University of Kentucky
UKnowledge

Theses and Dissertations--Physiology | Physiology

2021

Metabolic and Electrophysiological Effects of Fibroblast Growth Factor 19 in the Dorsal Vagal Complex

Jordan Wean
University of Kentucky, wean.jordan@gmail.com
Author ORCID Identifier:
https://orcid.org/0000-0002-9459-0093
Digital Object Identifier: https://doi.org/10.13023/etd.2021.383

Right click to open a feedback form in a new tab to let us know how this document benefits you.

Recommended Citation

Wean, Jordan, "Metabolic and Electrophysiological Effects of Fibroblast Growth Factor 19 in the Dorsal Vagal Complex" (2021). *Theses and Dissertations--Physiology*. 54.
https://uknowledge.uky.edu/physiology_etds/54

This Doctoral Dissertation is brought to you for free and open access by the Physiology at UKnowledge. It has been accepted for inclusion in Theses and Dissertations--Physiology by an authorized administrator of UKnowledge. For more information, please contact UKnowledge@lsv.uky.edu.

STUDENT AGREEMENT:

I represent that my thesis or dissertation and abstract are my original work. Proper attribution has been given to all outside sources. I understand that I am solely responsible for obtaining any needed copyright permissions. I have obtained needed written permission statement(s) from the owner(s) of each third-party copyrighted matter to be included in my work, allowing electronic distribution (if such use is not permitted by the fair use doctrine) which will be submitted to UKnowledge as Additional File.

I hereby grant to The University of Kentucky and its agents the irrevocable, non-exclusive, and royalty-free license to archive and make accessible my work in whole or in part in all forms of media, now or hereafter known. I agree that the document mentioned above may be made available immediately for worldwide access unless an embargo applies.

I retain all other ownership rights to the copyright of my work. I also retain the right to use in future works (such as articles or books) all or part of my work. I understand that I am free to register the copyright to my work.

REVIEW, APPROVAL AND ACCEPTANCE

The document mentioned above has been reviewed and accepted by the student's advisor, on behalf of the advisory committee, and by the Director of Graduate Studies (DGS), on behalf of the program; we verify that this is the final, approved version of the student's thesis including all changes required by the advisory committee. The undersigned agree to abide by the statements above.

Jordan Wean, Student

Dr. Bret N. Smith, Major Professor

Dr. Ken Campbell, Director of Graduate Studies

METABOLIC AND ELECTROPHYSIOLOGICAL EFFECTS OF FIBROBLAST GROWTH FACTOR 19 IN THE DORSAL VAGAL COMPLEX

DISSERTATION

A dissertation submitted in partial fulfillment of the requirements for the degree of Doctor of Philosophy in the College of Medicine at the University of Kentucky

By
Jordan Bruce Wean
Lexington, Kentucky

Director
Bret N. Smith, Ph.D.
Chair, Department of Neuroscience
Professor of Neuroscience and Physiology
Lexington, Kentucky

Copyright © Jordan Bruce Wean 2021
https://orcid.org/0000-0002-9459-0093

ABSTRACT OF DISSERTATION

METABOLIC AND ELECTROPHYSIOLOGICAL EFFECTS OF FIBROBLAST GROWTH FACTOR 19 IN THE DORSAL VAGAL COMPLEX

The dorsal vagal complex (DVC) is an important homeostatic regulatory center located in the hindbrain that alters vagal parasympathetic activity in response to central, viscerosensory, and humoral cues. Within the DVC, second-order sensory neurons in the nucleus tractus solitarius (NTS) integrate ascending vagal sensory input with descending regulatory inputs from higher brain areas and respond to circulating hormones and glucose. In turn, the NTS projects to the dorsal motor nucleus of the vagus (DMV) which is comprised of cholinergic motor neurons and regulates gastric motility, hepatic glucose production, and pancreatic hormone release functions, among others.

Fibroblast growth factor 19 (FGF19) is a protein hormone that produces antidiabetic effects when administered intracerebroventricularly in the forebrain. Lateral or third ventricle administration of FGF19 was shown to increase glucose tolerance, decrease body weight, and decrease food intake. However, no studies have been performed to understand the effects of FGF19 in the DVC. Neurons in the DVC express FGF receptors and regulate many of the processes that have been proposed to explain the antidiabetic effects of FGF19. Thus, this study was performed to understand both the cellular effects of FGF19 in the DVC as well as effects on systemic glucose regulation.

First, the FGF19 was applied to the hindbrain to understand its effects on blood glucose. Fourth ventricle administration of FGF19 produced no effect on blood glucose concentration in control mice, but induced a significant, peripheral muscarinic receptor-dependent decrease in systemic hyperglycemia for up to 12 hours in streptozotocin (STZ)-treated mice, a model of type 1 diabetes. Patch-clamp recordings from DMV neurons in vitro revealed that FGF19 application altered synaptic and intrinsic membrane properties of DMV neurons, with the balance of FGF19 effects being significantly modified by a recent history of systemic hyperglycemia.

Since the previous data indicated that FGF19 alters firing in glutamatergic neurons upstream from the DMV, the next study was aimed at understanding the electrophysiological effects of FGF19 on local glutamatergic circuits in the DVC. Receptor expression studies indicated that two nuclei were the most likely source of glutamatergic input to the DMV: The NTS and the area postrema (AP). Glutamate photolysis studies indicated that FGF19 does indeed increase the activity of glutamatergic neurons in the AP and NTS that project to the DMV. This effect was only seen in hyperglycemic mice. Further study indicated that FGF19 produced mixed effects on the intrinsic excitability of NTS neurons but increased

action-potential dependent glutamate release to the NTS in hyperglycemic mice. The source of this glutamate was confirmed to be the AP.

Overall, the in vitro effect of FGF19 on DVC neuron excitability was complex. FGF19 produced mixed effects on the intrinsic excitability of some cells while substantially increasing glutamatergic transmission at multiple synapses in the DVC of hyperglycemic mice. In vivo, FGF19 in the hindbrain decreased blood glucose concentration in diabetic mice, an effect that is consistent with its observed in vitro effects on glutamatergic transmission. These findings identify central parasympathetic circuitry as a novel target for FGF19 and suggest that FGF19 acting in the dorsal hindbrain can alter vagal output to produce its beneficial metabolic effects.

KEYWORDS: autonomic, vagus nerve, diabetes, fibroblast growth factor, dorsal vagal complex, EPSC

Jordan Bruce Wean

(Name of Student)

07-28-2021

Date

METABOLIC AND ELECTROPHYSIOLOGICAL EFFECTS OF FIBROBLAST GROWTH FACTOR 19 IN THE DORSAL VAGAL COMPLEX

By
Jordan Bruce Wean

Bret N. Smith, Ph.D
Director of Dissertation

Kenneth S. Campbell, Ph.D
Director of Graduate Studies

07-28-2021
Date

DEDICATION

This work is dedicated to my wife, Alyssa Wean

and

My parents, David and Pamela Wean

ACKNOWLEDGMENTS

I would like to thank my mentor, Dr. Bret Smith for the advice and guidance he provided along the way. I thank my advisory committee members: Dr. Olivier Thibault, Dr. Lisa Tannock, Dr. Ken Campbell, and Dr. John McCarthy. They asked the tough questions and helped bring new perspectives to my research. I thank the current and past members of the Smith laboratory who helped me along the way. To point out a few members regarding their roles. Thank you to: Drs. Jeff and Carie Boychuk, Cory Butler, and Isabel Derera for teaching me electrophysiology. Also, I would like to thank Dr. Katalin Smith, who helped so much with my failed molecular biology experiments and who also provided endless tasty Hungarian food.

I would also like to acknowledge my family. I thank my parents, David and Pamela Wean who always inspired me to be curious, courageous, and conscientious. I thank my siblings, David and Chloe Wean for all the amazing and strange things they do. Finally, I cannot thank enough my wife Alyssa, without whom, I would not be who I am and where I am today. She has been my best friend for as long as I can remember and an immense source of support, happiness, and advice though everything.

TABLE OF CONTENTS

ACKNOWLEDGMENTS iii

LIST OF FIGURES vii

LIST OF TABLES viii

1 Introduction 1

1.1 The Dorsal Vagal Complex 1
1.1.1 Overview of DVC Circuitry 1
1.1.2 The Vago-Vagal Reflex Arc 2
1.1.2.1 Ascending Input to the DVC 2
1.1.3 The NTS 3
1.1.4 The DMV 4
1.1.5 The Area Postrema 6
1.1.6 Other Inputs to the DVC 7
1.1.6.1 Actions of Hormones and Glucose in the DVC 7
1.1.6.2 Connections between the DVC and Other Nuclei 8

1.2 Diabetes 11

1.3 Fibroblast Growth Factors 12
1.3.1 Fibroblast Growth Factor Overview 12
1.3.2 Canonical and Intracellular FGFs 14
1.3.3 Endocrine FGFs 16
1.3.4 FGFs and metabolic regulation 17
1.3.4.1 FGF19 17
1.3.4.1.1 FGF19 Overview 17
1.3.4.1.2 FGF19 Actions in the Liver 21
1.3.4.1.3 FGF19 Actions in Adipose Tissue 22
1.3.4.1.4 FGF19 Actions in the Brain 22
1.3.4.1.5 FGF19 and Bariatric Surgery 26
1.3.4.2 FGF21 28
1.3.4.3 FGF1 30
1.3.5 FGF Receptors 33

2 Materials and Methods Summary 35

2.1 Animals 35

2.2 Brain Slice Preparation 35

2.3 Electrophysiological Recordings 36

2.4 Drugs Used for Electrophysiology Experiments 37

2.5 Statistical Analysis 37

3 FGF19 acts in the hindbrain to lower blood glucose concentration and alter excitability of dorsal vagal motor neurons in hyperglycemic mice 38

3.1 Introduction *38*

3.2 Research Design and Methods *39*
3.2.1 Animals 39
3.2.2 Intracranial Injection 40
3.2.3 Electrophysiology 41
3.2.4 Immunofluorescence 43
3.2.5 Statistics and Analysis 44

3.3 Results *45*
3.3.1 Hindbrain application of FGF19 decreases blood glucose concentration in hyperglycemic mice via a parasympathetic mechanism 45
3.3.2 Differential effects of FGF19 on synaptic excitability 49
3.3.3 Effects on resting membrane potential and input resistance 54
3.3.4 Action potential frequency 57
3.3.5 FGF19 decreases A-type K^+ current amplitude in control, but not in T1DM mice 59

3.4 Discussion *63*

4 Fibroblast growth factor 19 increases the excitability of pre-motor glutamatergic neurons in the dorsal vagal complex of hyperglycemic mice 70

4.1 Introduction *70*

4.2 Materials and Methods *72*
4.2.1 Animals 72
4.2.2 Electrophysiology 73
4.2.3 Statistics and Analysis 77

4.3 Results *77*
4.3.1 FGF19 increases the excitability of glutamatergic AP and NTS neurons that project to the DMV in hyperglycemic mice 77
4.3.2 FGF19 produces mixed effects on intrinsic excitability of NTS neurons. 80
4.3.3 FGF19 increases sEPSC frequency in NTS neurons from T1DM mice. 83
4.3.4 FGF19 does not alter mEPSC frequency in NTS neurons from T1DM mice. 85
4.3.5 FGF19 increases the excitability of glutamatergic AP neurons that project to the NTS in hyperglycemic mice. 88

4.4 Discussion *90*

5 General Discussion 98

5.1 Review of Major Findings *98*

5.2 Effects of Central Delivery of FGF19 on Blood Glucose *101*
5.2.1 Previous Findings 101
5.2.2 The DVC and Blood Glucose 103
5.2.2.1 DVC Regulation of the Pancreas 104
5.2.2.2 DVC Regulation of the Liver 105
5.2.2.3 Potential Involvement of Other Organs 106
5.2.3 Involvement of the Hypothalamus 107

5.3 The Cellular Effects of FGF19 in the DVC: Implications for Metabolism *109*

5.4 The Effects of Diabetes on the Brain *112*
5.4.1 The Effect of Diabetes on the DVC 113

5.4.2 The Effect of Diabetes on FGFR Signaling Pathways 114
5.5 Final Conclusions *116*
Appendices **119**
Abbreviations *119*
Equipment Used *123*
Patch-clamp rig diagram *124*
Patch Clamp Frequency Response Calculator and Circuit Diagram *125*
References **126**
VITA **148**

LIST OF FIGURES

Figure 3.1. Hindbrain application of FGF19 decreases blood glucose concentration in diabetic mice through a parasympathetic mechanism. 47

Figure 3.2. FGF19 decreases sEPSC frequency in neurons of the dorsal motor nucleus of the vagus (DMV) in slices from normoglycemic, control mice and increases sEPSC frequency in DMV neurons from hyperglycemic, T1DM mice. 52

Figure 3.3. Effects on input resistance and resting membrane potential. 55

Figure 3.4. FGF19 variably affects action potential frequency. 58

Figure 3.5. FGF19 decreases A-type K^+ current amplitude in DMV neurons from control, but not in T1DM mice. 60

Figure 3.6. The effect of FGF19 on the A-type K^+ current in normoglycemic mice is prevented by 4-AP or intracellular Cs^+. 62

Figure 4.1. FGF19 increases the excitability of glutamatergic AP and NTS neurons that project to the DMV in hyperglycemic mice. 79

Figure 4.2. FGF19 produces mixed effects on intrinsic excitability of NTS neurons. 82

Figure 4.3. FGF19 increases sEPSC frequency in NTS neurons from T1DM mice. 84

Figure 4.4. FGF19 does not alter mEPSC frequency in NTS neurons from T1DM mice. 87

Figure 4.5. FGF19 increases the excitability of glutamatergic AP neurons that project to the NTS in hyperglycemic mice. 89

LIST OF TABLES

Table 3.1. Intrinsic membrane properties of DMV neurons in response to FGF19 56

1 Introduction

1.1 The Dorsal Vagal Complex

1.1.1 Overview of DVC Circuitry

The dorsal vagal complex (DVC), located in the caudal brainstem, is the central hub of parasympathetic regulation of visceral homeostasis. The basic circuitry of the DVC can be compared to a standard reflex arc, with a sensory limb located in the periphery, a central limb that integrates sensory information, and an effector limb that projects to the periphery to regulate homeostatic processes. Despite the seemingly simplistic topology DVC circuitry, there are abundant points of modulation and specialization that allow this relatively small area of the brain to maintain tight, nuanced control of many disparate and vital peripheral systems.

The first limb of this “vago-vagal” reflex is comprised of sensory neurons in the vagus nerve that detect several types of homeostatic signals in the viscera and transmit this information to neurons in the DVC, specifically, the nucleus tractus solitarius (NTS). The NTS integrates numerous convergent inputs, both neural and humoral, and subsequently projects to neurons in the dorsal motor nucleus of the vagus (DMV) which make up the effector limb of the reflex arc. Cholinergic motor neurons in the DMV then project through the descending vagus nerve to regulate much of the viscera. The DVC is an efficient homeostatic regulatory center that can produce drastic changes in the periphery in response to an array of signals. As such, it is paramount to understand how circuitry in the

DVC can be modified to alter the outcome of chronic diseases such as diabetes. Further detail will now be given regarding the specifics of DVC signaling.

1.1.2 The Vago-Vagal Reflex Arc

1.1.2.1 Ascending Input to the DVC

The ascending limb of the DVC reflex arc is comprised of vagal sensory neurons with cell bodies in the bilateral nodose ganglia – found in the jugular foramen at the base of the skull. Vagal afferents significantly outnumber efferents, suggesting that the primary function of the vagus is sensory in nature [1]. Vagal afferents are found throughout the length of the alimentary tract with the highest innervation found in the esophagus, stomach, and duodenum [2]. There is further innervation throughout the intestines up to the left colic splenic flexure of the colon. These neurons are organized in a manner analogous to the dorsal root ganglion in that they are pseudounipolar, with distal processes in the gut containing sensory terminals and proximal processes that terminate centrally [3]. This allows for a high volume of viscerosensory information to be transmitted monosynaptically from gut to brain [3-6].

Vagal afferents can be differentiated into classes based on location of the receptive field and the type of signal that is transduced. Muscular afferents innervate the smooth muscle fibers of the GI tract or in the surrounding myenteric ganglia and contain mechanosensitive terminals [7-9]. These neurons respond to muscular tension, signaling the distension and contraction of the gastrointestinal tract [7]. Mucosal afferents innervate the mucosal lamina propria and can contain

both mechano- and chemosensitive terminals. Mucosal afferents, while not sensitive to tension per se, respond to light deformation to the mucosa with a high sensitivity, likely detecting luminal particulate material [7, 10]. Chemosensitive mucosal afferents primarily terminate in the small intestine [11] and are sensitive to chemosensory cues such as pH, nutrients, osmolarity, and temperature [10, 12, 13] as well as circulating hormones, perhaps most notably CCK [14]. The proximal processes of vagal afferents terminate in the NTS in a viscerotopic manner with, for example, esophageal and stomach wall afferents terminating within different NTS subnuclei [4]. Vagal afferents communicate to the NTS primarily through glutamate [6].

1.1.3 The NTS

The NTS comprises the central integration leg of the canonical vago-vagal reflex arc. The NTS receives glutamatergic input from the aforementioned vagal afferent sensory neurons and integrates these signals with inputs from several brain areas. Afferent input to the NTS is organized viscerotopically, with sensory inputs from different organs terminating in different NTS subnuclei [4, 15, 16]. Unlike DMV neurons (discussed below), NTS neurons do not exhibit pacemaker activity and need to be driven by synaptic connections [17-19]. NTS neurons are primarily GABAergic [20-22], glutamatergic [21-23] and catecholaminergic [24, 25]. The NTS also exhibits bidirectional communication with several other brain areas (for more, see Chapter 1.1.6.2).

1.1.4 The DMV

The DMV makes up the last limb of the vago-vagal reflex arc and is the origin of parasympathetic motor supply to a large proportion of the viscera. This was best described via several tract-tracing studies using retrograde labelling [26-28]. The DMV is a paired structure that lies at the ventral edge of the DVC adjacent to the central canal in the caudal DVC and ventral to the fourth ventricle in the rostral DVC. The DVC is comprised of ~20,000 neurons [12, Chapter 31] that innervate nearly every digestive organ, though projections to the stomach are the densest [29]. Most DMV neurons (>95%) are cholinergic although a small proportion express catecholamines and NOS [30-34]. Finally, there are a small population of DMV neurons that likely serve as inhibitory interneurons although their function is not understood [35].

The efferent vagus contains several branches and retrograde tracing data show that DMV neurons are organized mediolaterally according to which branch they project through [26]. The medial DMV contains neurons that project to the gastric vagal branches, the lateral DMV projects through the celiac vagal branches, and a small portion of neurons in the left DMV project to the hepatic vagal branch. A single organ may be innervated via multiple vagal branches. For example, the stomach is innervated by the gastric and hepatic branches and the duodenum is innervated by the gastric and celiac branches [29, 36].

The activity of DMV neurons regulates numerous important visceral processes. The largest proportion of DMV neurons project to the stomach and much of the research into the functions of DMV neurons has focused here. The

DMV heavily regulates gastric motility through both excitatory and inhibitory pathways [37]. Vagal efferent outflow, likely originating in the DMV, also stimulates gastric secretion [38-40]. The DMV is also the primary source of vagal control over both endocrine and exocrine pancreatic secretions. Electrical stimulation of the DMV greatly increases plasma insulin concentrations and this effect was blocked via atropine and vagotomy, heavily suggesting a vagus-dependent mechanism [41]. Additionally, disinhibition of the DMV via $GABA_A$ receptor blockade in the DVC or inhibition of the DMV via chemogenetics modulates pancreatic endocrine and exocrine secretions [42-44].

The actions of the DMV on the liver are not fully understood. Retrograde labeling using a modified pseudorabies virus (PRV) indicates that there are DMV neurons that project to the liver [45]. However, anterograde labeling from the DVC shows that DMV neurons do not terminate in the hepatic parenchyma or on hepatic nerves or paraganglia [46]. Despite this, there is evidence that the DMV regulates glucose metabolism through the vagus nerve. Pocai *et al.* found that the hypothalamus controls hepatic glucose production (HGP) by exciting DMV neurons and that this effect was blocked via a vagotomy [47]. Moreover, injection of NMDA into the DVC lowers HGP, which was also blocked by a vagotomy [48].

DMV neurons display a diverse set of electrophysiological phenotypes. Most DMV neurons sustain a slow pacemaker activity (1-2 Hz action potentials) [49-51]. This implies that small changes in DMV excitability through modification of either membrane potential or synaptic input can produce dramatic differences in vagal motor output [52, 53]. DMV neurons receive primarily glutamatergic and

GABAergic inputs from the NTS, although it is thought that GABAergic control dominates under normal circumstances [22, 23, 25, 54]. DMV neurons also display electrophysiological and morphological heterogeneity depending on their target organ [55]. Finally, DMV neurons display heterogeneity regarding the presence of several voltage-gated and subthreshold potassium currents [53, 55].

1.1.5 The Area Postrema

The area postrema (AP) is an important part of the DVC although it is traditionally not considered part of the canonical vago-vagal reflex. As a circumventricular organ, the AP lacks a functional blood-brain barrier and serves as a chemoreceptive sensory organ for the detection of humoral components [56]. The AP is located at the caudal end of the fourth ventricle and is located immediately dorsal and medial to the NTS. The AP is traditionally considered the primary emetic center of the brain [57]. Electrical stimulation in the AP causes nausea and emesis and lesions of the AP abolish nausea responses to intravenous poisons [58, 59].

Recent research has highlighted the importance of the AP in metabolic regulation. AP neurons respond to a number of metabolic hormones including GLP-1, amylin, and GDF15 [60-65]. Interestingly, the AP may also participate in vago-vagal reflex actions. The AP receives vagal afferent input and projects glutamatergic outputs to the NTS and DMV [66-68]. The function of the AP to NTS/DMV connection is not understood. However, it seems likely that the AP may serve as a secondary integration center for afferent vagal input, similar to the NTS.

The AP also projects to more distal metabolic nuclei such as the hypothalamus and parabrachial nucleus [66-68].

1.1.6 Other Inputs to the DVC

1.1.6.1 Actions of Hormones and Glucose in the DVC

There is a large body of evidence suggesting that the DVC is able to sense blood-borne components and alter parasympathetic output accordingly. Due to local fenestrated capillaries, much of the DVC has access to circulating hormones and nutrients that might typically be excluded by the blood brain barrier [56, 69]. Indeed, neurons in the DVC respond to numerous humoral metabolic signals although in most cases it is not known what part these responses play in normal homeostatic regulation.

Some neurons in the DVC are glucosensitive and different subsets of DVC neurons can respond with increased or decreased activity in response to a given change in extracellular glucose. For example, GABAergic NTS neurons respond with either increased (40%) or decreased (33%) excitability in response to an increase in ambient glucose from 2.5 to 15 mM [70]. These effects remained after the chemical blockade of synaptic input, indicating that these neurons directly sensed the changes in glucose. Furthermore, GLUT2-expressing neurons in the NTS sense hypoglycemia which and alter the activity of GABAergic connections to the DMV accordingly [71]. This produces an increase in vagus nerve activity, leading to a counterregulatory increase in glucagon secretion.

DVC neurons respond to numerous gastrointestinal hormones. For example, NTS and DMV neurons respond to leptin [49, 72]. Exogenous leptin administration to the fourth ventricle or the DVC reduces food intake for at least 24 h and decreases food-seeking behavior [73, 74]. Leptin sensitizes neurons in the DVC to signals of gastric distension [75], and knockdown of leptin signaling in the NTS leads to hyperphagia and increased body weight and adiposity [76]. This suggests that leptin functions to fine-tune DVC neuronal responses to gastric signals during homeostatic regulation of food intake.

The DVC also responds to insulin. Insulin produces effects on both DMV intrinsic excitability and on synaptic input to the DMV in a slice preparation [50, 77]. This suggests that insulin acts on DMV neurons directly and on either AP or NTS neurons that are immediately afferent to the DMV. The existence of direct actions on the DMV by insulin is unsurprising when considering that pancreatic insulin secretion is under the direct control of a subpopulation of DMV neurons [78]. When exogenous insulin is administered to the DVC, it produces an ERK1/2-dependent decrease in HGP. These examples are far from exhaustive, as the DVC also responds to glucagon [79], GLP-1 [64, 80-84], and ghrelin [85-87] among others.

1.1.6.2 Connections between the DVC and Other Nuclei

There is abundant evidence showing that DVC neurons make reciprocal connections with several other brain areas, though little is known about the functions of these connections. Early tract tracing studies showed that the NTS

projects to the hypothalamus, amygdala, parabrachial nucleus, and several motor nuclei including the DMV [28, 88]. Early studies also confirmed that the AP projects to the NTS, the parabrachial nucleus, and dorsal tegmental nucleus [67]. Subsequently, it was identified that the NTS receives extensive projections from higher brain areas including the prefrontal cortex, stria terminalis, amygdala, and the hypothalamus [89, 90]. The projections from other nuclei to the NTS are arranged so that cortical projections terminate in the dorsal NTS and subcortical projections terminate in the ventral NTS. The paraventricular hypothalamus also innervates the DMV. Finally, the hypothalamus also innervates the AP.

Relatively little is known about the functions of the various connections between the DVC and other brain areas. The best studied of these is the descending hypothalamic to DVC connection. Evidence suggests that hypothalamic regulation of HGP in response to sensation of circulating nutrients involves a descending hypothalamus-DVC-liver circuit [47, 91]. Pocai *et al.* found that ICV infusion of a fatty acid oxidation inhibitor ST1236 decreased HGP to such a degree as to require exogenous glucose infusions to prevent hypoglycemia in rats [47]. The authors found that central blockade of fatty acid metabolism activated hypothalamic K_{ATP} channels, which subsequently led to an activation of AP, NTS, and DMV neurons as measured by c-fos expression. The effect on HGP was blocked via vagotomy. It was found that activation of this circuit decreased hepatic gluconeogenesis by decreasing liver expression of G6Pase and PEPCK, gluconeogenetic enzymes. A subsequent study found that the hypothalamus-DVC-hepatic glucose production regulatory circuit requires NMDA receptor

activation in the DVC [92]. Together, these data indicate that the ability of the hypothalamus to regulate HGP in response to nutrient sensing relies on a NMDA receptor-dependent connection to the DVC.

Less is known about the functions of efferent connections from the DVC to other brain areas but a recent example highlights the potential power that these connections possess. GDF15 is a member of the TGFß superfamily that is typically associated with anorexia and cancer cachexia [93, 94]. It has been long known that GDF15 potently decreases body weight through suppression of food intake, although only recent research identified a mechanism. In 2017, four independent pharmaceutical company laboratories identified GFRAL, the receptor for GDF15 [61-63, 95]. Intriguingly, GDF15 is expressed in the AP and to a lesser degree the NTS, with no expression anywhere else in the body. Administration of GDF15 activates GFRAL-expressing AP neurons, which then leads to activation of neurons in the NTS, hypothalamus, parabrachial nucleus, and amygdala [61, 94, 96, 97]. It has been suggested that the primary mechanism of action is the activation of an AP to parabrachial nucleus to amygdala circuit that leads to conditioned taste avoidance and suppression of feeding. Much further work is required understanding the connections to and from the DVC. However, the examples above highlight powerful impact that activation of these circuits can produce.

1.2 Diabetes

Diabetes is too expansive a topic to be succinctly covered here. The following information will be a brief overview of the disease with specifics that relate to the current project. Diabetes is characterized by derangements of glucose metabolism, leading to high glucose concentrations in the blood. Type I diabetes involves autoimmune destruction of pancreatic ß-cells, leading to a loss of insulin production and secretion [98]. Type II diabetes involves progressive insulin resistance, due to a combination of genetics and chronic excessive energy intake [99, 100].

The brain is responsible for approximately 50% of glucose disposal while adipose and muscle tissue dispose of approximately 25% [101-103]. The remainder is disposed in the liver, red blood cells, and kidney. Diabetes decreases glucose clearance and induces insulin resistance in muscle tissue [104, 105]. However, muscular insulin resistance can only account for approximately 10% of the dysfunctional glucose clearance observed in diabetes [105]. This suggests that derangements in central metabolism are the primary cause of decreased glucose clearance. Diabetes causes elevated plasma glucose concentrations in the fasted state as well. This is likely due to decreased insulin signaling in the liver leading to high rates of HGP [106-109]. Since the body (usually) spends much more time in a post-absorptive state than in a postprandial state, it is therefore likely that the primary contributor to high fasting glucose levels associated with diabetes is the liver.

CNS control of blood glucose was first suggested by the physiologist Claude Bernard in 1854 after he observed that diabetes (as measured by glucosuria) could be induced by puncturing the ventral wall of the fourth ventricle in rabbits [110]. However, after the discovery of insulin in 1921, most study into metabolic regulation shifted to the periphery. Despite this, a wide body of recent research has highlighted that the brain contains a distributed neuronal network that can produce dramatic effects on glycemia when challenged with certain signals [for reviews, see: 111, 112-115]. Briefly, neurons primarily in the hypothalamus and brainstem have been shown to respond to glucose levels as well as numerous gut hormones. In response, these neurons regulate neuroendocrine hormone release, autonomic nervous system activity, and ingestive behavior. Current treatments for diabetes are primarily focused on peripheral metabolic signaling and do not take into account the important role that the CNS plays in metabolic regulation. Thus, research into centrally mediated modulation of blood glucose is paramount to develop new therapies.

1.3 Fibroblast Growth Factors

1.3.1 Fibroblast Growth Factor Overview

The fibroblast growth factor (FGF) family contains a diverse group of signaling molecules that regulate numerous aspects of life. The field of FGF research began as early as 1939 when it was shown that embryo extracts were able to promote the growth of chicken fibroblasts, though no individual molecules were identified [116]. The first members of the family (FGF1 and FGF2, initially

known as acidic FGF and basic FGF respectively) were identified in the 1970s and 1980s when it was discovered that bovine brain extracts were able to stimulate the growth of 3T3 fibroblasts [117-122]. Further members of the family were discovered via cell culture growth, identification of oncogenes tagged by retroviruses, identification of genes responsible for hereditary disease, or by homology-based searches of the genome [for review, see 123].

There are currently 23 known FGFs that differ widely according to function, receptor specificity, expression patterns, and secretion characteristics. FGFs are typically divided into three groups: canonical FGFs (further subdivided into 5 families), intracellular FGFs (iFGF), and endocrine FGFs. The overall grouping is based on secretion characteristics (i.e. whether the FGF is secreted or not) and whether the FGF interacts with heparin sulfate (HS).

FGFs are classified in part by their interactions with HS, a long linear chain of repeating sulfated disaccharides that varies in length and amount of sulfation. Typically, HS is found in the form of heparin sulfate proteoglycans (HSPG). HSPGs are complex cell surface molecules composed of heparin sulfate covalently linked to core proteins such as syndecan, perlecan, glypican, and agrin. Depending on which core protein is present, HSPGs can be cell surface transmembrane proteins, cell surface anchored proteins, or diffusible proteins in the extracellular matrix [124-129].

HSPGs modify FGF activity in two primary ways. First, HS is a required co-factor for the binding of all canonical FGFs to FGFRs [130-134]. Second, interaction with HS serves to sequester FGFs, thereby restricting their spread

[135]. The physical characteristics of HSPGs themselves also regulate FGF signaling. HS chain length and sulfation pattern regulate FGF signaling. Specific HS chains regulate cell-specific patterns of FGF-FGFR interaction [136-138]. Moreover, higher levels of HS sulfation increases FGF signaling activity [139, 140]. Finally, cleavage of the core HSPG protein increases FGF signaling by releasing FGFs that had been previously sequestered [138].

1.3.2 Canonical and Intracellular FGFs

Canonical FGFs are secreted signaling molecules that act in an autocrine or paracrine fashion due to their high affinity for HSPGs. These FGFs are further divided into 5 subgroups. The FGF1 subfamily contains only FGF1 and FGF2. This group is defined by its lack of any classical secretory signal. Despite this lack, they are still translocated across the cell membrane via chaperone proteins [141, 142]. FGF1 is notable in that it is the only FGF known to activate all FGFRs. More will be said regarding FGF1 later regarding its effects on metabolism. The FGF4 subfamily is comprised of FGF4, FGF5, and FGF6. The members of this family contain N-terminal signal peptides that control secretion characteristics and activate IIIc splice variants of FGFRs 1-3 and FGFR4 [131, 132]. The FGF7 subfamily contains FGF3, FGF7, FGF10, and FGF22. This family is defined by the fact that they activate the IIIb splice variant of FGFR1 and FGFR2 [131, 132]. For further information regarding FGFR splice variants, see Chapter 1.3.5.

The FGF8 subfamily contains FGf8, FGF17, and FGF18. These FGFs contain a cleaved N-terminal signal peptide and activate IIIc splice variants of

FGFRs 1-3 and FGFR4 [131, 132]. The FGF19 subfamily contains FGF9, FGF16, and FGF20. The members of this family are notable in that they contain an internal hydrophobic sequence instead of a classical N-terminal signaling peptide. This targets members of this family for transport into the endoplasmic reticulum as well as for secretion from cells [143-145]. This family activates the IIIb splice variants of FGFR3, FGFR4, and the IIIc splice variants of FGFRs 1-3 [131, 132].

Canonical FGFs participate in a diverse array of physiological processes starting from the very first stages of development. FGF4 is expressed in the preimplantation embryo and is required for inner cell mass proliferation [146, 147]. In later developmental stages, canonical FGF signaling is key in regulating organogenesis and limb development [148-150]. Canonical FGFs, primarily FGF8, are also vital for nervous system development. FGF8 signals the anterior to posterior structuring of the telencephalon [151]. Canonical FGF signaling also regulates myelination, and FGF22 and FGF7 are required for the synaptogenesis of excitatory and inhibitory synapses respectively [152-154].

Intracellular FGFs (knowns as iFGFs) are notable in that they are not secreted and do not interact with FGFRs [155]. The iFGF family is comprised of FGF11, FGF12, FGF13, and FGF14. iFGFs interact with voltage-gated sodium channels (Na_v). The iFGFs serve to regulate the localization of Na_v channels, helping to concentrate them at the axon hillock and axon initial segment. Moreover, iFGFs regulate the gating properties of Na_v channels in numerous cell types including neurons and cardiomyocytes [156-160].

1.3.3 Endocrine FGFs

The final group of FGFs is the endocrine FGFs, comprised of FGF 15/19, FGF 21, and FGF23. FGF15 and FGF19 are considered to be orthologs in mice and humans respectively and can be thought to serve the same function. For more information, see the section on FGF19. Endocrine FGFs are secreted, similar to the canonical group, yet there exists an important distinction in that endocrine FGFs interact weakly with HS. This allows members of this group to freely diffuse away from their tissues of origin and act as endocrine hormones [161].

Instead of HS, endocrine FGFs require the presence of members of the klotho family as co-receptors to activate FGFRs [162]. FGF15/19 and FGF21 signals using ß-klotho while FGF23 signals using α-klotho [163-167]. Importantly, klotho distribution is a vital determinant of endocrine FGF tissue specificity. This is because, although FGFRs are heavily distributed throughout the body, klotho distribution is much more restricted [168]. FGF23 primarily functions in phosphate metabolism and thus is of little importance here. However, FGF15/19 and FGF21 produce remarkable effects on metabolism throughout the body. These two members of the family, along with FGF1, will be discussed in the following section on FGFs and metabolic regulation.

1.3.4 FGFs and metabolic regulation

There is an enormous body of research over the past 80 years regarding the functions of FGFs that was only briefly addressed above. However, it was only relatively recently discovered (~20 years) that FGF signaling is important in the regulation of energy metabolism. The FGFs outlined within this group have all been linked to the actions of nuclear receptors that are well known to modulate metabolism. FGF1 is involved in adipose signaling and is regulated by PPARγ, a lipid sensor [169]. FGF15/19 is involved in cholesterol and bile metabolism and is regulated by the bile acid sensor FXR [170]. Finally, FGF21 is involved in the fasting response and is targeted by PPARα, a fatty acid sensor [171].

1.3.4.1 FGF19

1.3.4.1.1 FGF19 Overview

FGF15 and 19 are considered to be orthologs in the mouse and human respectively. Most FGFs are heavily conserved between mice and humans, showing a 90% or greater agreement in amino acid sequence yet FGF15 and FGF19 only show ~43% agreement [172] between species. Despite this, FGF15 and 19 show similar expression patterns [168, 172] and produce similar effects on metabolism and gene expression in mice [170, 173]. Because FGF19 is more stable than FGF15 and produces the same beneficial metabolic effects even when administered to mice, most research in this area has focused exclusively on

FGF19. Thus, the remainder of this section will discuss FGF19 unless specifically noted.

FGF19 was first identified using a PCR/cDNA-based screen for novel FGFs in human fetal brain tissue [172]. FGF15 has been shown to participate in the organization of the CNS by promoting differentiation of neural precursors [174, 175], thus it is likely that FGF19 performs similar functions in humans. After development, FGF15 is no longer expressed in the CNS [168] and is thereafter primarily involved in the regulation of bile acid metabolism.

Bile acids are small amphipathic detergent molecules that serve to break up lipid droplets and solubilize them for absorption [176]. Bile acids are produced in the liver released from the gall bladder into the small intestine after a meal. They travel to the distal small intestine (the ileum) where they are reabsorbed and transported back to the liver via the portal vein. Because bile acids are toxic to cells, their synthesis and release must be tightly regulated. This is accomplished by altering the transcription of several proteins found in the bile acid synthesis pathway.

A primary determinant of bile acid synthesis is the cholesterol 7α-hydroxylase enzyme (CYP7A1). It was suggested well before the discovery of FGF19 that there must be some secreted factor that regulates bile acid synthesis since intestinal administration of bile acids suppresses CYP7A1 expression [177]. Subsequent research found that specific bile acids (cholic acid and chenodeoxycholic acid) in the ileum stimulate the farnesoid X receptor (FXR), a member of the nuclear receptor family [178].

Since FXR agonists were shown to induce FGF19 release from human hepatocytes, it was suggested that FGF15/19 could be the missing secreted factor [179]. Further studies confirmed this hypothesis by showing that FXR was unable to repress CYP7A1 activity in FGF15-KO mice [170]. Additionally, administration or sequestration of bile acids in humans has been shown to increase or decrease circulating FGF19 in humans respectively, suggesting that the pathway is conserved between species. Bile acid stimulation of FXR causes FGF19 to be released from the ileum into the portal vein, where it travels back to the liver. FGFR4 and ß-klotho knockout mice show increased CYP7A1 expression and fail to reduce bile acid synthesis in response to exogenous FGF15/19 [170, 180-182]. Thus, FGF15/19 interacts with hepatic FGFR4 to decrease bile acid synthesis.

Shortly after the discovery of FGF19, pioneering work from the pharmaceutical company Genentech identified several beneficial metabolic effects caused by systemic FGF19. Transgenic overexpression of FGF19 was found to decrease body weight and adiposity despite increasing food intake [183]. These mice also failed to become obese or hyperglycemic when maintained on a high-fat diet (HFD). This was explained via multiple mechanisms. First, it was found that the transgenic FGF19 mice displayed increased metabolic rate without any change in activity. Interestingly, there was no difference in fasted metabolic rate between the groups, suggesting that the FGF19-induced increase in metabolism was reliant on energy availability. Second, FGF19 increased the mass of brown adipose tissue (BAT) depots in these mice. Mice with genetically induced reductions in BAT mass become obese and hyperphagic [184]. Furthermore,

FGF19 increased fourfold the uncoupling protein UCP-2 in BAT depots in these mice. UCP-2 is inversely correlated with body fat in humans [185].

Similar work from within the same laboratory showed that recombinant FGF19 produced many of the same effects. In mice fed a HFD, exogenous FGF19 increased metabolic rate and prevented weight gain with no effects on food intake [186]. Additionally, FGF19 treatment prevented or reversed diabetes in mouse models with genetic ablation of BAT or with leptin (ob/ob mice). This study found that FGF19 also increased liver expression of the leptin receptor and decreased hepatic acetyl coenzyme A carboxylase 2, leading to increased fatty acid oxidation. However, the most interesting result from this study was the finding that FGF19 alters metabolism when administered centrally. FGF19 injected into the lateral ventricle increased metabolic rate. This is unlikely to be due to spillover into the periphery since a small dose (0.5 μg) given centrally produced an effect on metabolic rate while the same dose given peripherally did not.

The initial studies outlined above were the first to identify FGF19 as a metabolically active hormone but failed to establish a mechanism for these effects. There has been much subsequent research subsequent identifying the effects of FGF19 throughout several metabolically important tissues. It appears that FGF19 (as well as the other two metabolic FGFs) primarily signal in the liver, adipose tissue, and the brain.

1.3.4.1.2 FGF19 Actions in the Liver

In light of FGF19's established effects on the liver via FGFR4, initial research focused on this system. FGF15 and FGFR4 knockout mice became hyperglycemic and showed increased rates of gluconeogenesis [173]. Similarly, another study found that FGFR4 knockout caused hyperlipidemia, glucose intolerance, and insulin resistance [187]. Interestingly, this same study found through re-expressing FGFR4 in the livers of FGFR4-KO mice, that hepatic FGFR4 was required for whole-body lipid metabolism but dispensable for glucose metabolism.

Subsequent studies found that FGF19 affects hepatic glucose metabolism by causing hepatic protein and glycogen synthesis similar to the effects of insulin on the liver [188]. While insulin requires the Akt-mTOR intracellular cascade to achieve this effect, FGF19 was found to work through an ERK-RSk signaling pathway. Since diabetic insulin resistance occurs primarily upstream of Akt, this indicates that FGF19 may be able to circumvent some of the dysregulated pathways seen in type II diabetes [189]. One additional important discovery regarding the actions of FGF19 in the liver is that FGF19 has mitogenic properties. By activating FGFR4, FGF19 can cause the proliferation of hepatocytes and can induce hepatocellular carcinomas [190]. To combat this, specific FGF variants have been created that retain their beneficial metabolic effects without activating FGFR4 [191, 192].

1.3.4.1.3 FGF19 Actions in Adipose Tissue

FGF19 signals primarily through FGFR1 and FGFR4 [193]. Multiple studies have shown that FGF19 interacts with FGFR1, not FGFR4 to improve glucose metabolism [194, 195]. Since FGFR1 is only sporadically expressed in the liver, it was hypothesized that FGF19 may alter metabolism via interactions with other tissues [168]. One potential target is adipose tissue since both white adipose tissue (WAT) and BAT express high levels of FGFR1 and ß-klotho. However, WAT-specific knockout of FGFR1 does not prevent FGF19's beneficial effects on blood glucose. Moreover, genetic ablation of ß-klotho in adipose tissue does not block the effects of FGF19 [196]. Given the aforementioned increases in BAT mass, it is likely that FGF19 does alter adipose signaling. However, it does not seem to alter glucose regulation through this tissue.

1.3.4.1.4 FGF19 Actions in the Brain

Recent research has suggested that the brain is the primary target for FGF19's beneficial metabolic effects. Lan et al. showed that ablation of ß-klotho in the brain blocked the effect of FGF19 on weight loss whereas ablation of ß-klotho in either adipose tissue or hepatocytes did not. As mentioned previously, early research established that low dose FGF19 increased metabolic rate when injected into the lateral ventricles [186]. These findings inspired four key studies as well as those included in Chapter 3 of this work. The overall message of the combined research in this area is clear: FGF19 injection into the brain produces potent antidiabetic effects. However, there are several differences between the

studies regarding mechanisms and techniques. Each study was performed by a different research group and no groups performed more detailed follow-up studies. As such, there remains a lack of consensus regarding the effects of FGF19 in the brain and a somewhat shallow understanding of each individual effect.

The first detailed study on FGF19 in the brain came from the Seeley lab and established several interesting effects [197]. This study was performed in lean and high-fat diet fed rats. Firstly, it was shown that HFD was able to reduce the expression of FGFR1 and FGFR4 in the hypothalamus. This suggested that intracerebroventricular (ICV) FGF19 would not be as effective at regulating metabolism in these mice, although this was not the case. ICV FGF19 was able to reduce 24 hr food intake and body weight in both chow-fed and HFD mice in approximately equal amounts. The researchers further established that ICV FGF19 significantly improves glucose tolerance in an insulin-independent manner. Interestingly, this study also showed that CNS regulation of metabolism also involves endogenous FGFR signaling since the ICV administration of an FGFR antagonist increased food intake and decreased glucose tolerance. While these results were promising, they failed to establish any mechanistic details

The second key study in this area came from the Schwartz group and was the first to propose a mechanism for ICV FGF19's beneficial effects on blood glucose regulation [198]. These studies were performed in leptin-deficient ob/ob mice. First, researchers established the ability of FGF19 to decrease fasting blood glucose and glucose tolerance in these mice in an insulin-independent manner. To understand the contribution of CNS FGFR signaling to the systemic FGF19-

induced antidiabetic effects, FGF19 was administered intraperitoneally with concurrent ICV FGFR antagonist administration. It was found that FGF19's actions in the CNS account for approximately 50% of its total systemic actions on blood glucose. To understand how FGF19 was able to improve glucose tolerance, the authors used a frequently sampled i.v. glucose tolerance test (FSIGT) combined with the minimal model analysis. This methodology allows for quantitative measures of, among others, insulin secretion, insulin sensitivity, and glucose effectiveness (GE) [199, 200]. GE is the body's ability to dispose of glucose independently of insulin and GE is impaired in humans and mice with diabetes [199, 201]. The authors found that FGF19 was able to improve glucose homeostasis by increasing GE, with no effects on insulin secretion or sensitivity. This was hypothesized to occur via increased metabolism of glucose to lactate, possibly through changes in liver enzyme expression. Finally, the authors showed that ICV FGF19 does not activate hypothalamic POMC neurons and still reduces blood glucose in melanocortin-4 receptor-KO mice, suggesting that ICV FGF19 does not work through the melanocortin system.

The third study in this area was the first to establish a CNS mechanism for the central delivery of FGF19 [202]. These studies were performed in HFD and leptin-deficient (ob/ob) mice. Firstly, the authors showed that systemic delivery of FGF19 was able to stimulate ERK signaling in AGRP/NPY but not POMC neurons in the hypothalamus. Phosphorylated extracellular signal-related kinase (pERK) is often used as a hallmark for FGFR activation. Using c-Fos staining, the authors further established that FGF19 inhibited AGRP/NPY neurons. Importantly, the

authors showed that the FGF19-mediated improvements in blood glucose are reliant upon ERK signaling since ICV administration of an ERK inhibitor blocked these effects. Thus, these data identified a central mechanism: FGF19 inhibits AGRP/NPY neurons in the hypothalamus by activating intracellular pERK signaling.

The fourth and final study on FGF19 in the brain is unique in both methodology and animal model used [203]. First, the authors of this study chose to use a type I diabetic (T1DM) rat model. All prior research in this area had been performed in WT rodents or models of diet-induced obesity (DIO) or leptin deficiency (ob/ob). However, all previous findings pointed towards an insulin-independent mechanism, suggesting that ICV FGF19 would also work in a T1DM model. The methodology used here also differed from others in that the authors measured HGP, whole-body glycolysis, and whole-body glycerol and palmitate turnover. This was measured by injection of radioactive glucose, glycerol, and palmitate with subsequent analysis via scintillation counter and gas chromatography. The authors found that ICV FGF19 lowered blood concentrations of glucose, corticosterone, ACTH, fatty acids, and glycerol with no changes to adrenergic hormones, glucagon, or insulin. The authors then found that ICV FGF19 decreased HGP, whole body palmitate turnover, and whole-body glycerol turnover. Importantly all effects of FGF19 were reversible by co-administration of corticosterone. The authors concluded that ICV FGF19 suppressed the hypothalamic-pituitary-adrenal axis, thereby reducing blood glucose concentrations. Moreover, this paper established that not only does ICV

FGF19 not alter insulin secretion, but that it also does not require intact insulin signaling to produce its effects.

1.3.4.1.5 FGF19 and Bariatric Surgery

There is a growing body of research linking FGF19 to the antidiabetic effects of bariatric surgery procedures [204]. Bariatric surgery procedures such as the Roux-en-Y gastric bypass (RYGB) and vertical sleeve gastrectomy (VSG) provide long-term improvements to blood glucose concentration in addition to body weight. Bariatric surgery involves either reduction of the size of the stomach (VSG) or stomach reduction with the additional rerouting of the small intestine (RYGB). Although initial theories held that the primary benefits of these surgical procedures were the result of a smaller stomach, there is evidence that this is not the case. A large proportion of patients with diabetes can cease taking their diabetic medications within several days of receiving surgery [205]. This effect was not replicated in patients that lost weight and improved glycemic control via traditional medical therapy. This suggests that there must be a distinct underlying mechanism that is induced by surgical means that is absent from other treatments.

Bariatric surgery causes numerous changes in gut physiology but one of the most promising involves bile acid regulation. In both humans and rodent models, bariatric surgery alters the levels and composition of bile acids [206-209]. The changes in bile acid regulation seen in bariatric surgery are not observed in patients on a hypocaloric diet that produced similar amounts of weight loss [210]. Moreover, studies have shown that bile acid supplementation can produce a host

of beneficial metabolic effects including increased metabolic rate, increased BAT activity, decreased appetite, and improved glucose metabolism [211-214]. Interestingly, surgical diversion of bile acids into the ileum of DIO rodents recapitulates the effects of RYGB on body weight, fat loss, and carbohydrate metabolism [215, 216].

One likely explanation for these effects involves FXR and FGF19. Unbiased pathway analysis revealed that VSG regulates FXR, which is perhaps unsurprising considering the effects of VSG on bile acid dynamics [217]. However, the same study showed that the effects of VSG were blocked in FXR knockout mice. While VSG decreased food intake, body weight, and blood glucose concentrations in WT mice compared to sham counterparts, FXR-KO mice showed no difference in body weight and increased food intake and blood glucose concentration compared to their counterparts.

Bariatric surgery rapidly increases circulating FGF19 in both rodents and humans [218, 219]. Moreover, post-VSG/RYGB bile acid and FGF19 levels are predictive of improvements in diabetic outcomes [220]. Finally, VSG performed in FGF15 knockout mice reduces body weight but fails to improve blood glucose [221]. However, the authors of this study are careful to point out that there are caveats regarding the differences between FGF15 and FGF19. In contrast to FGF19, high circulating levels of FGF15 do not correspond to improvements in blood glucose or pancreatic ß-cell mass [222]. These caveats are not particularly detrimental to the theory, although clinical trials in humans are needed. Together,

these data suggest that bariatric surgery improves blood glucose by increasing circulating FGF19 secondary to an increase in bile acid secretion.

1.3.4.2 FGF21

FGF21, another member of the endocrine FGFs, shares a number of similarities with FGF19 regarding metabolic effects and receptor activity. However, there are several important differences as well. FGF21 was first discovered during a screen for new FGFs in a mouse embryo cDNA library [223]. Kharitonenkov et al. then showed that FGF21-transgenic mice were resistant to diet-induced obesity and exogenous FGF21 lowered plasma glucose and triglycerides in ob/ob and db/db mice [224]. Subsequent studies found that FGF21 was effective at lowering body weight, blood glucose, insulin, and triglycerides as well as improving LDL/HDL cholesterol balance in rodent and primate metabolic models [224-227].

FGF21 profoundly increases insulin sensitivity. Acute injection of FGF21 decreases blood glucose and increases insulin sensitivity in ob/ob mice and DIO mice [228]. Moreover, chronic FGF21 (3-6 weeks) lowers HGP and improves insulin-stimulated glucose uptake in several tissues [229]. It is likely that FGF21 acts in roughly the same target tissues as FGF19, since FGF19 and FGF21 require the presence of ß-klotho and have similar FGFR affinities [131]. Consistent with this, FGF21 stimulates ERK phosphorylation in the liver, WAT, and BAT [164, 230]. Moreover, ICV FGF21 into DIO rats increases insulin sensitivity by increasing insulin-induced suppression of HGP [231]. Although the antidiabetic effects of ICV FGF21 are broadly similar to FGF19, ICV FGF21 also increased

food intake. This suggests that even the small differences in FGFR affinities between FGF19 and FGF21 are sufficient to cause opposite effects.

Interestingly, the physiological actions of FGF21 run somewhat contrary to those observed with pharmacological doses. FGF21 is released during prolonged fasting and regulated by PPARα, a nuclear fatty acid sensor [171]. PPARα is a crucial component of the starvation response. PPARα-KO mice show impaired hepatic fatty acid metabolism but this phenotype can be partially rescued with exogenous FGF21 [171]. FGF21 is also heavily induced by a low carbohydrate, high fat “ketogenic” diet [232]. Additionally, transgenic mice with consitutively increased FGF21 show increased hepatic gluconeogenesis, fatty acid metabolism, and ketogenesis [229].

FGF21 also contributes to both increases and decreases of body temperature, depending on the circumstance. FGF21 is implicated in the mouse torpor response. Torpor is a phenomenon where starvation leads to decreased physical activity and body temperature in an attempt to conserve energy [233]. FGF21 transgenic mice display an increase in extrapancreatic lipases – a sign of torpor [234]. 24-h fasted FGF21 transgenic mice present with a 10°C drop in body temperature along with a substantial decrease in physical activity [171]. FGF21 is also part of the cold adaptation response. Cold ambient temperature induces FGF21 in BAT [235, 236]. Exogenous FGF21 stimulates the expression of UCP-1 and deiodinase-2 (thermogenic genes) in BAT and UCP-1 in WAT [226, 237]. It is not entirely known how FGF21 contributes to both increases and decreases in

body temperature but it is hypothesized that the differences in effects can be explained by target tissue and energy balance state.

1.3.4.3 FGF1

Although FGF1 is not considered an endocrine FGF, it produces some of the most potent and lasting metabolic effects known of any molecule. FGF1 is produced in many tissues but is found primarily in the brain, kidney, heart, and lung [168]. Within the CNS, the highest expression of FGF1 is found in the spinal cord and brain stem although most areas surveyed showed at least moderate expression. FGF1 is well known to participate in would healing, neurogenesis, angiogenesis, and development. Despite this, FGF1 knockout mice are viable and do not display an apparent deficiency in these processes [238, 239]. However, FGF1 seems to be involved in the response to aberrant energy intake, since FGF1-KO mice show pronounced hyperglycemia and insulin resistance when fed a HFD [191].

FGF1 was the first FGF that was demonstrated to be involved in central regulation of food intake. Ependymal cells lining the third ventricle were shown to release FGF1 (then known as acidic FGF or aFGF) in response to an increase in circulating glucose after feeding [240]. The authors then found that ICV FGF1 dose-dependently suppressed food intake. As discussed previously in Chapter 1.3.2, FGF1 is a member of the canonical FGF family. As such, in physiological situations, FGF1 acts in an autocrine or paracrine manner due to HSPG binding. When FGF1 is secreted from ependymal cells, FGF1 acts locally within the lining

of the third ventricle to excite tanycytes and hypothalamic astrocytes [240-243]. When FGF1 is administered to the third ventricle, feeding suppression is sustained for 24 h but is greatest within 2-6h [242-244]. Interestingly, internalized radioactive FGF1 is observed in neurons at 18 h, not 5 h, after ICV administration [245]. This suggests that the stronger initial phase of FGF1-mediates food intake suppression is mediated through actions in astrocytes where the later phase may be mediated by direct actions on neurons.

The glucose-lowering effect of FGF1 was only recently discovered but has garnered attention due to the magnitude and duration of effects. A single ICV injection of FGF1 was significant to normalize blood glucose for at least 17 weeks in ob/ob mice [246]. The authors of this study further tested this paradigm in db/db and DIO + low dose streptozotocin mice as well as Zucker diabetic fatty (ZDF) rats and found similar results. Similar to previous studies, the authors found that ICV FGF1 activated hypothalamic tanycytes. The peripheral mechanism for this action is not completely understood but appears to involve several tissues. The authors found that ICV FGF1 increased glucose clearance rate and basal circulating lactate. This implies an increase in metabolism of glucose to lactate similar to the mechanism proposed for FGF19. However, the authors also found an increase in hepatic glycogen content, implying increased rates of glycogen storage. Finally, the authors found that skeletal muscle glucose clearance was increased.

The findings above inspired a string of subsequent studies by the same research group aimed at identifying the effects of ICV FGF19. First, pERK staining was performed after ICV FGF1. This identified the hypothalamic arcuate nucleus-

median eminence as a prime target [247]. Direct parenchymal injections of low dose FGF1 were sufficient to cause >3 week remission of hyperglycemia whereas the same dose injected into other hypothalamic nuclei failed to produce an effect. In another study, the authors identify multiple key details about the peripheral response [248]. The authors show that ICV FGF1 delays the onset of ß-cell dysfunction in ZDF rats and increases hepatic glucose uptake through a twofold increase in liver glucokinase activity.

The next study from this group showed that perineuronal nets are necessary for the effect of ICV FGF1 [249]. Perineuronal nets are an extracellular matrix subtype that surrounds certain neurons and greatly influences their excitability. The authors show that enzymatic digestion of the perineuronal nets surrounding the arcuate median eminence shortens the duration of the antidiabetic effect of ICV FGF1. In the most recent paper, the research group identifies the cell types affected by ICV FGF1 via single cell transcriptomic analysis [250]. As previously suggested, these findings showed that ICV FGF1 preferentially activated non-neuronal populations with tanycytes and ependymal cells dominating the early response and oligodendrocytes dominating the later response. Together, these data suggest that ICV produces a potent and long lasting response through several central and peripheral mechanisms. The duration and potency of the effects indicate that central FGF1 signaling may be a promising and potentially paradigm-shifting drug development candidate.

1.3.5 FGF Receptors

There is an enormous body of research identifying FGFRs and their functions. What follows will serve as a brief survey of FGFR discovery and function. FGFR1 was first discovered by crosslinking a radioactive variant of FGF2 in fractions of chicken embryo membrane [251]. The receptor was sequenced using a trypsin degradation and subsequent matching to a cDNA library. FGFRs 2-4 were discovered using homology based cloning against FGFR1[252-256]. FGFRs 1-3 also display two alternative splicing variants (termed IIIb and IIIc) that greatly affect ligand binding affinities [257-261]. Thus, there are seven total FGFRs. The actions of FGFs are dictated in part by their receptor affinities and FGF1 is the only known FGF that activates all FGFR subtypes [131]. FGFR splice variation is a key regulator of organogenesis and limb formation. For example, mesenchymal tissue expresses IIIc variants of FGFR1 and FGFR2 which are most often activated by epithelial-derived FGFs [262, 263]. Conversely, epithelial tissues express IIIb FGFR splice variants, which are most often activated by mesenchymal-derived FGFs [264, 265]. This reciprocal signaling pattern is important for the spatial patterning of structures such as the lung, limb buds, and skin.

FGFRs are tyrosine kinase receptors and, as such, signal through receptor dimerization, leading to trans/autophosphorylation of tyrosine residues [266]. Once the receptor dimer is activated, it recruits four major intracellular signaling pathways by phosphorylating certain adaptor proteins. The major signaling pathways are: RAS-MAPK, PI3K-AKT, PLCγ, and STAT (1,3,5). Activation of the

RAS-MAPK pathway by FGFRs leads to induction of the MAP kinases ERK1/2. JNK, and p38 [267-271]. As noted elsewhere in this document, measurement ERK1/2/ phosphorylation is the primary method by which researchers confirm FGFR engagement. FGFR activation of the PI3K-Akt pathway leads to inactivation of FOXO1 and activation of mTOR complex 1. Both of which serve pro-survival/proliferation, anti-apoptotic functions [272]. FGFR phosphorylation of PLCγ hydrolyzes PIP_2, leading to IP_3 and DAG. This leads to increased intracellular calcium release and activation of protein kinase C. Finally, FGFR phosphorylation of STAT (1,3,5) leads to the activation of many target genes which play roles in cancer, inflammation, and numerous other processes [273].

2 Materials and Methods Summary

2.1 Animals

Adult (3-12) week old male and female GIN mice (FVB-Tg (GadGFP) 4570Swn/J; Jackson Laboratory) were used for all experiments. These mice express GFP in somatostatin-expressing GABA neurons, which allows for easier targeting of specific subpopulations of neurons. This property was of no use for the experiments in Chapter 3, as the neurons targeted (DMV) are cholinergic. However, it was expected that further experiments were to be performed in the NTS (Chapter 4) and using the same mouse model throughout the project allows for better comparability of results. Using this model is crucial for targeting glutamatergic NTS neurons. Most experiments were performed in both normoglycemic and hyperglycemic mice. Hyperglycemic mice were produced using streptozotocin (STZ) to produce a model of Type 1 diabetes (T1DM). All procedures and experiments were approved by the University of Kentucky Institutional Animal Care and Use Committee.

2.2 Brain Slice Preparation

Mice were anesthetized with isoflurane inhalation to effect (i.e. lack of foot pinch response) and decapitated. The brain was rapidly removed and submerged in ice-cold, oxygenated (2-4°C; 95% O_2/5% CO_2) artificial cerebrospinal fluid (ACSF) composed of (in mM): 124 NaCl, 3 KCl, 26 $NaHCO_3$, 1.4 NaH_2PO_4, 11 glucose, 1.3 $CaCl_2$, and 1.3 $MgCl_2$. The hindbrain was mounted to a sectioning

stage and coronal brainstem slices (300 μm) were cut using a vibratome (Series 1000; Technical Products International, St. Louis, MO). Slices were transferred to a holding chamber and incubated for 1 hour in warmed (30-33°C), oxygenated ACSF. For experiments, a single slice was transferred to the recording chamber on a fixed-stage, upright microscope (BX51WI; Olympus, Melville, NY) and continuously superfused with warmed (30-33°C) ACSF, identical to the slicing ACSF except when drugs were added, as described.

2.3 Electrophysiological Recordings

Whole-cell, patch-clamp recordings were performed under visual control using infrared illumination and differential interference contrast (i.e., IR-DIC) optics. Glass recording pipettes (1.65 mm OD, 1.2 mm ID; King Precision Glass, Claremont, CA) were filled with a solution containing (in mM): 130 K-gluconate (or Cs-gluconate), 1 NaCl, 5 EGTA, 10 HEPES, 1 $MgCl_2$, 1 $CaCl_2$, 3 KOH, 2 Mg-ATP; pH=7.2–7.3, adjusted with 5M KOH (or CsOH). In some experiments, Cs^+ was used as the primary cation charge carrier in the recording pipette, which prevents K^+ current-dependent drug effects. Open tip resistance was 3-5 MΩ; seal resistance was 1-7 GΩ. For cell-attached recordings, pipettes were filled with 150 mM NaCl. Neuronal activity was recorded using a Multiclamp 700B amplifier, Digidata 1440A digitizer, and pClamp 10.6 software (Molecular Devices, Axon Instruments, Sunnyvale, CA). Data were recorded at 20 kHz and filtered at 3 kHz.

2.4 Drugs Used for Electrophysiology Experiments

All drugs used for electrophysiology experiments and their respective concentrations were: Fibroblast growth factor 19 (FGF19; 230 pM; ProspecBio, Ness Ziona, Israel), tetrodotoxin (TTX; 2 μM; Alomone Labs, Jerusalem, Israel), kynurenic acid (KYN; 1 mM; Sigma-Aldrich), 4-aminopyridine (4-AP; 5 μM; Sigma-Aldrich), tetraethylammonium chloride (TEA; 10 μM; Sigma-Aldrich), picrotoxin (100 μM; Alomone Labs), and 4-Methoxy-7-nitroindolinyl-caged-L-glutamate (MNI caged glutamate; 250 μM; Tocris/BioTechne, Minneapolis, MN, USA).

2.5 Statistical Analysis

Recordings were analyzed using pClamp 10.6 (Axon Instruments), Minianalysis 6.0.7 (Synaptosoft, Decatur, GA), and Prism 8 (GraphPad Software, San Diego, CA). Within-cell analysis of multi-event recordings (e.g. EPSCs before and after drug application) was performed using the two-sample Kolmogorov-Smirnov (K-S) test. Grouped analyses were performed using a Student's T-test, Wilcoxon matched pairs test, or 1-way ANOVA, as appropriate. In vivo glucose measurements were analyzed using a repeated-measures 2-way ANOVA with Tukey multiple comparisons test. Significance was set at $p<0.05$ for all analyses.

3 FGF19 acts in the hindbrain to lower blood glucose concentration and alter excitability of dorsal vagal motor neurons in hyperglycemic mice

3.1 Introduction

Fibroblast growth factor 19 (FGF19) is a post-prandially released hormone that is closely linked to metabolic homeostasis. When administered to the lateral or 3rd cerebral ventricles (ICV), FGF19 improves insulin sensitivity, decreases food intake, and decreases blood glucose concentration in an insulin-independent fashion in both type I and type II diabetes models [198, 203]. Autonomic or neuroendocrine mechanisms have been proposed to mediate these effects [197, 198, 202]. While previous studies have focused on the effects of FGF19 in the hypothalamus, studies identifying the direct actions of FGF19 in the brainstem dorsal vagal complex (DVC), the primary parasympathetic regulatory center, have not been performed.

The DVC is principally comprised of the area postrema, nucleus tractus solitarius (NTS), and dorsal motor nucleus of the vagus (DMV). Vagal afferents convey viscerosensory information to second-order sensory neurons in the NTS, which integrate this information with neural input from other brain areas and effects of humoral factors. NTS neurons make excitatory and inhibitory connections with DMV motor neurons, whose axons comprise the efferent vagus nerve and regulate visceral homeostatic processes that regulate blood glucose concentration [37, 44, 48, 71, 274-276].

The DVC contains fenestrated capillaries that allow diffusion of humoral components, potentially including peptides like FGF19, which might typically be excluded by the blood-brain barrier [56, 69]. DVC neurons respond to changing glucose concentration as well as several metabolic hormones, including leptin, insulin, glucagon, and GLP-1 [50, 70, 72, 79, 80]. Importantly, FGF receptors 1 and 3 (FGFR1 and FGFR3) and β-klotho (an obligate co-receptor) are expressed in the DVC, which suggests that DVC neurons participate in endogenous FGF signaling [277-279]. Manipulation of neuronal activity in the DVC is directly linked to changes in blood glucose concentration [44, 48]. Thus, alteration of neuronal activity in this area by FGF19 could contribute to regulation of systemic blood glucose. This study tests the hypothesis that FGF19 affects neural excitability in the DVC to lower blood glucose concentration. Identifying antidiabetic effects of FGF19 in the brainstem will improve understanding of how blood glucose can be regulated via central mechanisms.

3.2 Research Design and Methods

3.2.1 Animals

Experiments were performed on juvenile (3-8 weeks old) male and female FVB mice [FVB-Tg(GadGFP)4570Swn/J, FVB; The Jackson Laboratory, Bar Harbor, ME] housed in the University of Kentucky Division of Laboratory Animal Resources facilities under normal 14:10 light-dark conditions with food (Teklad 2018) and water available ad libitum, except where noted. Roughly equal numbers

of males and females were used and results from both sexes were aggregated. The University of Kentucky Animal Care and Use Committee approved all animal procedures.

To induce necrosis of insulin-secreting pancreatic ß-cells, mice were fasted for 6 hr prior to receiving an intraperitoneal injection (i.p.; 0.15 mL) of either citric acid vehicle (CA; 0.1 M) or streptozotocin in CA (STZ; 200mg/kg; Sigma-Aldrich, St. Louis, MO). After injection, mice were returned to their home cages. Blood glucose was monitored by tail lance (Nova Max Plus, Nova Diabetes Care, Billerica, MA), and animals were used for experiments after ≥5 days (range: 5-19 days) of sustained hyperglycemia (≥300mg/dL) [280, 281]. Similar periods of continuous hyperglycemia have been associated with persistent changes in intrinsic and synaptic properties of NTS and DMV neurons [280-285]. Mice with sustained hyperglycemia after STZ injection were considered a model of early type 1 diabetes mellitus (T1DM).

3.2.2 Intracranial Injection

Fasted mice (2 hr) were anesthetized using isoflurane (5% induction, 3% maintenance) and placed in a stereotaxic frame. Mice were kept on a heating pad during surgery to prevent hypothermia. The skull was exposed using a midline incision, and a ~2 mm diameter midline craniotomy was made 2mm posterior to lambda. Vehicle (VEH; 1 µL, PBS) or FGF19 (3 µg) in VEH was delivered to the fourth ventricle (4V) using a 5 µL syringe equipped with a 26 gauge flat-tipped needle (Hamilton, Reno, NV) over a period of 10 min. The needle was allowed to

stay in place for 3 min before withdrawing. After surgery, mice were returned to their home cage and given buprenorphine (0.1 mg/kg, analgesic). Mice recovered rapidly from surgery and resumed normal feeding behavior within 10 minutes of anesthesia withdrawal. Blood glucose was measured 30 min prior to and at 10 min and 6, 12, and 24 hr after 4V injection. The first post-surgery analysis time point (6hr) was chosen to allow for sufficient time to recover from surgery. Similar experiments were performed with the addition of (-)-scopolamine methyl bromide (methylscopolamine; MSA; 1 mg/kg; i.p) to block peripheral muscarinic receptors and consequent parasympathetic output [44]. MSA was administered 30 minutes prior to and every 2 hours after surgery until the conclusion of the experiment (6hrs post-surgery).

3.2.3 Electrophysiology

For complete methods, see general methods in Chapter 2. Seal resistance was typically 1-5 GΩ measured using square voltage steps applied through the recording pipette at 100 Hz. Acceptable series resistance was considered to be <25 MΩ (range=3.48-23.57 MΩ; mean=12.88±0.32 MΩ) and was regularly monitored; recordings were discarded if series resistance or cell capacitance changed by ≥ 20% during recording.

FGF19 (ProspecBio, Ness Ziona, Israel) was bath applied at 230 pM. This concentration was shown to stimulate approximately half-maximal glucose uptake and phosphorylated extracellular signal-related kinase (pERK) induction in cell culture assays [286]. FGF19 was applied only once per slice to prevent the

influence of potential long-term effects. Added to the ACSF for specific experiments were the following: tetrodotoxin (TTX; 2 μM; Alomone Labs, Jerusalem, Israel), kynurenic acid (KYN; 1 mM; Sigma-Aldrich), 4-aminopyridine (4-AP; 5 μM; Sigma-Aldrich), tetraethylammonium chloride (TEA; 10 μM; Sigma-Aldrich), and picrotoxin (100 μM; Alomone Labs). Incubation time for FGF19 was 5 min; antagonists or channel blockers were applied for ≥10 min prior to and during agonist application.

DMV neurons were identified by their morphology (>20 μm soma width, multipolar) and location in the slice [35, 55]. Once in whole-cell configuration, neurons were held near the resting membrane potential for 10 min to allow equilibration of the pipette solution and cytoplasm. Voltage values were corrected post-hoc to account for the liquid junction potential (-15 mV). Excitatory post-synaptic currents (EPSCs) were recorded at a holding potential of -85 mV and inhibitory post-synaptic currents (IPSCs) were recorded at a holding potential of -15 mV. For event-based recordings (e.g., action potentials, EPSCs), 3 min of continuous activity (typically 300-3000 events) was examined. In these recordings, neurons were rejected if the initial event frequency was less than 0.4 Hz to ensure an adequate number of events for analysis. Input resistance (R_{in}) was measured in current-clamp mode from responses to 500 ms current steps ranging from -20 to 0 pA in 5 pA increments; R_{in} was calculated as the slope of the line that best fit these points using linear regression. A peptide-induced change in input resistance of more than 20% was considered responsive.

Potassium currents were measured in neurons voltage-clamped at -75 mV using a voltage step protocol. The protocol consisted of a 500 ms step to -125 mV, followed by a 3000 ms depolarizing step to the test potential, after which the cell was returned to -75 mV. The test potentials ranged from -75 mV to +35 mV in 10 mV increments. Peak current was measured at the first 50 ms of the depolarizing step and steady-state current was measured over the last 500 ms of the step, once the current had saturated. Peak values were recorded as the difference between peak and steady-state amplitudes within the same step. When the peak current was blocked (i.e. 4-AP or intracellular Cs^+), only the steady-state value was measured.

3.2.4 Immunofluorescence

DMV neurons were recovered by staining for biocytin (0.2% added to the internal solution; Sigma-Aldrich). After recording, brainstem slices were fixed overnight in 4% paraformaldehyde in 0.15M phosphate buffer. Slices were rinsed 3 times with 0.01 M phosphate buffered saline (PBS; Sigma-Aldrich) and immersed in avidin conjugated to AMCA Avidin-D (1:400; Vector Laboratories) in PBS containing 1% Triton X-100 for 3-4 hr at room temperature. Slices were then rinsed three times with PBS and then visualized to identify slices that contained biocytin-filled neurons. Slices containing biocytin-filled neurons were placed in a 30% sucrose solution in PBS overnight for cryoprotection, sectioned on a cryostat at 20 μm thickness, and rinsed with PBS. The sections were then immersed in 5% normal goat serum in PBS for 30 minutes, then in PBS containing 1% normal goat

serum, 0.5% Triton X-100, and FGFR1 antibody (Rabbit mAB; 1:500; Cell Signaling Technologies 9740T; [287]) for 24 hr, rinsed for 15 minutes three times with PBS, and immersed in a goat anti-rabbit secondary antibody (1:400; Alexafluor 568; Invitrogen, Carlsbad, CA; [288]). Sections were washed again for 15 minutes three times with PBS and then mounted on slides and air dried, covered with Vectashield H-1000 (Vector Laboratories, Burlingame, CA), and coverslipped. Sections were visualized using epifluorescence (BX-41; Olympus) and imaged using a Spot RT camera and software (Diagnostic Instruments, Sterling Heights, MI). Final images were adjusted for brightness and contrast for illustrative clarity only. Omission of either the primary or secondary antibody resulted in no labeling (n=4).

3.2.5 Statistics and Analysis

Recordings were analyzed using pClamp 10.6 (Axon Instruments), Minianalysis 6.0.7 (Synaptosoft, Decatur, GA), and Prism 8 (GraphPad Software, San Diego, CA). Within-cell analysis of multi-event recordings (e.g. EPSCs before and after drug application) was performed using the two-sample Kolmogorov-Smirnov (K-S) test. Grouped analyses were performed using a Student's T-test, Wilcoxon matched pairs test, or 1-way ANOVA, as appropriate. In vivo glucose measurements were analyzed using a repeated-measures 2-way ANOVA with Tukey multiple comparisons test. Significance was set at $p<0.05$ for all analyses.

3.3 Results

3.3.1 Hindbrain application of FGF19 decreases blood glucose concentration in hyperglycemic mice via a parasympathetic mechanism

To determine whether FGF19 alters blood glucose concentration by interacting with the dorsal hindbrain, FGF19 (3 µg) was administered via 4V infusion in fasted control or STZ-treated mice with sustained (≥5 days), continuous hyperglycemia (i.e., T1DM mice). Blood glucose concentration was measured 2 hr before injection (i.e., before fasting) and at 10 min, 6 hr, 12 hr, and 24 hr after 4V administration. In control mice, FGF19 did not significantly alter blood glucose concentration at any time point after injection, compared to vehicle (VEH; $n = 12$; $p > 0.05$; Figure 3.1A). In T1DM mice, FGF19 significantly decreased blood glucose concentration at 6 and 12 hrs post-4V administration, compared to VEH injection (6hr: VEH, 577.17 ± 21.273 mg/dL; FGF19, 349.66 ± 33.98 mg/dL; $n = 12$; $p < 0.01$; 12hr: VEH, 577.67 ± 18.45 mg/dL; FGF19, 353.00 ± 41.763 mg/dL; $n = 12$; $p < 0.01$; Figure 3.1A). Blood glucose returned to pre-injection concentration by the 24-hour time point and was not statistically significant relative to VEH ($p > 0.05$). FGF19 also decreased the post-injection glucose area under the curve (AUC) in T1DM mice (VEH, 13,588 ± 467 mg•hrs/dL; FGF19, 9576 ± 544 mg•hrs/dL; $p < 0.0001$; Figure 3.1B). FGF19 did not significantly alter AUC in control mice (VEH, 4170 ± 166 mg•hrs/dL; FGF19, 4233 ± 99 mg•hrs/dL; $p > 0.05$). FGF19 infusion into 4V therefore significantly reduced blood glucose concentration in hyperglycemic, but not normoglycemic mice.

Since 4V administration of FGF19, but not VEH, significantly reduced blood glucose concentration in T1DM mice, the involvement of parasympathethic output in the response was determined in a cohort of T1DM mice that were pre-treated with MSA (1 mg/kg; i.p.) prior to FGF19 application (Figure 3.1C; n = 5). MSA blocks peripheral muscarinic receptors mediating parasympathetic output to the viscera, but does not cross the blood-brain barrier to block central muscarinic receptors [289]. MSA may also prevent activation of sympathetic superior cervical ganglion neurons [290] and sympathetic activation can be associated with an increase in blood glucose concentration [291]. Considering this, a peripheral sympathetic blockade might be expected to decrease blood glucose. However, pretreatment with MSA in fasted T1DM mice was not found to significantly alter blood glucose concentration (Fasted, 544 ± 20.1 mg/dL; Fasted+MSA, 558 ± 35.7 mg/dL; n = 5; $p > 0.05$; Figure 3.1C1). The effect of 4V administration of FGF19 on blood glucose was abolished in mice pre-treated with MSA ($p > 0.05$; Figure 3.1C), indicating that the glucose-lowering effects of 4V infused FGF19 were most likely mediated by parasympathetic activity.

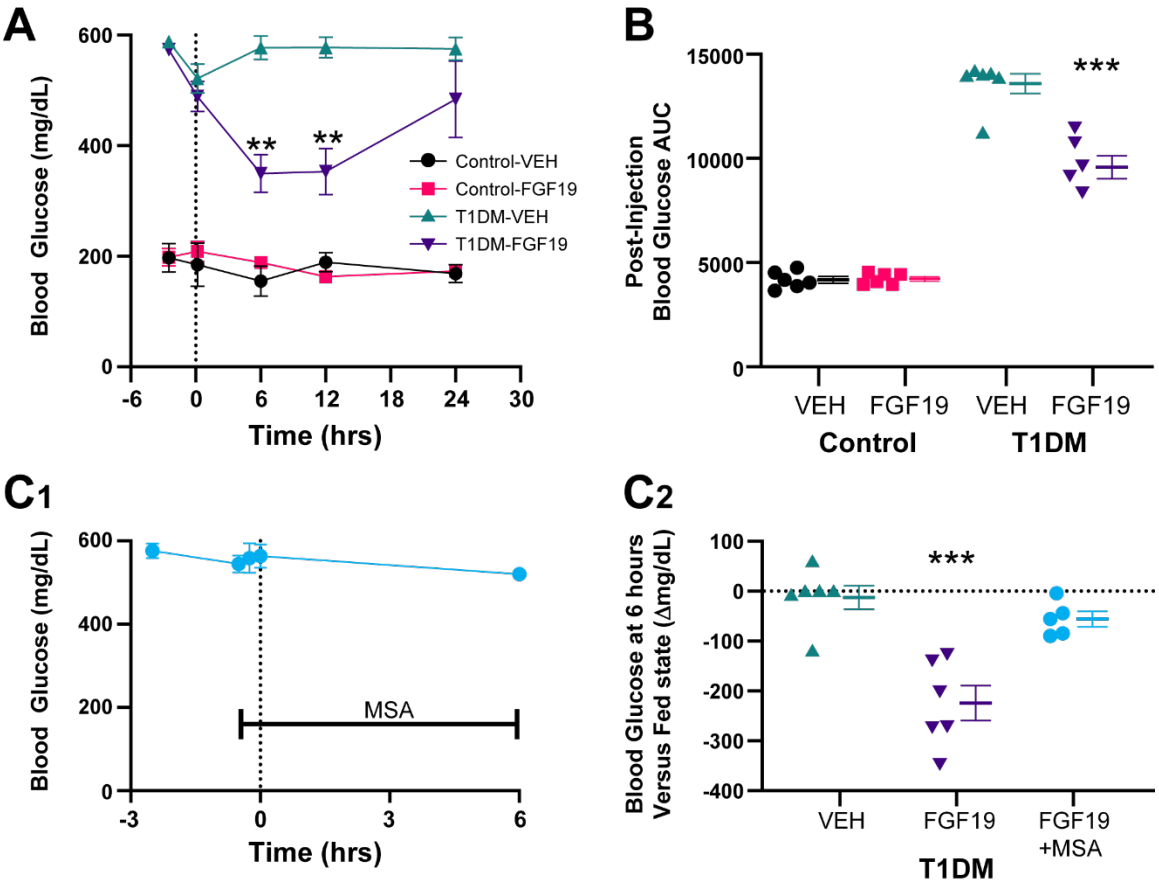

Figure 3.1. Hindbrain application of FGF19 decreases blood glucose concentration in diabetic mice through a parasympathetic mechanism.

(A) Blood glucose concentration measured 2 hours before injection (before fasting), and at 10 minutes, 6 hours, 12 hours, and 24 hours after fourth ventricle microinjection of VEH (1 μL PBS) or FGF19 (3 μg in VEH) in normoglycemic (control) and hyperglycemic mice with type 1 diabetes mellitus (T1DM). Asterisk indicates significance versus VEH for T1DM mice (**$p < 0.01$; $n = 24$; repeated measures 2-way ANOVA with Tukey's multiple comparison test). **(B)** Post-injection blood glucose area under the curve values calculated for the data shown in A. Asterisk indicates significance versus VEH (***$p < 0.001$; $n = 24$; 1-way ANOVA). **(C1)** Blood glucose concentrations measured at -2.5 hrs (fed), -30

minutes (fasted), -15 minutes (after MSA injection), 0 minutes, and 6 hours in relation to FGF19 injection **(C2)** Change in blood glucose from fed state to 6-hour time point. Pretreatment with systemic methylscopolamine (MSA) prevented the glucose lowering effect of FGF19. VEH and FGF19 group data were calculated from A. Asterisk indicates significance versus VEH (***$p < 0.001$; $n = 17$; unpaired t-test).

3.3.2 Differential effects of FGF19 on synaptic excitability

Whole-cell patch-clamp recordings were made from DMV neurons in acutely prepared brainstem slices to assess the effects of FGF19 on excitatory synaptic transmission. DMV neurons were voltage-clamped at -85 mV and spontaneous EPSCs (sEPSCs) were recorded while bath-applying FGF19 (230 pM; Figure 3.2). In neurons from control mice, FGF19 significantly decreased spontaneous EPSC (sEPSC) frequency in 4 out 8 neurons, determined by within-recording K-S test. Overall, mean sEPSC frequency was modestly, but significantly reduced (19%) by FGF19 (ACSF, 2.152 ± 0.44 Hz; FGF19, 1.807 ± 0.37 Hz; $n = 8$; $p < 0.05$; Figure 3.2E). There was no significant effect of FGF19 on sEPSC amplitude (ACSF, 21.45 ± 4.28 pA; FGF19, 22.91 ± 2.49 pA; $n = 7$; $p > 0.05$; Figure 3.2F).

Consistent with previous reports, sEPSC frequency was significantly greater in DMV neurons from T1DM mice than in controls ($p < 0.05$) [282, 284]. In DMV neurons from T1DM mice, FGF19 consistently and significantly increased sEPSC frequency in each of 7 neurons ($p < 0.02$; K-S test; Figure 3.2E). Mean sEPSC frequency was significantly increased by 43% in the presence of FGF19 (ACSF, 8.63 ± 1.57 Hz; FGF19, 12.33 ± 1.62 Hz; $n = 7$; $p < 0.02$; Figure 3.2E). There was no significant change in sEPSC amplitude (ACSF, 17.70 ± 2.34 pA; FGF19, 19.55 ± 3.52 pA; $p > 0.05$; Figure 3.2F). Thus, FGF19 led to a modest, but significant decrease in excitatory synaptic input to DMV neurons in slices from normoglycemic mice, but the peptide further increased the already enhanced excitatory synaptic drive to DMV neurons from T1DM mice.

To determine whether the effects of FGF19 on EPSC frequency were due to activation of receptors located on presynaptic terminals, miniature EPSCs (mEPSCs) were recorded in the presence of TTX (2 μM), a blocker of action potential-dependent synaptic activity. In control mice, there was no significant change in mean mEPSC frequency during FGF19 application (ACSF, 4.26 ± 1.00 Hz; FGF19, 4.00 ± 0.95 Hz; $n = 7$; $p > 0.05$; Figure 3.2G), although significant changes in frequency could be detected in four of seven neurons (increase, $n = 2$; decrease, $n = 2$; $p < 0.02$; K-S test). There was no significant difference in mean mEPSC amplitude (ACSF, 12.4 ± 2.51 pA; FGF19, 12.2 ± 2.39 pA; $n = 7$; $p > 0.05$; Figure 3.2H).

FGF19 also produced no significant change in overall mEPSC frequency in T1DM mice (ACSF, 7.93 ± 2.06 Hz; FGF19, 7.77 ± 2.14 Hz; $n = 7$; $p > 0.05$; Figure 3.2G). In this group, only one neuron produced a significant change of mEPSC frequency as measured by the K-S test ($p < 0.01$). Similarly, there was no significant difference in mEPSC amplitude (ACSF, 12.9 ± 1.08 pA; FGF19, 13.1 ± 1.05 pA; $p > 0.05$; Figure 3.2H). FGF19 therefore modestly decreased excitatory synaptic input to DMV neurons in control mice, but significantly increased sEPSC frequency in DMV neurons from T1D mice, and these effects were mostly prevented when action potential-dependent synaptic activity was blocked.

To assess possible effects of FGF19 on inhibitory synaptic activity, spontaneous IPSCs (sIPSCs) were recorded. No effects on sIPSC frequency were observed in control (ACSF, 4.19 ± 1.06 Hz; FGF19, 3.87 ± 1.16 Hz; $n = 5$; $p > 0.05$) or T1DM mice (ACSF, 2.72 ± 1.07 Hz; FGF19, 2.53 ± 0.96 Hz; $n = 5$; $p >$

0.05). Additionally, baseline sIPSC frequency was not significantly different between the two groups (control; 4.19 ± 1.06 Hz; T1DM; 2.72 ± 1.07 Hz; $p > 0.05$; $n = 10$). Similarly, FGF19 did not change sIPSC amplitude in control (ACSF, 29.5 ± 3.67 pA; FGF19, 25.7 ± 4.56pA; $n = 5$; $p > 0.05$) or T1DM mice (ACSF, 33.5 ± 1.74 pA; FGF19, 27.4 ± 3.56 pA; $n = 5$; $p > 0.05$). FGF19 therefore selectively modulated glutamate release in the DMV, being decreased in control and increased in T1DM mice, with no significant effect on inhibitory synaptic activity.

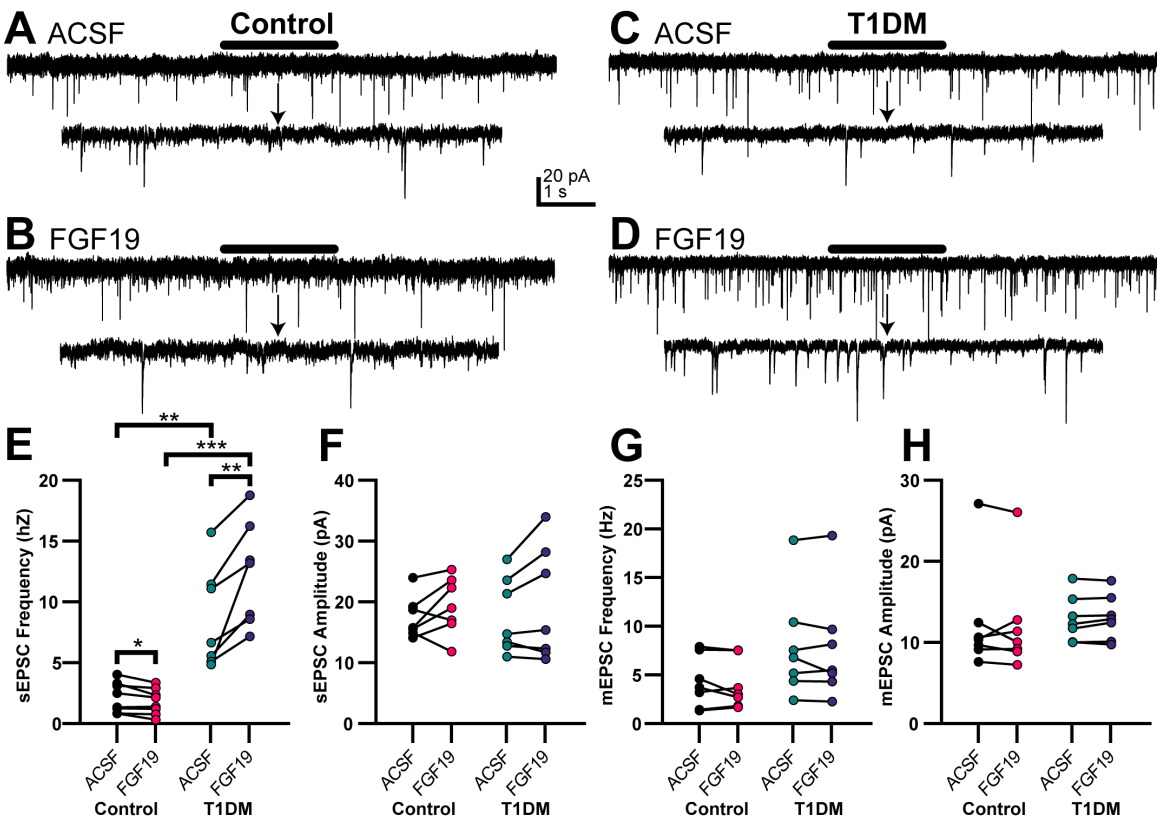

Figure 3.2. FGF19 decreases sEPSC frequency in neurons of the dorsal motor nucleus of the vagus (DMV) in slices from normoglycemic, control mice and increases sEPSC frequency in DMV neurons from hyperglycemic, T1DM mice.

(A) Voltage clamp recordings of sEPSCs in a DMV neuron from a control mouse and **(B)** after addition of FGF19 (230 pM). **(C)** Recording of sEPSCs in a DMV neuron from a T1DM mouse and **(D)** in FGF19. Lower traces indicated by arrows in **A-D** are expanded from the area indicated with a bar in the top traces in each set; all sEPSC measurements were from neurons voltage-clamped at -85 mV. **(E)** FGF19 significantly decreased mean sEPSC frequency in control mice (n = 8) and increased mean sEPSC frequency in T1DM mice (n = 7). sEPSC frequency was significantly greater in neurons from T1DM mice than from control

mice (*$p < 0.05$; **$p < 0.01$; ***$p < 0.001$). **(F)** FGF19 did not affect mean sEPSC amplitude in control ($n = 8$) or T1DM mice ($n = 7$; $p > 0.05$). sEPSCs were recorded from: Control; 2 male and 2 female; T1DM 3 male and 2 female mice. In the presence of tetrodotoxin (TTX; 2 μM), FGF19 did not affect mean mEPSC frequency **(G)** or amplitude **(H)** in control ($n = 7$; $p > 0.05$) or T1DM mice ($n = 7$; $p > 0.05$). mEPSCs were recorded from: Control; 2 male and 2 female; T1DM 2 male and 2 female mice.

3.3.3 Effects on resting membrane potential and input resistance

To confirm the presence of FGF receptors in DMV neurons, immunolabeling of FGFR1 was performed. Figure 3.3A shows an example of a biocytin filled DMV neuron and FGFR1-like immunoreactivity in the DVC. To investigate the effects of FGF19 on membrane properties of DMV neurons, input resistance (R_{in}) and resting membrane potential (RMP) were recorded in current-clamp mode in the presence of TTX (2 μM) to prevent spontaneous action potentials (Figure 3.3B-G). Neither RMP nor R_{in} differed significantly between control and T1DM mice ($p > 0.05$). In control mice, FGF19 significantly hyperpolarized the RMP whereas in T1DM mice, FGF19 did not significantly alter mean RMP (Table 1). Despite the lack of an overall effect, 7/10 T1DM neurons were hyperpolarized by >3 mV, suggesting inhibition of most neurons. In control mice, the overall effect of FGF19 on R_{in} was not significant, whereas in T1DM FGF19 significantly decreased overall R_{in} (Table 1). In DMV neurons from both control and T1DM mice, FGF19 induced a >20% decrease R_{in} in approximately half of neurons in each group. Excluding one neuron in the T1DM group that depolarized in response to FGF19, a decrease in R_{in} was always accompanied by a concomitant hyperpolarization of RMP, suggesting the opening of a channel at resting membrane potential. The predominant effects of FGF19 on RMP and R_{in} were therefore inhibitory, consisting of a membrane hyperpolarization and decrease in R_{in}, in DMV neurons from both normoglycemic and hyperglycemic mice.

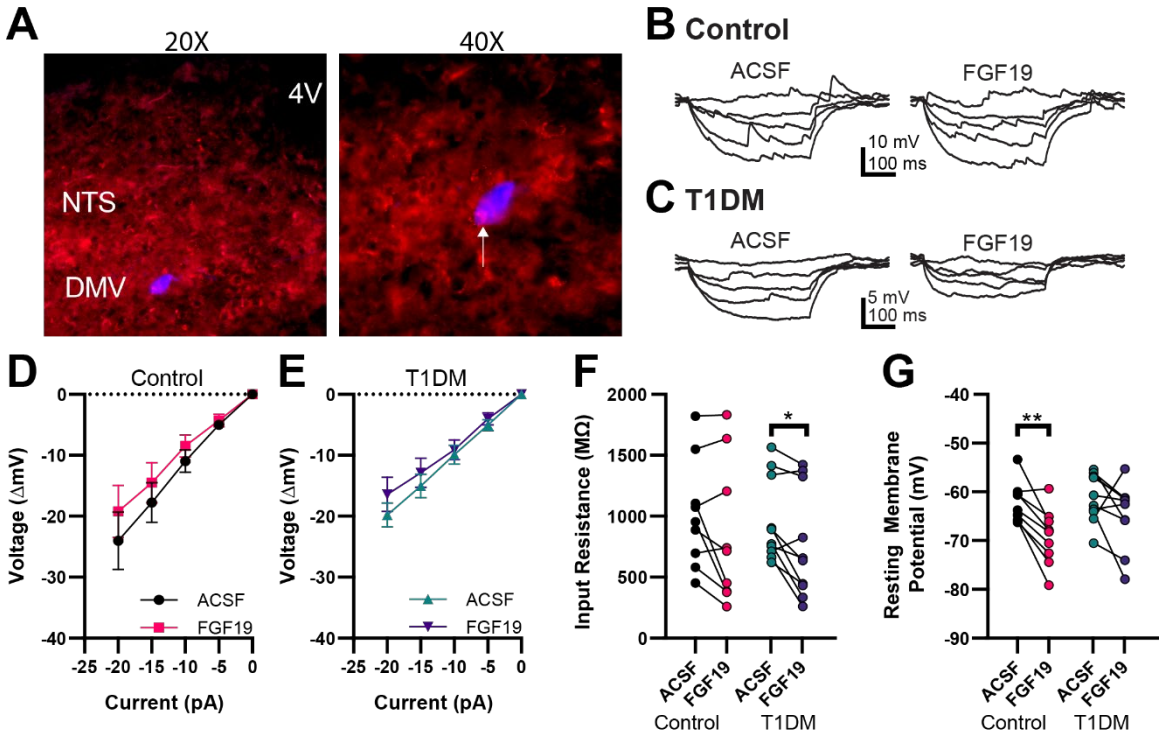

Figure 3.3. Effects on input resistance and resting membrane potential.

(A) Fluorescence images showing a recorded, biocytin-filled DMV neuron (blue) and immunofluorescence staining for FGFR1 (red) at two magnifications. Arrow indicates an area of label overlap (purple), suggestive of FGFR1 localization on the recorded DMV neuron. **(B)** Current injection recordings of DMV neurons from a control mouse and **(C)** T1DM mouse. **(D)** I-V plots for responses of DMV neurons to FGF19 application from control mice (n = 9) and **(E)** T1DM mice (n = 10). The slope of the lines in D and E reflect input resistance. **(F)** FGF19 did not alter mean input resistance in control mice (n = 9; $p > 0.05$) but significantly decreased input resistance in T1DM mice (n = 10; $*p < 0.05$). **(G)** FGF19 significantly hyperpolarized neurons from control mice (n = 9; $**p < 0.01$) but did not alter mean resting membrane potential in T1DM mice (n = 10; $p > 0.05$). All

recordings in TTX (2 μM). Recorded from: Control; 2 male and 2 female; T1DM 4 male and 2 female mice.

Table 3.1. Intrinsic membrane properties of DMV neurons in response to FGF19

	Control Mice			
	ACSF	**ACSF+FGF19**	**pval**	**n**
RMP (mV)	-62.3±1.40	-69.3±1.92	$p < 0.01$	9
R_{in} (MΩ)	1013±148	844±193	n.s.	9
Action Potential Frequency (Hz)	0.99±0.112	1.12 ± 0.171	n.s.	14

	T1DM Mice			
	ACSF	**ACSF+FGF19**	**pval**	**n**
RMP (mV)	-61.2±1.55	-64.7±2.10	n.s.	10
R_{in} (MΩ)	964±109	771±142	$p < 0.05$	10
Action Potential Frequency (Hz)	1.46±0.277	1.06±0.274	$p < 0.05$	8

3.3.4 Action potential frequency

To investigate the effects of FGF19 on spontaneous action potential current (I_{AP}) frequency, neurons were recorded in cell-attached configuration (Figure 3.4). In control mice, there was no significant change in mean I_{AP} frequency during FGF19 application (Table 1). However, I_{AP} frequency in individual neurons was significantly altered (increased, n = 6; decreased n = 4; $p < 0.02$ K-S test). In T1DM mice, there was a significant decrease in mean I_{AP} frequency during FGF19 application (Table 1). I_{AP} frequency in individual neurons was predominantly decreased (n = 7; $p < 0.02$; K-S test), with an increase in frequency in one neuron.

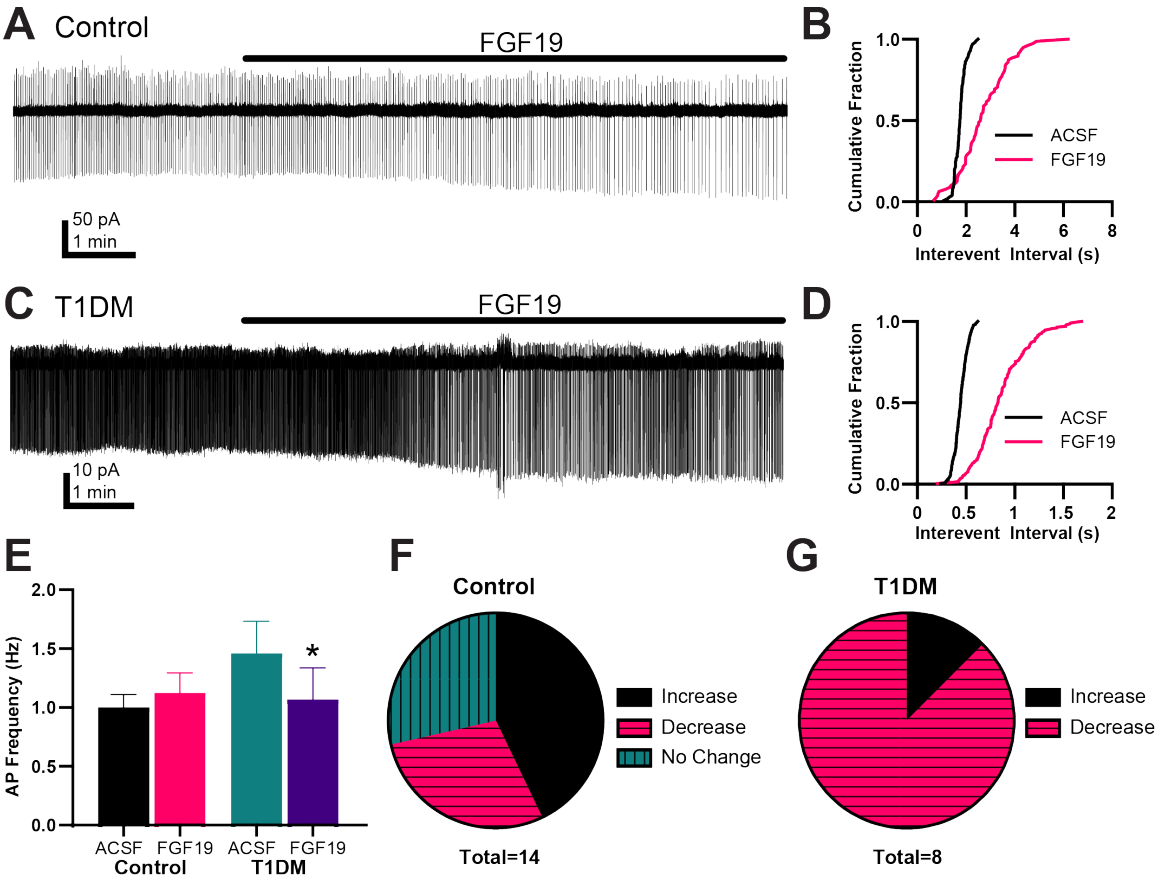

Figure 3.4. FGF19 variably affects action potential frequency.

(A) Representative traces showing effects of FGF19 on spontaneous sodium-dependent action potential currents (I_{AP}) in cell-attached recordings in a DMV neuron from a control mouse. **(B)** Cumulative probability plot of the traces in **A**. **(C**) Representative traces showing effects of FGF19 on I_{AP} frequency in a DMV neuron from a T1DM mouse. **(D)** Cumulative probability plot of the traces in **C**. **(E)** FGF19 did not alter mean I_{AP} frequency in control mice ($n = 14$; $p > 0.05$) but significantly decreased I_{AP} frequency in T1DM mice ($n = 8$; $p < 0.05$). Asterisk indicates significance versus ACSF. **(F)** Relative proportion of neurons with responses to FGF19 application in neurons from control mice indicate variable responses. **(G)** Proportions of responses in T1DM mice suggests a that FGF19 decreases I_{AP} frequency in most neurons. Recorded from: Control; 2 male and 2 female; T1DM 3 male and 2 female mice.

3.3.5 FGF19 decreases A-type K^+ current amplitude in control, but not in T1DM mice

Since inconsistent effects of FGF19 were observed on I_{AP} firing, we investigated the possibility that FGF19 altered voltage-gated K^+-current amplitude, in addition to its effects on passive membrane properties of DMV neurons. To determine the effects of FGF19 on voltage-gated K^+ current amplitudes, a step protocol was performed in voltage-clamp mode in the presence of TTX (2 μM), PTX, a $GABA_A$ receptor blocker (100 μM) and KYN, an ionotropic glutamate receptor blocker (1 mM). To either block or help isolate the A-type current, ACSF included either 4-AP, an A-type current blocker (5 mM) or TEA, a delayed-rectifier current blocker (10 mM). To adjust for any potential differences in cell size, current values were normalized to cell capacitance to yield current density (pA/pF).

In the presence of TEA, FGF19 significantly decreased the amplitude of the peak current density measured at 50 ms in DMV neurons from control mice (ACSF, 50.5 ± 6.61 pA/pF; FGF19, 38.3 ± 5.46 pA/pF; $n = 9$; $p < 0.05$; Figure 3.5). Unlike in controls, FGF19 produced no significant change in peak current density in neurons from T1DM mice (ACSF, 65.7 ± 7.22 pA/pF; FGF19, 64.8 ± 6.04 pA/pF; $n = 8$; $p > 0.05$).

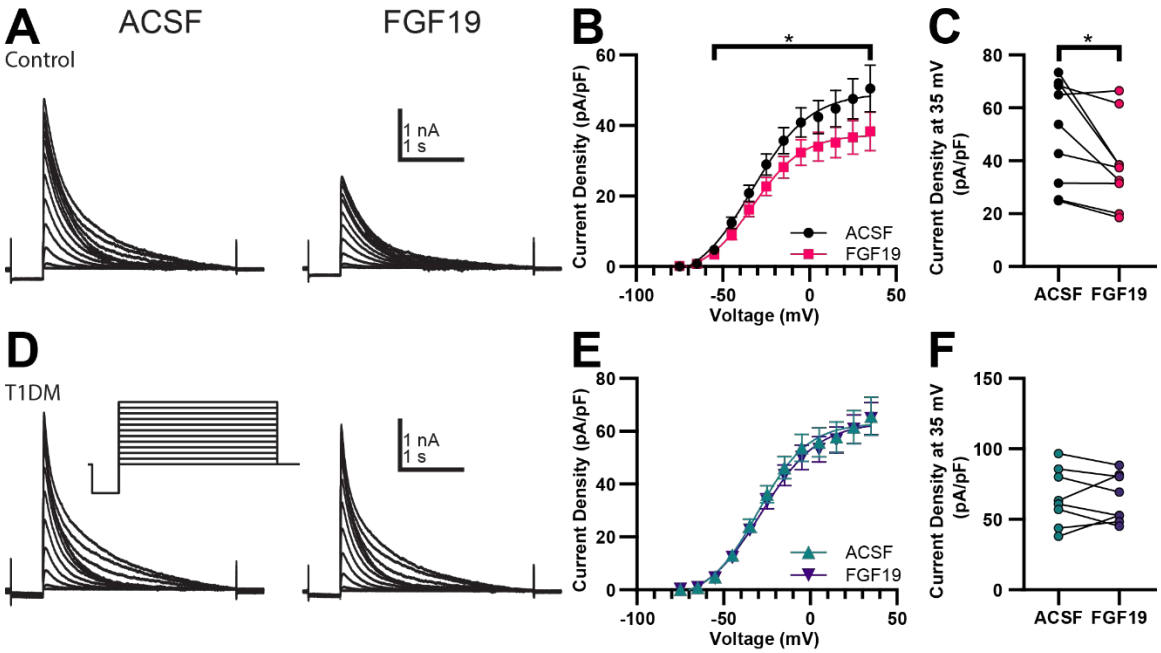

Figure 3.5. FGF19 decreases A-type K^+ current amplitude in DMV neurons from control, but not in T1DM mice.

(A) Voltage activation step recording a from control mouse in ACSF and in the presence of FGF19 (230 pM). Traces shown are peak data only (i.e. steady state current has been subtracted). **(B)** Graphed peak current density data from control mice (n = 9) indicate an FGF19-mediated reduction in peak current density at potentials at and above -45 mV (*p<0.05). **(C)** Effect of FGF19 on peak current density for the +35 mV step for individual neurons (n = 9; *p < 0.05). **(D)** Voltage activation step recording from T1DM mouse in ACSF and in the presence of FGF19. **(E)** Peak current density in DMV neurons from T1DM mice (n = 8). **(F)** The effect of FGF19 on peak current density for the +35 mV step was not significant at any potential (n = 8; p>0.05). All recordings in tetrodotoxin (TTX; 2 μM), picrotoxin (PTX; 100 μM), kynurenic acid (KYN; 1 mM), and tetraethylammonium (TEA; 10 μM). Recorded from: Control; 4 male and 3 female; T1DM 2 male and 2 female mice.

Since FGF19 only altered voltage-dependent K^+ currents in DMV neurons from control mice, additional experiments to further identify the nature of this effect were restricted to this group. The effects on FGF19 on K^+ current amplitude were blocked by 4-AP (ACSF, 106.0 ± 11.1 pA/pF; FGF19, 99.2 ± 11.6 pA/pF; $n = 6$; $p > 0.05$; Figure 3.6A-C) or when recording pipettes contained Cs^+ (ACSF, 51.7 ± 4.16 pA/pF; FGF19, 56.6 ± 3.20 pA/pF; $n = 5$; $p > 0.05$; Figure 3.6D-F). FGF19 therefore reduced the peak current amplitude of the 4-AP sensitive, putative A-type K^+ current in control, but not T1DM mice.

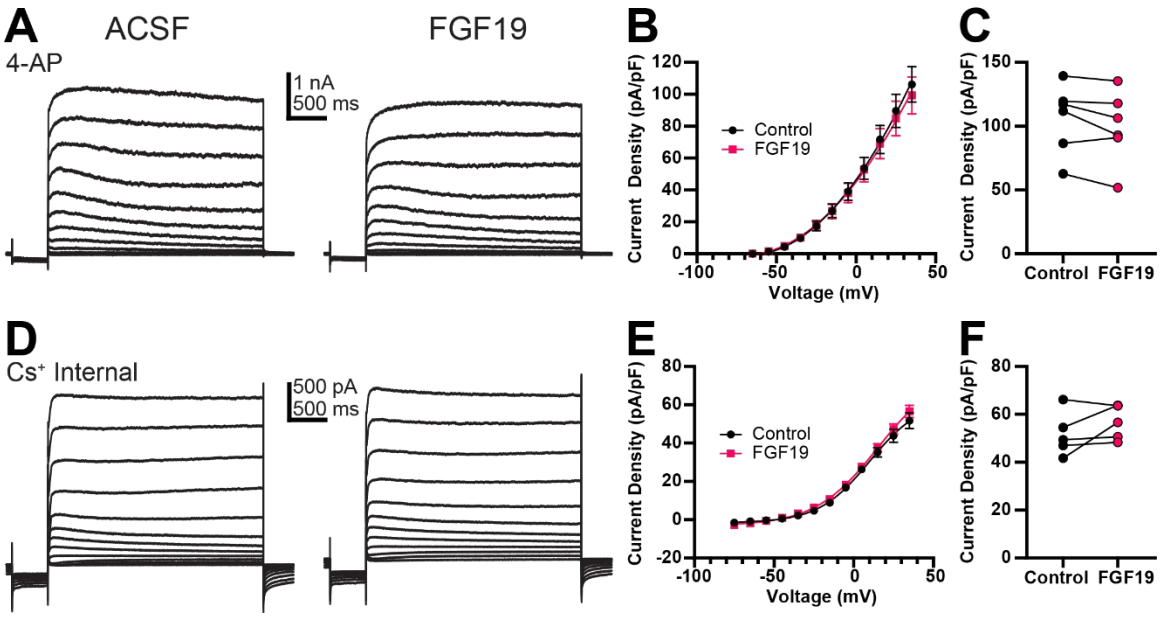

Figure 3.6. The effect of FGF19 on the A-type K^+ current in normoglycemic mice is prevented by 4-AP or intracellular Cs^+.

(A) Representative voltage activation step recording in the presence of 4-AP (5 mM). **(B)** Steady-state current density in DMV neurons from in the presence of 4-aminopyridine (4-AP; 5 μM; n = 6). **(C)** FGF19 effect on steady-state current density plotted for individual neurons from the 35 mV step in **B** (n = 6; p>0.05). 4-AP recordings were from 2 male and 1 female mouse. **(D)** Representative voltage activation step recording using a Cs^+ internal solution. **(E)** Steady-state current density in DMV neurons using a Cs^+ internal solution (n = 5). **(F)** FGF19 effect on steady-state current density plotted for individual neurons from the 35 mV step in **E** (n = 5; p>0.05). Cs^+ recordings were from 1 male and 1 female mouse. All recordings are from normoglycemic mice and performed in TTX (2 μM), PTX (100 μM), KYN (1 mM).

3.4 Discussion

This report identifies the brainstem DVC as a previously underappreciated target for the antidiabetic effects of FGF19. Previous research on the metabolic effects of centrally applied FGF19 has focused on hypothalamic circuits, since third ventricle administration led to lower blood glucose levels that were correlated with decreased plasma ACTH and suppression of AgRP/NPY neuron activity [202, 203]. The DVC contains FGFR1, FGFR3, and ß-klotho, suggesting that DVC neurons can respond to exogenous FGF and engage in endogenous FGF signaling [277-279]. Importantly, DVC neurons regulate autonomic control of HGP, food intake, and hepatic enzyme expression [44, 47, 292-294], all of which are mechanisms proposed to mediate the antidiabetic actions of ICV FGF19 [197, 198, 203]. While the findings from previous studies are consistent with the hypothesis that FGF19 regulates metabolism and interacts with hypothalamic neurons, the present data suggest that actions of the peptide in the DVC may be sufficient to produce significant effects on systemic glucose concentration under hyperglycemic conditions.

The effects of FGF on hypothalamic neurons could also function to lower blood glucose levels by signaling through the DVC and vagus nerve [47, 90]. ICV FGF19 activation of hypothalamic neurons decreases DVC c-fos expression and vagus nerve activity in response to neuroglucopenia [295]. Furthermore, some reports suggest that hypothalamic regulation of HGP works through DVC neuron activation and requires an intact vagus nerve [47, 92]. Consequently, interactions

of FGF19 with DVC circuits may provide a more direct path for FGF19-mediated antidiabetic effects.

Acute 4V administration of FGF19 produced a significant, reversible decrease in blood glucose concentration in hyperglycemic mice for at least 12 hours. Consistent with the effects of FGF19 application in the diencephalon, the glucose-lowering ability of FGF19 applied to the hindbrain was only observed in hyperglycemic mice [246, 296]. The effects on blood glucose are unlikely to the result of anesthesia or recovery from surgery, as all mice resumed normal feeding behavior rapidly after surgery and returned to baseline glucose levels, except the T1DM-FGF19 group. Diffusion of FGF19 to the hypothalamus is unlikely, as cerebrospinal fluid flows rostrocaudally and FGF19 was injected slowly into 4V to prevent backflow rostrally [297]. To wit, 4V application is often used as a substitute for direct DVC parenchymal injections [74, 85, 293, 298]. Altered activity of DMV motor neurons has been linked with blood glucose regulation, which is mediated by parasympathetic regulation of pancreatic and hepatic vagal activity [44, 48, 71]. Moreover, the effect of 4V FGF19 on blood glucose was prevented when peripheral muscarinic receptors were blocked by MSA, suggesting a parasympathetic mechanism. Previous studies did not reach a consensus regarding the mechanism by which FGF19 decreases blood glucose in diabetic mice. Taken together, they suggest that FGF19 in the brain may work by altering hepatic metabolism with no effects on insulin or glucagon levels [186, 198, 203]. However, no further investigation into this mechanism was performed here. While

insulin is unlikely to play a role due to the use of a T1DM model, we cannot rule out the potential involvement of glucagon in the response to FGF19.

A previous report found that third-ventricular FGF19 was able to decrease blood glucose concentration by >200 mg/dL in T1DM rats – similar in magnitude to the results found here - and this was associated with a 50% decrease in HGP [203]. Manipulation of DVC neuron excitability has been shown to decrease HGP by ~50% [47, 48, 92, 293], suggesting that FGF19 modulation of DVC excitability can alter HGP sufficiently to produce the decrease in blood glucose shown in Figure 3.1. Notably, the largest proportion of DMV neurons project to the stomach [29]. Since FGF19 altered excitability of most DMV neurons, this suggests effects on GI function, which may alter blood glucose indirectly and warrants further research. While this study was performed in a T1DM mouse model, similar results would likely be found in a type II diabetes (T2DM) model, since previous reports indicate that FGF19 functions independently of insulin to lower blood glucose concentration in both T1DM and T2DM models [198, 203]. The reduced insulin availability in this model of hyperglycemia is consistent with an insulin-independent effect of FGF19 acting in the DVC. The FGF19 effects in the hindbrain neurons are therefore sufficient to lower systemic glucose concentration in hyperglycemic mice.

FGF19 produced a complex set of electrophysiological responses in DMV neurons that differed as a function of disease state (i.e. presence or absence of hyperglycemia). While FGF19 modestly decreased action potential-dependent glutamate release onto DMV neurons from control mice, it produced a robust and

consistent increase in synaptic excitation of DMV neurons from T1DM mice. The FGF19-mediated effects on glutamate release are mainly due to activity of the peptide on action potential firing of neurons with intact projections to the DMV, since blockade of action potentials with TTX prevented the overall effect of FGF19 on glutamate release. Interestingly, analysis of IPSC frequency and amplitude revealed no significant effect of FGF19 on GABA release, suggesting relatively selective effects of the peptide on upstream excitatory circuits. Because intact NTS neuron projections to the DMV are contained within the slice [299], and FGFRs are present in the NTS [277, 279], it is likely that FGF19 increases activity of premotor, glutamatergic NTS neurons to affect increased synaptic excitability of vagal motorneurons in the DMV of T1DM mice, but effects on other local circuits cannot be discounted. Thus, the effects of FGF19 appear to impinge on central vagal circuitry that participates in vago-vagal reflexes, possibly including the gut-brain-liver glucose regulatory circuit [300]. Phasic glutamatergic input profoundly affects vagal motor activity in vitro [21, 37], injection of glutamatergic agonists into the DVC lowers HGP [48], and blockade of glutamate receptors in the NTS prevents vagally-mediated, reflexive modulation of hepatic gluconeogenesis [300]. Glutamate release is persistently increased in the DMV of T1DM mice, and NMDA receptor function in glutamatergic NTS neurons is enhanced [282, 284]. Glutamate system plasticity in the DVC could also underlie the differences in FGF19 effects on EPSC frequency between control and T1DM mice. Consequently, the effect of FGF19 on EPSC frequency in T1DM mice may prove to be the primary determinant of its effects on blood glucose.

The effect of FGF19 on intrinsic excitability in DMV neurons was inconsistent and modest. In control mice, FGF19 produced mixed effects on action potential firing, whereas it mainly decreased firing in T1DM mice. Most neurons from both groups displayed a decrease in R_{in} and membrane hyperpolarization in response to FGF19 application. While these effects tend to be inhibitory, FGF19 also decreased the magnitude of an A-type K^+ current in control mice. Where the decreased synaptic excitation and generally inhibitory effect on RMP and R_{in} by FGF19 in control mice suggest a decrease in cellular excitability, the decrease in A-type K^+ current might contribute to increased AP firing during periods of membrane depolarization [301]. Due to recording constraints, effects on PSCs, intrinsic membrane properties, APs, and A-type K^+ channels were recorded separately. Thus, opposing pre and post-synaptic effects were not observed within the same neuron. DMV neurons display considerable heterogeneity regarding morphological and electrophysiological properties that may also contribute to their considerable variation in response to FGF19 [53, 55]. Notably, the inhibitory effects on DMV EPSC frequency and R_{in} in control mice are shared with both leptin and insulin [49, 50]. The marked FGF19-induced increase in synaptic excitability in DMV neurons from T1DM mice suggests that this factor may underlie the differential effects of the peptide on blood glucose in T1DM mice.

It is not fully understood how DMV activity corresponds to changes in blood glucose. The increase in sEPSC frequency in DMV neurons from T1DM mice reported here and previously may represent a compensatory response to hyperglycemia [282, 284]. This suggests a model where an increase in synaptic

excitation of DMV motor neurons results in decreased blood glucose concentration. Correspondingly, microinjection of NMDA in the DVC decreases HGP [48]. This model is also consistent with our previous findings showing that increased synaptic inhibition of DMV neurons by depolarization of GABAergic afferents results in increased blood glucose in mice [44]. Here, FGF19 increased the already elevated sEPSC frequency in T1DM mice, which would be predicted to decrease blood glucose in this model.

Diabetic hyperglycemia leads to profound changes in synaptic activity and postsynaptic responsiveness in the DVC, including increased glutamate release in the DMV and increased NMDA receptor function in the NTS [282-284]. This plasticity of excitatory circuitry in the DVC may contribute to the different metabolic and neuronal responses in hyper- and normoglycemic mice. The nature of the differences in electrophysiological effects between disease groups (e.g. diabetes reversed and amplified effects on sEPSCs while abolishing effects on A-type K^+ currents) suggests that hyperglycemia may differentially regulate discrete intracellular pathways downstream from the FGFR. Indeed, FGFRs signal via MAP kinases, PLCγ, and PKC[123], all of which are also modulated by hyperglycemia/diabetes [302-304]. In addition, FGFRs signal through the PI3K-Akt pathway, which is dysregulated in the brains of diabetic rats [305]. Moreover, the insulin receptor and FGFR share several intracellular signaling pathways that likely exhibit significant crosstalk [123, 306, 307]. Since the DVC responds to insulin [50, 293] and changing glucose concentrations [70, 276], and has access to circulating insulin and glucose via local fenestrated capillaries [56], it is to be

expected that the changes in peripheral metabolism in T1DM mice would produce profound effects on FGFR signal transduction in the DVC. Thus, differential responses to FGFs between disease groups may be linked to diabetes-induced changes in the intracellular pool of signaling machinery. As such, future study is warranted to investigate this possibility.

The cellular responses of DMV neurons confirm that FGF19 modulates DMV neuron excitability, consistent with the hypothesis that FGF19 normalizes blood glucose in T1DM mice by altering autonomic output to the viscera. Despite this, it cannot be discounted that the antidiabetic effects found here could be partially mediated through interactions with other brain areas, since the NTS communicates with neurons in hypothalamic and ventral brainstem areas that regulate sympathetic and neuroendocrine functions, in addition to the DMV [90, 308, 309]. However, MSA blocked the antidiabetic actions of FGF19, suggesting a predominantly parasympathetic mechanism.

In conclusion, this study identified the dorsal hindbrain as a novel target tissue for the glucose-lowering effects of centrally acting FGF19 in hyperglycemic mice. The cellular and synaptic effects of FGF19 on DMV neurons were consistent with a parasympathetically-mediated effect on blood glucose in T1DM mice. This research highlights the importance of the DVC in FGFR-mediated glucoregulation and suggests that understanding FGF activity in central vagal circuitry may reveal new targets for brain-centered therapies to relieve diabetic hyperglycemia.

4 Fibroblast growth factor 19 increases the excitability of pre-motor glutamatergic neurons in the dorsal vagal complex of hyperglycemic mice

4.1 Introduction

Fibroblast growth factor 19 (FGF19) is an ileal-derived protein hormone that produces potent, anti-diabetic, and anti-obesogenic effects. Although early work suggested that these effects could be mediated by FGF19 acting on peripheral targets, several reports have now found that acute intracerebroventricular (ICV) administration of FGF19 may act at multiple distinct sites in the brain to regulate energy balance. Lateral ventricle administration of FGF19 increases metabolic rate [186], while 3rd ventricular administration was found to decrease food intake, lower insulin resistance, improve glucose tolerance, and reduce blood glucose concentrations in rodent models of diabetes and obesity [198, 202, 203, 217]. These findings suggest a hypothalamic mechanism since FGF19 was found to suppress AGRP/NPY activity [202] and decrease plasma ACTH [203]. However, we demonstrated that 4th ventricular administration of FGF19 also decreases blood glucose in type 1 diabetic (T1DM) mice, suggesting the hindbrain as an underappreciated target tissue for this system [51].

The brainstem dorsal vagal complex (DVC) is an important homeostatic regulatory center that tightly controls parasympathetic output in response to numerous convergent inputs, both neuronal and humoral. The DVC is principally comprised of the area postrema (AP), the nucleus tractus solitarius (NTS), and the dorsal motor nucleus of the vagus (DMV). The NTS integrates

vagal afferent, viscerosensory information with input from several brain areas, including the hypothalamus and AP [37, 67, 89, 310]. In turn, the NTS regulates neural activity in the DMV through both glutamatergic and GABAergic projections [54, 299]. Finally, DMV neurons project cholinergic outputs through the efferent vagus nerve to regulate hepatic glucose production, gastric motility, and pancreatic exocrine secretion, among other visceral regulatory functions [44, 48, 71, 274, 276, 311]. Additionally, the AP and NTS contain fenestrated capillaries that permit the passage of humoral components that may be excluded by the blood-brain barrier elsewhere [56, 69]. DVC neurons respond to many primary metabolic hormones including insulin, leptin, ghrelin, glucagon, GLP-1 [50, 72, 79, 81, 86] and importantly, FGF19 [51]. The DVC, especially the AP and NTS, contains multiple FGF receptors (FGFR) as well as ß-klotho, an obligate co-receptor [277-279], suggesting that neuronal activity in the DVC may regulate metabolic homeostatic mechanisms in response to endogenous FGF signaling.

In a mouse model of type 1 diabetes (T1DM), FGF19 consistently and robustly increased action potential-dependent excitatory synaptic transmission to the DMV [51]. This suggests that FGF19 alters the excitability of glutamatergic neurons immediately afferent to the DMV, which remain intact in the slice preparation. A likely source of these glutamatergic inputs is the NTS since the NTS to DMV connection is well documented [299, 312-314] and is open to modulation via various other peptides and neurotransmitters [49, 314-316]. Interestingly, receptor expression data suggest that the AP could also be a target for FGF19 since the AP expresses significantly more FGFR than surrounding

areas [277] and expresses more ß-klotho and FGFR2 than any other brain area, in addition to high levels of FGFR1 and FGFR3 [278]. Moreover, glutamatergic AP neurons project extensively to the NTS and DMV [68]. Taken together, these findings suggest that FGF19 may act on intrinsic DVC circuitry to modify synaptic input to the DMV and consequently modulate vagally-mediated glucoregulation.

This study tests the hypothesis that FGF19 increases excitatory neurotransmission in the DVC by altering excitability of NTS and AP neurons. In addition to functioning within local DVC circuits, the NTS and AP communicate bidirectionally with other brain areas thought to be involved in regulating energy metabolism [67, 88, 89]. Thus, FGF19-mediated alteration of excitability in these areas is likely to have wide-reaching metabolic effects by modulating vago-vagal circuit dynamics as well as influencing other brain areas that regulate ingestive behaviors and energy balance through autonomic or neuroendocrine means.

4.2 Materials and Methods

4.2.1 Animals

All mice used for experiments were juvenile (3-8 weeks old) male and female FVB mice (FVB-Tg(GadGFP)4570Swn/J, FVB; Jackson Laboratory, Bar Harbor, ME, USA). This mouse expresses enhanced green fluorescent under the control of the GAD67 promoter and allows for the visual identification of GABAergic neurons. Animals were housed under 14:20 light-dark conditions in the University of Kentucky Division of Laboratory Animal Resources facilities with food and water available ad-libitum. Approximately equal numbers of both sexes

were used and results from both sexes were aggregated. All animal procedures were approved by the University of Kentucky Animal Care and Use Committee.

To destroy insulin-secreting pancreatic β-cells, mice were given an intraperitoneal injection of streptozotocin (STZ; 200 mg/kg in 0.15mL of 0.1 M citric acid; Sigma-Aldrich, St. Louis, MO, USA) after a 6-hour fast. After injection, mice were returned to their home cages and blood glucose was monitored daily by tail lance (Nova Max Plus, Nova Diabetes Care, Billerica, MA, USA). Mice were used for experiments after ≥5 days of hyperglycemia (≥ 300 mg/dL). It has been previously established that a similar period of hyperglycemia is sufficient to produce lasting changes in both synaptic and intrinsic properties of NTS and DMV neurons [280-285]. Mice that displayed persistent hyperglycemia after STZ injection were considered a model of T1DM.

4.2.2 Electrophysiology

Mice were anesthetized using isoflurane inhalation (confirmed using foot pinch response) and decapitated. The brain was then rapidly removed and placed in ice-cold, oxygenated (2-4 °C; 95% O_2/5% CO_2) artificial cerebrospinal fluid (ACSF). In all experiments (except where the addition of drugs is noted), ACSF was composed of (in mM): 124 NaCl, 3 KCl, 26 $NaHCO_3$, 1.4 NaH_2PO_4, 11 glucose, 1.3 $CaCl_2$, and 1.3 $MgCl_2$. The hindbrain was mounted to a sectioning stage via cyanoacrylate glue and submerged in ACSF. Coronal brainstem slices (300 μm) were made using a vibratome (Series 1000; Technical Products

International, St. Louis, MO, USA). After cutting, slices were incubated in a holding chamber for 1 hour in warmed (30°C-35°C), oxygenated ACSF.

For recordings, slices were transferred to a recording chamber on a fixed-stage, upright microscope (BX51WI; Olympus, Melville, NY, USA) and superfused with warmed ACSF (32-34 °C). Whole-cell patch-clamp recordings were performed under visual control and cells were identified using infrared illumination with differential interference contract optics. Glass recording pipettes (1.65 mm OD, 1.2 mm ID; King Precision Glass, Claremont, CA, USA) were filled with internal solution that contained (in mM): 130 K-gluconate, 1 NaCl, 5 EGTA, 10 HEPES, 1 MgCl2, 1 CaCl2, 3 KOH, and 2 Mg-ATP; pH = 7.2-7.3, adjusted with 5 M KOH. using a Multiclamp 700B amplifier, Digidata 1440A digitizer, and pClamp 10.6 software (Molecular Devices, Axon Instruments, Sunnyvale, CA, USA). Data were recorded at 20 kHz and filtered at 3 kHz.

Added to the ACSF for specific experiments were the following: fibroblast growth factor 19 (FGF19; 230 pM; ProspecBio, Ness Ziona, Israel), 4-Methoxy-7-nitroindolinyl-caged-L-glutamate (MNI caged glutamate; 250 μM; Tocris/BioTechne, Minneapolis, MN, USA), tetrodotoxin (TTX; 2μM; Alomone Labs, Jerusalem, Israel), and picrotoxin (100 μM; Alomone Labs). The concentration for FGF19 was chosen because we have previously shown that this concentration alters intrinsic and synaptic properties of DMV neurons [51]. Additionally, this concentration has been shown to stimulate approximately half-maximal glucose uptake and phosphorylated extracellular signal-related kinase

(pERK) induction in cell culture assays [286]. FGF19 was applied for 5 minutes and was applied once per slice to avoid any lasting effects of prior applications.

DMV neurons were identified via morphology (elongated, tear-drop-shaped soma ≥ 20 μm) and by their location in the slice (located along the ventral edge of the DVC). NTS neurons were also identified by morphology and location in slice (dorsal to the DMV). The mouse model used here expresses enhanced green fluorescent protein (EGFP) under a GAD67 promoter. This allows for visual identification of a large proportion of GABAergic NTS neurons. Since previous research suggested that FGF19 altered glutamatergic but not GABAergic transmission in the DVC, EGFP-negative NTS neurons were targeted to increase the likelihood of recording from a glutamatergic neuron [51].

Once whole-cell configuration was achieved, neurons were held near their resting membrane potential (RMP) for at least 5 minutes to allow proper equilibration of the cytoplasm and pipette solution. Acceptable series resistance was considered to be <25 MΩ (range = 6.044-24.89 MΩ; mean = 13.21 MΩ) and was regularly monitored; recordings were discarded if series resistance or cell capacitance changed by ≥ 20% during recording. All voltage values were corrected post-hoc for the liquid junction potential (calculated at -15 mV). Excitatory postsynaptic currents (EPSCs) were recorded at -85 mV, the approximate reversal potential for Cl^-, to prevent interference by inhibitory currents. For continuous recordings of EPSCs, 2 min of activity was analyzed. Input resistance (R_{in}) was calculated as the slope of the line that best fit the points produced by 500 ms negative current injections ranging from -20 pA to 0 pA in 5

pA increments. Neurons were considered responsive if FGF19 produced a ≥20% change in R_{in}. Current versus action potential frequency (I-F) analysis was made in the same group of neurons that were used to measure R_{in} by measuring action potentials resulting from positive current injections ranging from 0 pA to 20 pA in 5 pA increments.

Similar to previous reports of glutamate photoactivation in the DVC [49, 299, 316], MNI-caged glutamate (250 μM) was added to recirculating ACSF and uncaged using 30 ms pulses of UV light (UV filter; Chroma Technology, Rockingham, VT). UV light, controlled by an automated shutter system (Uniblitz VMM-D1, Vincent Associates, USA), was directed to the slice through the 40X water immersion objective. Aperture width was set to minimum to stimulate a small patch of neurons (approximately 75 μm diameter stimulation region). When light was positioned directly over the recorded cell, UV pulses produced large, fast inward currents in voltage-clamp mode and significant depolarization in current-clamp mode (typically >200 pA and >20 mV, respectively). To find extant glutamatergic connections, the objective was systematically moved throughout the AP or NTS until the UV pulse produced a detectable synaptic response. Recordings consisted of 10 repetitions of: A 1-second pre-stimulus period, a 30 ms UV pulse, then a 2-second post-stimulus period. Results were reported as a difference in EPSC frequency during the 500 ms immediately after stimulation versus that in the 1-second period before stimulation. Successful glutamate uncaging was defined as a >1 Hz change in frequency.

4.2.3 Statistics and Analysis

Recordings were analyzed using pClamp 10.6 (Axon Instruments), Minianalysis 6.0.7 (Synaptosoft, Decatur, GA, USA), SAS 9.4 (SAS Institute, Cary, NC, USA) and Prism 8 (GraphPad Software, San Diego, CA, USA). Within-cell analysis of multi-event recordings (e.g., EPSCs before and after drug application) was performed using the 2-sample Kolmogorov-Smirnov (K-S) test. Grouped analyses were performed using a paired t-test when one before/after pair was present or repeated measures generalized linear mixed model with Tukey multiple comparisons when multiple before/after pairs were present. Significance was set at $p<0.05$ for all analyses.

4.3 Results

4.3.1 FGF19 increases the excitability of glutamatergic AP and NTS neurons that project to the DMV in hyperglycemic mice

Previous reports found that FGF19 increased action potential-dependent glutamate release in the DMV of hyperglycemic, but not normoglycemic mice [6]. Both the NTS and area postrema (AP) remain intact in the slice preparation, express abundant FGF receptors, and have glutamatergic projections to the DMV [26, 28, 35]. Thus, it was posited that these areas were likely sources of excitatory input that was modified by FGF19. To identify the effect of FGF19 on excitatory neurotransmission from the NTS and AP to the DMV, glutamate photostimulation was made in these areas while recording EPSCs in DMV neurons (Fig 4.1). Briefly, the effect of glutamate uncaging was determined by measuring the difference in

EPSC frequency before and after UV light pulses. All recordings were made in the presence of picrotoxin (100 μM), a GABA receptor type-A blocker, to prevent network effects caused by stimulating local GABAergic neurons.

When glutamate photostimulation was performed in the NTS of control mice, FGF19 failed to alter the mean effect of glutamate photostimulation in the NTS on EPSC frequency in the DMV (ACSF: 5.78 ± 1.05 Hz; FGF19: 5.81 ± 1.38 Hz; $n = 7$; $p>0.05$). Since there was no overall effect on the response to photostimulation in the NTS, and since there was no effect of FGF19 on spontaneous EPSC (sEPSC) frequency in DMV neurons from control mice previously [6], no further uncaging experiments were performed in this group. When glutamate photoactivation was performed in the NTS of T1DM mice, FGF19 significantly increased the mean effect of glutamate photostimulation in the NTS on EPSC frequency in the DMV (ACSF: 5.18 ± 1.02 Hz; FGF19: 7.52 ± 0.91 Hz; $n = 10$; $p<0.05$). This represented an average 1.84-fold increase in the response. Similarly, when glutamate photolysis was performed in the AP in T1DM mice, FGF19 significantly increased the mean effect of glutamate photostimulation (ACSF: 3.62 ± 0.82 Hz; FGF19: 8.16 ± 1.21 Hz; $n = 5$; $p<0.01$). This represented an average 2.6-fold increase in the response. Together, these data suggest that FGF19 increases the excitability of glutamatergic neurons in the AP and NTS that project to the DMV in hyperglycemic mice.

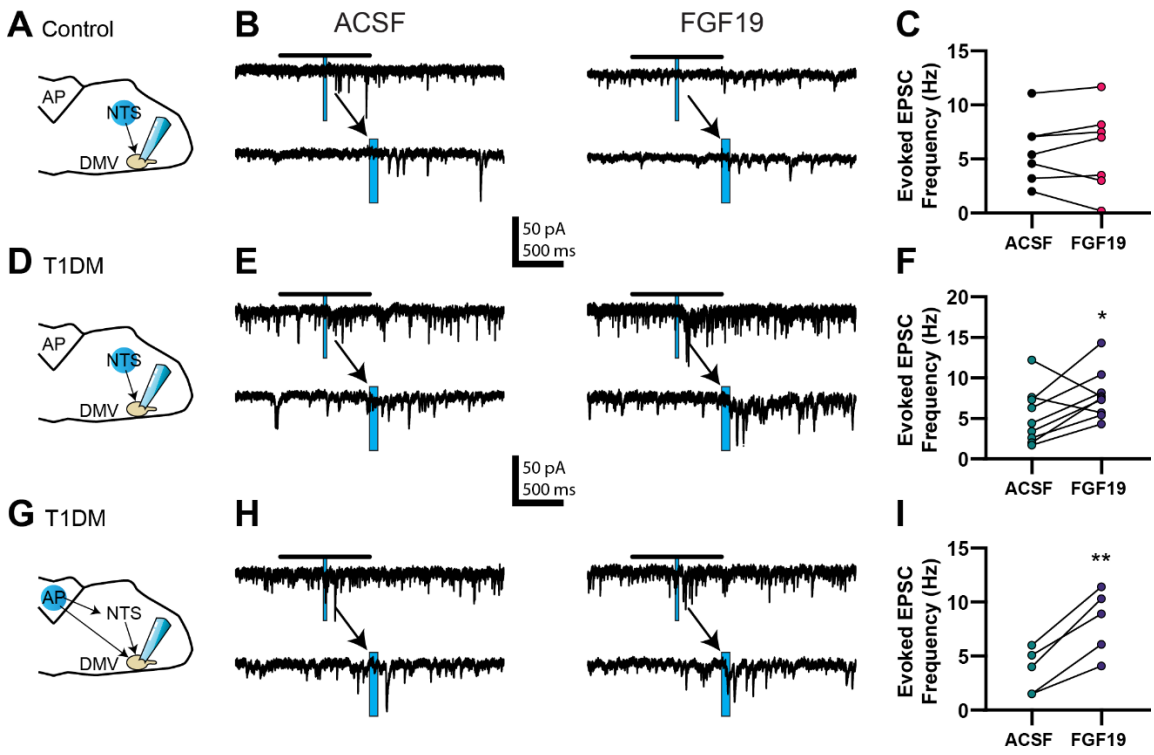

Figure 4.1. FGF19 increases the excitability of glutamatergic AP and NTS neurons that project to the DMV in hyperglycemic mice.

(A) Diagram showing a typical stimulation and recording location for cells in B and C. **(B)** Representative voltage clamp recordings of evoked EPSCs for the NTS to DMV circuit in control mice. **(C)** Evoked EPSC response in this group before and after addition of FGF19 (230 pM; n = 7; p > 0.05). **(C)** Diagram showing a typical stimulation and recording location for cells in E and F. **(E)** Representative voltage clamp recordings of evoked EPSCs for the NTS to DMV circuit in T1DM mice. **(F)** Evoked EPSC response in this group before and after addition of FGF19 (n = 10; *p<0.05). **(G)** Diagram showing a typical stimulation and recording location for cells in H and I. **(H)** Representative voltage clamp recordings of evoked EPSCs for the AP to DMV circuit in T1DM mice. **(I)** Evoked EPSC response in this group before and after addition of FGF19 (n = 5; **p<0.01). In representative traces, blue

rectangle indicates stimulation time and duration. Arrows point to an expanded trace showing 500 ms before and after stimulation. All cells recorded at -85 mV.

4.3.2 FGF19 produces mixed effects on intrinsic excitability of NTS neurons.

To determine the effects of FGF19 on intrinsic excitability of NTS neurons, resting membrane potential (RMP) and input resistance (R_{in}) were measured in current-clamp mode (Fig 4.2A-4.2F). Recordings were performed in control and T1DM mice to understand whether hyperglycemia modulates the effect of FGF19 in these neurons as suggested by previous findings [6]. A neuron that displayed a >20% change in R_{in} or >2 mV change in RMP was considered responsive to FGF19. In neurons from control mice, FGF19 modestly but significantly decreased mean R_{in} (ACSF: 1.38 ± 0.07 GΩ; FGF19: 1.21 ± 0.07 GΩ; n = 60; $p<0.01$). In this group, FGF19 produced a change in R_{in} in approximately 50% of neurons, with lower Rin observed in most responding neurons (8 increased; 21 decreased; 31 no change). FGF19 did not alter mean RMP in NTS neurons from control mice (ACSF: -63 ± 1.22 mV; FGF19; -63.6 ± 1.29 mV; n = 60; $p < 0.05$), but individual neurons responded with a change in RMP in similar proportions to those observed with R_{in} (8 increased; 16 decreased; 36 no change). In neurons from T1DM mice, FGF19 produced a similarly small but significant decrease in mean R_{in} (ACSF: 1.51 ± 0.11 GΩ; FGF19: 1.33 ± 0.14 GΩ; n = 26; $p<0.05$). In this group, FGF19 altered R_{in} in 50% of neurons with a predominately inhibitory effect in responding neurons (2 increased, 11 decreased, 13 no change). FGF19 also mildly

hyperpolarized the mean RMP in this group (ACSF: -59.5 ± 1.37 mV; FGF19: -62.3 ± 1.72 mV; n = 26; $p<0.001$).

Similarly to R_{in}, FGF19 altered RMP in approximately half of neurons (0 increased, 12 decreased, 14 no change). Neither R_{in} nor RMP differed between control and T1DM groups prior to FGF19 application. To identify the effects of FGF19 on action potential (AP) responsiveness in the NTS, positive current step recordings were performed in the same neurons to produce evoked APs (Fig 4.2G-4.2J). In neurons from control mice, FGF19 decreased mean AP frequency at the 10 pA current step (n = 60; $p<0.05$; paired t-test). In neurons from T1DM mice, FGF19 decreased mean AP frequency at the 10, 15, and 20 pA current steps (n = 26; $p < 0.05$).

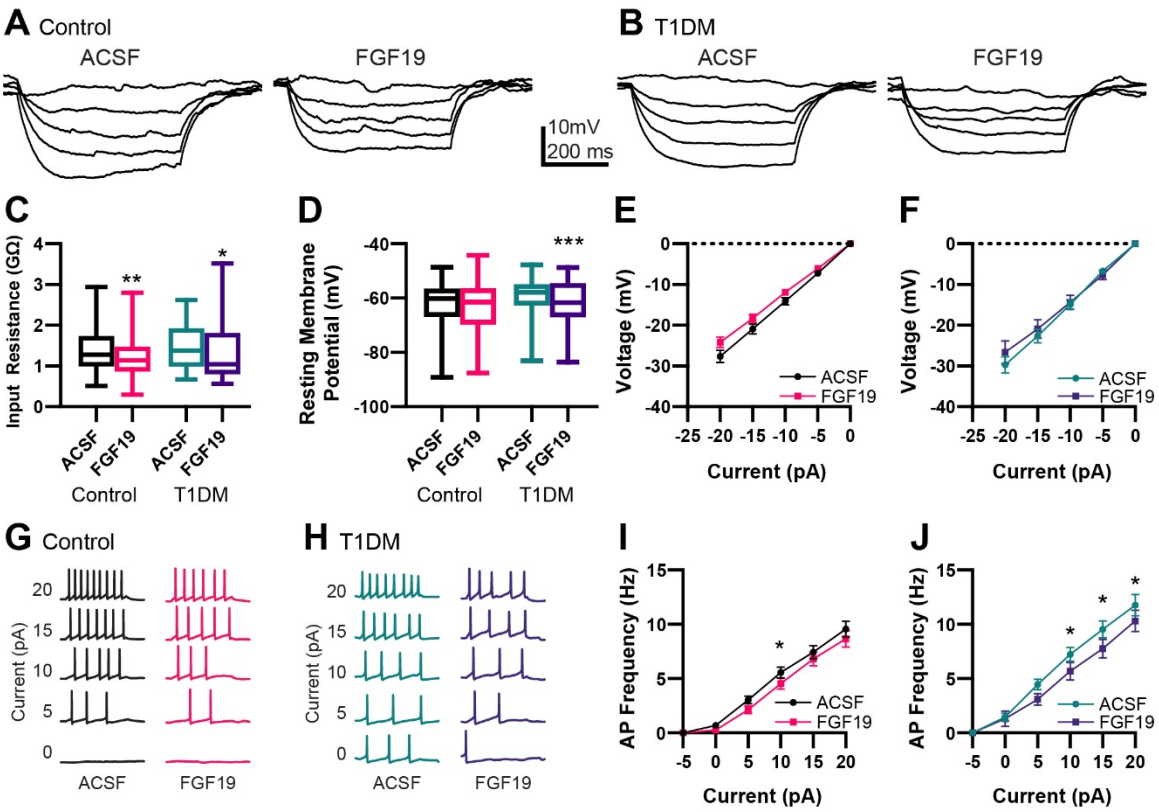

Figure 4.2. FGF19 produces mixed effects on intrinsic excitability of NTS neurons.

Representative current step recordings in current clamp mode from **(A)** control and **(B)** T1DM mice. **(C)** FGF19 significantly decreased mean input resistance in both control (n = 60; **p<0.01) and T1DM mice (n = 26; *p<0.05). **(D)** FGF19 did not alter mean resting membrane potential in control mice (n = 60; *p>0.05) but significantly hyperpolarized mean RMP in T1DM mice (n = 26; ***p<0.001). **(E)** Averaged current-voltage relationship in seen control mice (n = 60). **(F)** Averaged current-voltage relationship seen in T1DM mice (n = 26). Representative traces showing action potential response to positive current injections in control **(G)** and T1DM mice **(H)**. **(I)** Averaged action potential frequency response to positive current injections in control mice (n = 60; p<0.05).

(J) Averaged action potential frequency response to positive current injections in T1DM mice (n = 26; $p<0.05$). For all panels, * indicates $p<0.05$; ** indicates $p<0.01$, ***indicates $p<0.001$.

4.3.3 FGF19 increases sEPSC frequency in NTS neurons from T1DM mice.

Because FGF19's effects on intrinsic excitability were inconsistent with its effects on spontaneous EPSC frequency reported previously in DMV neurons [6], and since FGF19 consistently increased EPSCs in the DMV after glutamate photolysis in either the NTS or AP, excitatory neurotransmission to NTS neurons was measured. To assess this, NTS neurons were voltage-clamped at -85 mV to record sEPSCs before and after bath application of FGF19 (Fig 4.3). In neurons from control mice, FGF19 did not significantly alter mean sEPSC frequency (ACSF: 3.02 ± 0.51 Hz; FGF19: 2.89 ± 0.47 Hz; n = 14; $p>0.05$). In this group, FGF19 altered sEPSC frequency in 7 out of 14 neurons (2 increased; 5 decreased; $p < 0.02$; within recording K-S test). FGF19 also failed to produce effects on mean sEPSC amplitude in this group (ACSF: 14.4 ± 1.04 pA; FGF19: 14.0 ± 1.07 pA; n = 14; $p > 0.05$). In neurons from T1DM mice however, FGF19 significantly increased mean sEPSC frequency (ACSF: 3.60 ± 0.43 Hz; FGF19: 4.62 ± 0.57 Hz; n = 13; $p<0.001$). In this group, FGF19 altered sEPSC frequency in all neurons, with a predominately excitatory effect (11 increased; 2 decreased; $p<0.02$; K-S test). FGF19 did not alter mean sEPSC amplitude in this group (ACSF: 17.7 ± 1.31 pA; FGF19: 15.3 ± 1.09 pA; n = 13; $p > 0.05$). Neither sEPSC

frequency nor sEPSC amplitude differed between the control and T1DM groups prior to FGF19 application.

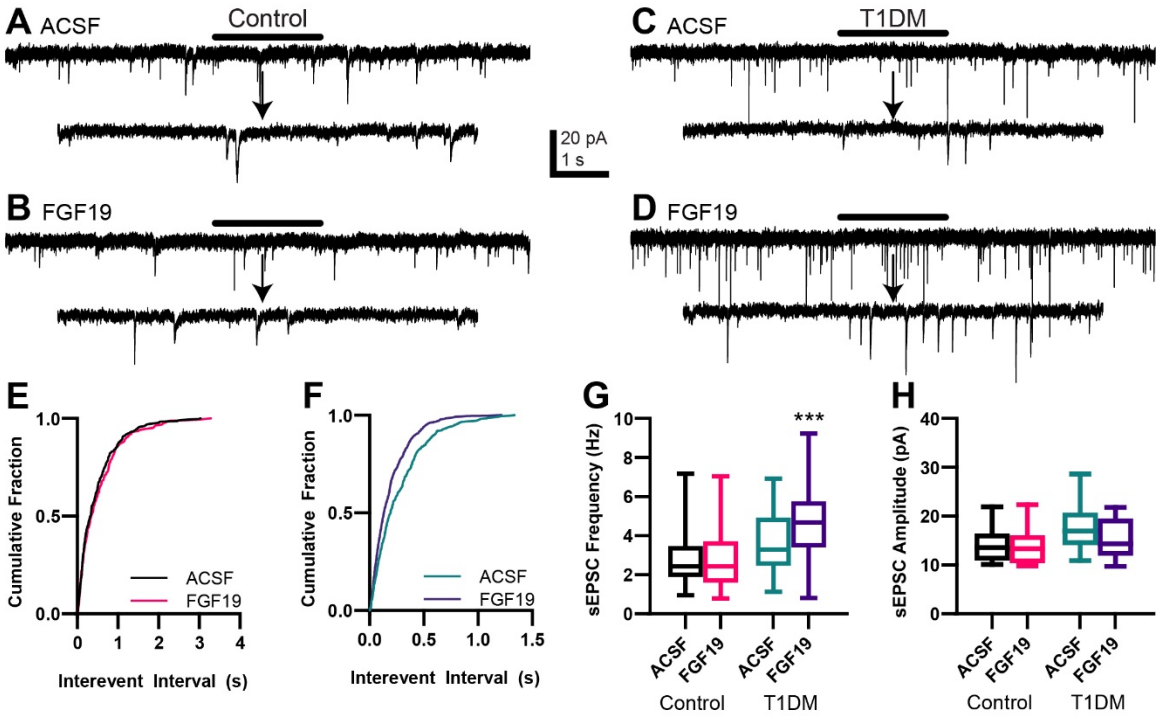

Figure 4.3. FGF19 increases sEPSC frequency in NTS neurons from T1DM mice.

(A-B) representative voltage clamp recordings of sEPSCs in NTS neurons from control mice. **(C-D)** Representative voltage clamp recordings of sEPSCs in NTS neurons from T1DM mice. **(E)** Cumulative fraction plot for the traces from A and B. **(F)** Cumulative fraction plot for the traces from C and D. **(G)** FGF19 does not alter sEPSC frequency in control mice (n = 14; p>0.05) but significantly increases sEPSC frequency in T1DM mice (n = 13; ***p<0.001). **(H)** FGF19 does not alter sEPSC amplitude in control mice (n= 14; p > 0.05) or in T1DM mice (n = 13; p>0.05). Arrow indicates 2 s expanded portions indicated by the black bar above the trace. All cells recorded at -85 mV.

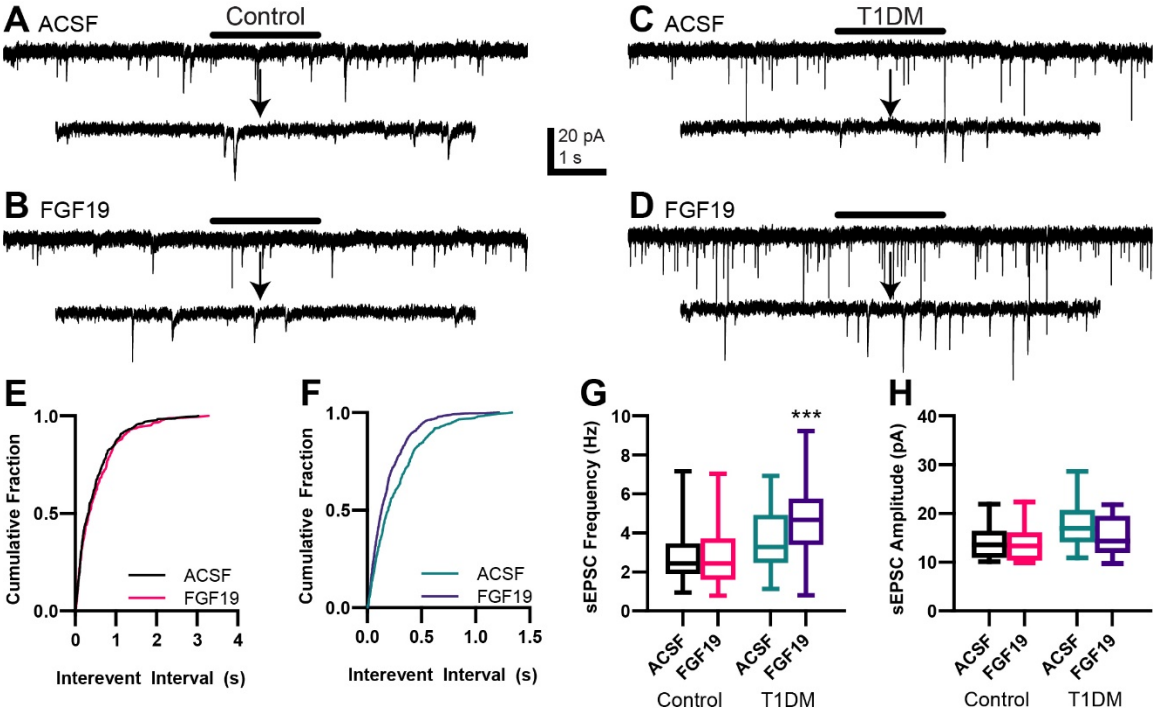

4.3.4 FGF19 does not alter mEPSC frequency in NTS neurons from T1DM mice.

FGF19 increased mean spontaneous excitatory transmission in neurons from T1DM, but not normoglycemic mice, so further experiments were performed to understand the nature of this effect in T1DM mice only. To determine whether the effect on sEPSCs was due to actions at the soma or terminal of the presynaptic neuron, action potential independent, “miniature” excitatory postsynaptic currents (mEPSCs) were recorded (Fig 4.4). NTS neurons from T1DM mice were recorded similarly to the sEPSC recordings above with the addition of TTX (2 μM) to prevent action potentials. Unlike for sEPSCs, FGF19 failed to alter mean mEPSC frequency in DMV neurons from T1DM mice (ACSF: 2.60 ± 0.47 Hz; FGF19: 2.26 ± 0.60 Hz; n = 9; $p > 0.05$). FGF19 did not alter mean

mEPSCs amplitude (ACSF: 26.0 ± 4.34 pA; FGF19: 23.1 ± 3.64 pA; $n = 9$; $p > 0.05$). These data, taken with the sEPSC results above suggest that FGF19 consistently produced a net increase in synaptic excitability in the NTS of T1DM mice. Because this increase in sEPSC is abrogated in the presence of TTX, FGF19 likely increases the excitability of intact glutamatergic neurons afferent to the NTS.

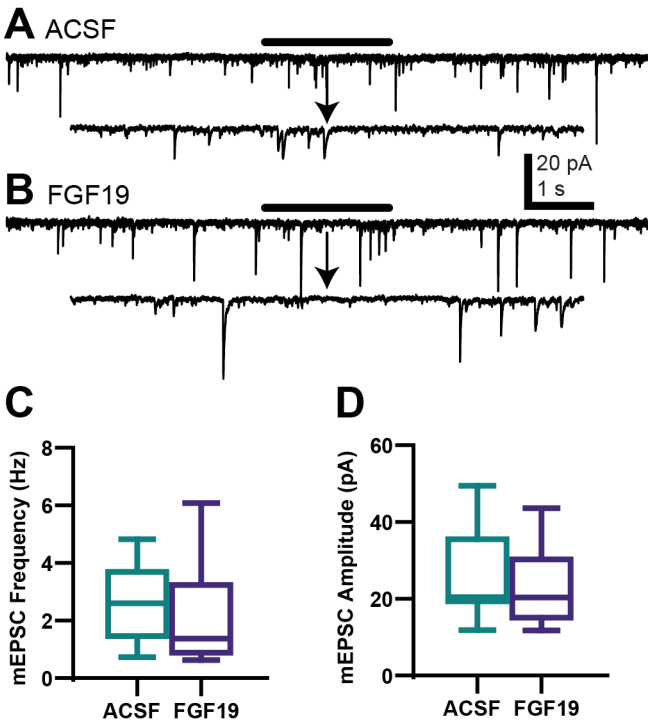

Figure 4.4. FGF19 does not alter mEPSC frequency in NTS neurons from T1DM mice.

(A-B) representative voltage clamp recordings in NTS neurons from T1DM mice in the presence of TTX (2 μM). **(C)** FGF19 failed to alter mean mEPSC frequency (n = 9; p>0.05). **(D)** FGF19 failed to alter mean mEPSC amplitude (n = 9; p>0.05). All cells recorded at -85 mV.

4.3.5 FGF19 increases the excitability of glutamatergic AP neurons that project to the NTS in hyperglycemic mice.

Since FGF19 was found to increase the effect of glutamate photolysis in the AP and since the AP projects glutamatergic projections to both the NTS and DMV [68], it was determined that the AP was also a likely source of local excitatory input to the NTS. To identify the effects of FGF19 on glutamatergic neurotransmission from the AP to the NTS, glutamate uncaging was performed to increase activity of AP neurons while recording from neurons in the NTS (Fig 4.5). Because FGF19 was found to increase sEPSC frequency in NTS neurons from T1DM mice only, further glutamate uncaging experiments were restricted to this group of mice. When uncaging was performed in the AP, FGF19 significantly increased the mean effect of uncaging on EPSC frequency in the NTS (ACSF: 4.34 ± 1.10 Hz; FGF19: 7.12 ± 0.98 Hz; $n = 5$; $p < 0.05$). Together, these data suggest that FGF19 increases the excitability of glutamatergic AP neurons that project to the NTS in hyperglycemic mice.

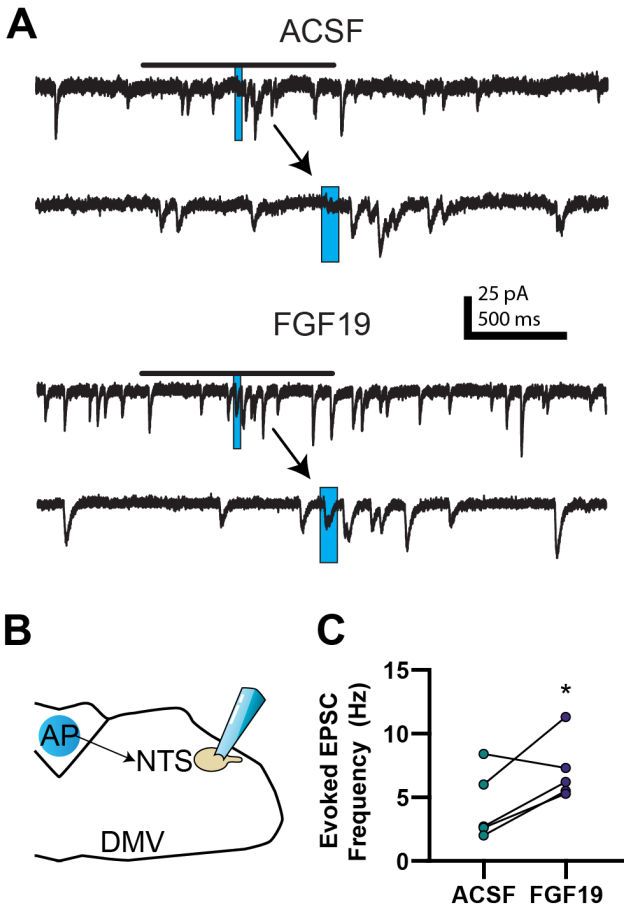

Figure 4.5. FGF19 increases the excitability of glutamatergic AP neurons that project to the NTS in hyperglycemic mice.

(A) Representative voltage clamp recordings of evoked EPSCs for the AP to NTS circuit in T1DM mice. **(B)** Diagram showing a typical stimulation and recording location for cells in A and C. **(C)** Evoked EPSC response in this group before and after addition of FGF19 (n = 5; $p<0.05$). In representative traces, blue rectangle indicates stimulation time and duration. Arrows point to an expanded trace showing 500 ms before and after stimulation. All cells recorded at -85 mV.

4.4 Discussion

These results indicate that FGF19 increases glutamatergic transmission at multiple points in DVC circuitry in hyperglycemic, but not normoglycemic mice, with multiple implications regarding the understanding of FGF19 activity in the hindbrain. We found previously that FGF19 decreased blood glucose in hyperglycemic mice through actions in the dorsal hindbrain, and this effect was abrogated by co-administration of a peripheral muscarinic receptor blocker [51], suggesting a parasympathetic mechanism. Similar to the current findings, we also found that FGF19 altered the excitability of DMV neurons in a complex manner that was heavily influenced by hyperglycemic state. These results suggested that FGF19 functioned in the DVC through a relatively restricted mechanism – i.e., that FGF19 modified the activity of central vago-vagal reflexes, resulting in altered parasympathetic output. The current findings expand upon what was established previously by identifying multiple local, excitatory synaptic circuits within the DVC that are modulated by FGF19. These results are especially intriguing considering that, while the DMV is typically associated with autonomic regulation, the NTS and AP show extensive interconnectivity with several other brain regions [67, 68, 88, 317-319]. This suggests that FGF19 in the hindbrain may regulate metabolism through multiple mechanisms in addition to autonomic changes, which is consistent with the diverse effects produced by ICV FGF19 reported previously [197, 198, 202, 203].

Previous data showed that the effect of FGF19 on EPSC frequency in the DMV was blocked by TTX, suggesting a neuronal source that remained intact

within slice preparation. Although the source was unknown, it was hypothesized to be the NTS, since it is a primary source of synaptic input to the DMV and expresses the required receptors/co-receptor required to respond to FGF19 [277, 278, 320, 321]. However, these same expression data suggested the intriguing hypothesis that the AP may also participate in the response of DMV neurons to FGF19. Indeed, the AP displays significantly higher expression of multiple FGFRs and ß-klotho than the NTS and shows some of the highest expression levels of any brain area [278]. Thus, neurons in the NTS and AP were tested regarding the effects of FGF19 on their glutamatergic connections to the DMV.

The glutamate uncaging experiments performed here demonstrated that FGF19 increases the excitatory influence of both the AP and NTS on DMV neurons. The involvement of the NTS was predicted, since the excitatory NTS to DMV circuit has been well-characterized [21, 37, 54, 299]. However, there is vanishingly little known about the role of the AP in local vagal circuitry. Interestingly, there is evidence to suggest that the AP may be an unappreciated participant in the canonical vago-vagal reflex circuit. Several early tracing studies [322-325], later confirmed via viral and genetic techniques [68, 326], found that the AP receives afferent vagal sensory input and projects glutamatergic output toward the NTS and DMV. This suggests that the AP may serve as a vagal sensory integration center, in a similar capacity as the NTS. Despite this, there are little to no existing electrophysiological studies exploring the role that the AP plays in regulating local DVC circuitry.

The current findings confirm that AP neurons modulate DMV activity via glutamatergic synaptic connections and that FGF19 increases the activity of this input. This does not necessarily imply the existence of a monosynaptic connection, since it is possible that the AP regulates DMV excitability exclusively through intermediary NTS neurons. However, considering the widespread glutamatergic innervation from the AP throughout the DVC and the extensive dendritic fields of DMV neurons, it is likely that the AP communicates to the DMV both mono- and polysynaptically [55, 68]. A priori, in light of the AP's traditional role as the principal emetic center in the brain, the existence of a monosynaptic connection from AP to DMV seems logical. This would allow direct and rapid control of gastric motility and stomach muscle contraction in response to noxious stimuli in the blood.

Uncaging glutamate over a neuron causes a transient membrane depolarization that subsides over a period of ~500 ms. Consequently, an increased response to uncaging, as was seen here, is presumed to be the result an increase in excitability in the afferent neuron. Initial uncaging experiments indicated an increase in glutamatergic NTS neuron excitability in T1DM mice. To understand this, we first measured the intrinsic excitability of these neurons in both control and T1DM mice. The mouse model used here expresses EGFP in GABAergic neurons, so to increase the likelihood of patching from glutamatergic neurons, only EGFP-negative neurons were targeted for recording, though this does not guarantee that all neurons were glutamatergic.

FGF19 produced a mixed effect on intrinsic excitability in these neurons, which did not appear to be dependent on hyperglycemic state. In both control and

T1DM groups, FGF19 failed to alter R_{in} and RMP in approximately half of NTS neurons. In the neurons that did respond, FGF19 tended to produce relatively subtle inhibitory effects, although a small proportion of neurons were excited by FGF19. Similarly, FGF19 produced a predominately inhibitory effect on evoked action potential firing in response to positive current injections. Often, large differences in evoked action potential response were also associated with effects on R_{in} and/or RMP, suggesting that the change action potential response was likely secondary to changes in membrane properties. These responses were mainly consistent with our previous findings in the DMV, which found moderate intrinsic inhibition in both control and T1DM groups in response to FGF19, suggesting that the peptide may interact with a common intracellular pathway downstream from the FGFR that is not modified by hyperglycemia [51].

The effects of FGF19 on NTS intrinsic excitability run contrary to the excitation that was predicted by glutamate uncaging. Although it is possible that the small proportion of NTS neurons that were excited by FGF19 was responsible for the increase in evoked EPSCs in T1DM mice, further experiments on synaptic excitability were warranted. FGF19 significantly increased sEPSC frequency in most NTS neurons from T1DM mice with no overall effect in control mice. This is consistent with the findings from Figure 4.1 and is likely a key driver of the FGF19-induced increase in NTS to DMV excitatory transmission. Intriguingly, and in contrast to several other metabolic hormones, this effect was abolished with the addition of TTX, suggesting the involvement of intact upstream neurons [72, 327]. FGF19 was also found to moderately decrease sEPSC amplitude. This effect was

not reproduced in mEPSC recordings, indicating a presynaptic mechanism. This is likely explained by the concurrent increase in sEPSC frequency, suggesting that FGF19 may increase the frequency of smaller EPSC events, thereby decreasing mean EPSC amplitude. Since FGF19 was found to increase the activity of the AP to DMV glutamatergic connection, the effect of AP input to the NTS was tested. As hypothesized, FGF19 increased glutamate release in the NTS that was due to increased activity of AP neurons. One alternative explanation for the discrepancy seen here between intrinsic properties and glutamate uncaging is the involvement of calcium. FGFR activation has previously been shown to increase activity of the L-type calcium channel [328, 329]. EGTA was included in the intracellular solution used here, so any FGF19-induced changes in calcium dynamics in recorded NTS neurons were likely blunted or abrogated.

Together, these data suggest that FGF19 increases glutamatergic neurotransmission at multiple points in the DVC circuit of T1DM mice. ICV administration of FGF19 decreases blood glucose concentration in T1DM but not control mice [51, 246, 296]. This suggests that the effects on blood glucose are likely to be determined by neurophysiological differences between control and T1DM groups. Although FGF19 produced intrinsic inhibition in some NTS neurons, this effect was broadly similar between both animal groups. Moreover, the effects on intrinsic excitability of NTS neurons does not appear to be consequential regarding their net excitatory influence on DMV neurons in T1DM mice. Rather, the more substantial effects of FGF19 on synaptic excitability in T1DM mice play a greater role in the peptide's effect on vagal motor output. The

NTS phenotype observed here is also consistent with our previous results showing that FGF19 produced a moderate decrease in EPSC frequency in some DMV neurons from control mice [51].

In addition to neuronal input, the DVC regulates metabolism in response to humoral signals. The AP and NTS lack a fully functional blood-brain barrier due to local fenestrated capillaries, which allows the diffusion of humoral components into the DVC that might typically be excluded [56]. Additionally, NTS and DMV neurons have a wide dendritic field [55, 330] that can extend to the AP border. As such, it is likely that neurons in all three DVC nuclei can sense and respond to humoral signals. Neurons in the DVC have been shown to respond to many primary metabolic hormones [49, 50, 72, 79, 81, 86, 293]. Similar to the effects of FGF19 described here, leptin, insulin, CCK-8, and ghrelin modify glutamatergic, not GABAergic transmission in the DVC [49, 50, 72, 85, 327]. Despite this, GABAergic transmission is considered to be the primary determinant of DMV excitability during resting conditions since blockade of glutamatergic transmission in this area fails to produce effects on gastric motility or pancreatic secretion in normoglycemic mice [37, 54]. Interestingly, chemogenetic silencing of GABAergic NTS neurons fails to alter blood glucose concentration in normoglycemic mice, whereas increasing GABA neuron activity in the dorsal hindbrain increases blood glucose concentration [44]. This suggests that glucoregulatory DMV neurons may not show the same GABA-dominant phenotype seen with other DMV subgroups.

The changes in cellular excitability in the DVC seen here are consistent with the beneficial metabolic effects associated with ICV administration of FGF19.

ICV FGF19 has been shown to decrease HGP [203] and hepatic expression of G6Pase, a key enzyme required for gluconeogenesis [198]. These effects can be replicated by injection of excitatory neurotransmitters into the DVC [48] or by increasing the excitability of DMV neurons as measured by c-fos staining [47]. Additionally, a common hallmark of FGFR activation is induction of phosphorylated extracellular signal-related kinase (pERK). Insulin activation of ERK signaling in the DVC is sufficient to decrease HGP, suggesting that FGF19 may share this mechanism [293]. Furthermore, the increase in excitatory neurotransmission to the DMV seen here is consistent with a decrease in blood glucose concentration. Injection of NMDA in the DVC lowers HGP and this effect was prevented by a hepatic vagotomy, suggesting that the effect was mediated via the synaptic excitation of DMV neurons [48]. Additionally, increasing synaptic inhibition to the DMV increases blood glucose concentration [44]. Together, these results are consistent with a model in which increased excitatory input to the DMV produces a decrease in blood glucose concentration [331]. Accordingly, the effects of FGF19 seen here on DVC circuit dynamics are likely to produce beneficial effects on blood glucose levels in diabetic animals.

The effects of FGF19 in the DVC found here may also modulate metabolism independently of autonomic mechanisms. Central delivery of FGF19 has been shown to decrease food intake, which could be explained via alterations in DVC excitability [197, 202]. Similar to the effects of insulin on HGP, satiation produced by CCK in the DVC requires induction of pERK, suggesting that FGF19 may decrease food intake via a shared mechanism. The NTS and AP also exhibit

significant connections to other nuclei associated with regulation of ingestive behavior including the lateral parabrachial nucleus (PBN) [68, 332] and the hypothalamus [333]. The experiments performed here focus on local circuitry within the DVC. As such, it is not known whether connections to other nuclei such as the PBN or hypothalamus are altered by FGF19. However, considering the significant expression of FGFR/β-Klotho throughout the NTS and AP, it is likely that FGF19 alters the activity of neurons that project distally as well as those that participate in local vago-vagal reflexes [277, 278].

The DVC is a key metabolic regulatory area of the brain. Although the DVC is typically associated with autonomic regulation of metabolism, the AP and NTS also serve as a communication hub between the DVC and several other key nuclei. Alterations in DVC excitability, such as those seen here, are likely to produce profound effects on multiple aspects of metabolism. Consistent with our previous work, these data suggest that FGF19 alters parasympathetic output in T1DM mice by increasing synaptic excitability of DMV neurons. Interestingly, our findings demonstrate a role for the AP in the direct regulation of the vago-vagal reflex mechanism and that this connection can be modified by a metabolic hormone. Though not confirmed, it is possible that other metabolic hormones work similarly in this area. Overall, the electrophysiological effects seen here are consistent with the beneficial metabolic effects of ICV FGF19. Although these findings implicate a primarily autonomic mechanism, FGF19 was also found to significantly alter AP and NTS excitability. This raises the possibility that FGF19 may interact with the DVC to produce an array of beneficial metabolic effects through alteration of vagal parasympathetic output and through regulation of several other important nuclei.

5 General Discussion

5.1 Review of Major Findings

It was previously established through the work of several research groups that FGF19 produces powerful antidiabetic effects when administered to the brain [186, 197, 198, 202, 203]. Excluding Fu *et al.*, all of these papers either explicitly or implicitly explored a hypothalamic site of action for ICV FGF19. This report is the first to identify the effects of FGF19 in the DVC. Chapter 3 of this dissertation first established that administration of FGF19 to the hindbrain was sufficient to significantly decrease blood glucose concentrations in T1DM mice. Similar to previous reports on ICV FGFs, this effect only occurred in hyperglycemic mice and did not produce hyperglycemia [246]. This effect was abrogated by co-administration of MSA, a peripheral muscarinic receptor blocker. Although not fully confirmative, this suggests that FGF19 decreased blood glucose by acting through the vagus nerve.

Chapter 3 also established several electrophysiological effects of FGF19 on DMV neurons. Since the in vivo data indicated a likely change in vagal parasympathetic output, the effect of FGF19 on DMV neurons was measured. FGF19 produced several effects that differed as a function of disease state (i.e. presence of hyperglycemia). In the DMV, FGF19 moderately decreased glutamate release from control mice and consistently increased glutamate release in T1DM mice. This effect was prevented with the addition of TTX, a Na_v/action potential

blocker, suggesting that FGF19 increased the activity of glutamatergic neurons immediately afferent to the DMV.

FGF19 produced mixed effects on the intrinsic excitability of DMV neurons. Quantitatively, FGF19 decreased the input resistance of neurons from T1DM mice and decreased the RMP of neurons from control mice. However, on an individual neuron level, FGF19 produced generally inhibitory effects on both measures from both sets of neurons. This suggests that hyperglycemia does not modify the intracellular process that produces these effects. Consistent with these data, FGF19 produced mixed effects on action potential (I_{AP}) frequency of DMV neurons. In control mice, FGF19 produced no change, an increase, or a decrease in I_{AP} frequency in approximately equal amounts while in T1DM mice, FGF19 decreased I_{AP} frequency in most neurons with an increase in one neuron.

Finally, FGF19 decreased A-type potassium channel (K_A) current amplitude in control mice only. First, it was found that FGF19 decreased the amplitude of the initial peak current elicited by voltage activation steps in control mice only. This effect was blocked in the presence of 4-AP, a K_A channel blocker, and when the internal solution contained Cs^+, a K^+ channel blocker, as the primary cationic charge carrier. Since the current was blocked by 4-AP and by Cs^+, it was determined to be K_A. Altogether, the data from Chapter 3 indicate that FGF19 decreases blood glucose, likely by altering DMV neuron excitability. In vitro studies revealed that FGF19 produced a complex phenotype of electrophysiological responses in the DMV and that this phenotype was heavily modified by the presence of hyperglycemia.

Chapter 4 of this dissertation explored the effects of FGF19 on neurons upstream to the DMV. Since FGF19 decreased blood glucose in T1DM mice only in Chapter 3, it was hypothesized that the most important electrophysiological responses must be the ones that occurred in T1DM mice and not in control mice. This suggested that the increased I_{AP}-dependent glutamate release in the DMV was the most likely driver of the beneficial effects on blood glucose. To explore this, Chapter 4 focused entirely on electrophysiology and these experiments were aimed at identifying the involvement of the NTS and AP in the FGF19-mediated increase in DMV glutamate. First, glutamate photolysis experiments were performed. Briefly, DMV neurons were recorded while caged glutamate was photoactivated in either the NTS or the AP. In control animals, FGF19 did not affect glutamate uncaging in the NTS. This was consistent with the results from Chapter 3. In T1DM animals, FGF19 increased glutamate release in the DMV when photoactivation was performed in either the AP or the NTS. These results confirmed the hypothesis that FGF19 increased the activity of glutamatergic neurons in the AP and NTS, leading to increased glutamate in the DMV. No experiments were performed to understand if the connection from AP to DMV was monosynaptic or if the NTS served as an intermediary.

Next, the effects of FGF19 in the NTS were explored. FGF19 produced unexpected effects on NTS intrinsic excitability. In both control and T1DM groups, FGF19 produced mixed effects on excitability with a definite trend towards inhibition. R_{in} was decreased in RMP was hyperpolarized in approximately half the cells of both groups. The remainder of cells tended to either show no change with

a small subset of cells showing excitatory effects. Considering the consistent responses seen in the glutamate uncaging experiments, these results ran somewhat contrary to what was expected. It is possible that the small number of neurons that were excited by FGF19 could be responsible for the increased glutamate release in the DMV but we hypothesized that the observed excitatory effects would likely be found in synaptic measurements. This hypothesis was indeed borne out. FGF19 increased EPSC frequency in the NTS in most cells from T1DM mice with no effect on mean EPSC frequency in control mice. This result was consistent with the previous findings from Chapter 3 and Figure 4.1. Further EPSC recordings were made in T1DM mice with the addition of TTX to block action potentials. The addition of TTX blocked the excitatory effect of FGF19 in the NTS, suggesting that the source of glutamate was from cells left intact in slice preparation and not, for example, glutamate terminals from vagal afferents. Finally, to confirm the source of this input, glutamate photolysis experiments were performed in the AP while recording in the NTS. It was found that FGF19 increased the activity of glutamatergic AP neurons that project to the NTS. The implications of these results and their roles within the larger context of CNS control of blood glucose will be discussed in detail below.

5.2 Effects of Central Delivery of FGF19 on Blood Glucose

5.2.1 Previous Findings

In Chapter 3, it was found that hindbrain application of FGF19 produced a significant decrease in blood glucose concentrations in T1DM mice only. This

effect was found to be dependent on peripheral muscarinic receptor signaling. However, no further experimentation was performed to understand the target tissue or mechanism. Therefore, it is unknown if the decrease in blood glucose was, for example, caused by a decrease in HGP, an increase in glucose disposal, or if hormones such as glucagon were involved.

Despite the lack of mechanistic details, certain parallels can be drawn with other studies that may give clues to the likely mechanism here. First, due to the use of a T1DM model, it can at least be safely assumed that insulin was not responsible here. This is consistent with previous studies on CNS FGF19. Morton *et al.* found that ICV FGF19 decreased blood glucose likely through increased metabolism of glucose to lactate and that there was no change in insulin secretion [198]. Ryan *et al.* found that insulin levels did not differ between ICV vehicle and ICV FGF19 groups at multiple time points after injection [197]. However, the latest time point for insulin measurements in this study was only 15 minutes, meaning that there could be a change in insulin at a later time point.

Perry *et al*. found that ICV FGF19 decreased blood glucose in T1DM rats with no changes in insulin levels between the groups [203]. At first glance, due to the similarities in models used, it could be assumed that this paper may be the closest to explaining the mechanism for FGF19 in the hindbrain. However, the authors determined that the decrease in blood glucose was the result of altered hypothalamic-pituitary-adrenal axis changes leading to decreased corticosterone. Thus, since in Chapter 3 it was found that the effect on blood glucose was

dependent on peripheral muscarinic receptor signaling, it is unlikely that the mechanism is shared.

Intriguingly, the results in Marcelin *et al.* run somewhat contrary to the three other studies and indeed indicate a change in insulin signaling [202]. This may be due to a difference in methodology since this study performed four daily ICV injections of FGF19 instead of a single injection. This study found that in ob/ob and HFD mice, FGF19 decreased fasting insulin levels, indicating an increase in insulin sensitivity. It was also found that, in the FGF19 groups, insulin secretion was increased in response to a glucose challenge, where in vehicle-injected groups it did not. This suggests that chronic FGF19 administration may produce additional effects on glucose-induced insulin secretion and insulin sensitivity as compared to acute injection.

5.2.2 The DVC and Blood Glucose

Since the experiments here involved acute administration of FGF19 and were dependent on peripheral muscarinic receptor engagement, the most likely mechanism involves vagus nerve-mediated effects on peripheral organs. Peripheral blockade of muscarinic receptors can be used as an indirect and less invasive alternative to a surgical procedure such as a vagotomy. Briefly, the DMV consists of preganglionic motor neurons that communicate to postganglionic neurons in the periphery through acetylcholine activation of nicotinic receptors [334, 335]. In turn, the peripheral postganglionic neurons exert their effects primarily through acetylcholine activation of muscarinic receptors on target tissues

[12, Chapter 31]. Although the DMV projects to most visceral tissues, the most likely target tissues for the effects seen here are either the liver or the pancreas.

5.2.2.1 DVC Regulation of the Pancreas

Pancreatic exocrine and endocrine release is heavily regulated through vagal cholinergic innervation. It is well known that the DMV regulates pancreatic exocrine secretions through a peripheral muscarinic receptor-dependent mechanism [43, 311]. Pancreatic exocrine secretions are vital for proper nutrient processing and loss of pancreatic exocrine function results in poor nutrient absorption and malnutrition. [336]. However, it is unlikely that ICV FGF19 works through this mechanism as it works through the activation of muscarinic receptors. Activating muscarinic receptors increases pancreatic exocrine secretions, leading to better nutrient absorption and likely higher blood glucose levels.

Pancreatic endocrine release is also under the control of peripheral muscarinic receptors. Unilateral electrical stimulation of the DMV increases plasma insulin levels by 100%-200% and this effect was blocked with a muscarinic blockade or vagotomy [41]. Bilateral electrical stimulation of the lateral DMV results in increased insulin and glucagon secretion [337]. Chemical disinhibition of the DMV also produces an increase in pancreatic insulin release [42]. The animals used here are a model of T1DM, and as such, have little to no ß-cells remaining. This suggests that increased insulin release is not involved.

Efferent projections from the DMV also regulate pancreatic glucagon secretion [337]. Acetylcholine release from efferent vagal terminals can stimulate glucagon release [337-340] and disruption of pancreatic M3 muscarinic receptor

signaling prevents acetylcholine-stimulated glucagon secretion [341]. Glucagon is traditionally thought of as a counterregulatory hormone, released from pancreatic α-cells, that increases blood glucose in response to hypoglycemia [342]. Both T1DM and T2DM are associated with hyperglucagonemia, leading to increased fasting blood glucose [343, 344]. Glucagon receptors are located primarily in the liver and kidney but are also found in the brain, heart, adipocytes, pancreas, and many other tissues [345]. Glucagon has many actions but the most relevant of these is regards HGP. Glucagon promotes glycogenolysis and gluconeogenesis while suppressing glycolysis and glycogenesis [346]. The resulting phenotype is one of greatly increased hepatic glucose release with a concurrent decrease in hepatic glucose breakdown and storage. However, it is again unlikely that hindbrain administration of FGF19 decreases glucagon release. The effects seen here rely on peripheral muscarinic receptor activation, which would be expected to increase glucagon levels.

5.2.2.2 DVC Regulation of the Liver

The most likely mechanism to explain the effects of hindbrain FGF19 on blood glucose is direct vagal modulation of hepatic glucose metabolism. In contrast to the effects seen in the pancreas, increasing the activity of vagal outputs to the liver results in a decrease in blood glucose. As noted elsewhere, the activation of neurons in the DVC leads to a decrease in HGP. Injection of NMDA, an excitatory neurotransmitter, into the DVC decreases HGP by ~50%, an effect that is blocked by a vagotomy [48]. Another study found similar results, where central regulation of HGP relied on the activation of DMV neurons and required an

intact hepatic branch of the vagus nerve [47]. Perfusion of isolated rat liver with acetylcholine causes an increase in glucose production and glycogen content, an effect that was abrogated by atropine, a muscarinic receptor antagonist [347]. This study also found that hepatocytes express M3 muscarinic receptors.

It is not fully known how vagal output produces its effects on hepatic glucose metabolism. There are no identified hepatic postganglionic neurons, suggesting a direct connection from the DMV to the liver [348]. Anterograde tracing studies from the DMV show no labeling in the hepatic parenchyma or in vagal nerves or paraganglia [46]. There was labeling found associated with bile ducts and portal vessels. Moreover, the vagal efferent markers acetylcholinesterase is not found in the liver parenchyma of humans or any other species surveyed [349-355]. Regardless, activation of DMV neurons leads to a vagus nerve hepatic branch-dependent suppression of HGP that was likely caused by decreases in glucose metabolism enzymes [47]. Importantly, during this experiment, hepatic glucose dynamics were measured under pancreatic clamp conditions to prevent changes in glucagon and insulin levels. Thus, it is likely that neurons in the DMV can act directly on the liver to regulate glucose metabolism. Although not confirmed, this is the most likely mechanism to explain the antidiabetic effects of FGF19 in the hindbrain.

5.2.2.3 Potential Involvement of Other Organs

The DMV projects to many organ systems so it is possible FGF19 could work through these tissues though it is unlikely. One alternative possibility to explain the hepatic branch-dependent actions outlined above in Pocai *et al.* [47]

is that the DMV may act indirectly through another organ system that is innervated by the hepatic branch of the vagus. This branch innervates not only the liver, but also the duodenum with additional sparse labeling in the stomach, jejunum, ileum, cecum, and colon [29, 46]. It is not known whether the results in Chapter 3 are dependent on the hepatic vagus and therefore could work through any organ that the DMV projects to, including the heart, lungs, stomach, esophagus, small intestine, and colon [12, 29, 356, 357]. It is not immediately clear how vagal actions within these organs might decrease blood glucose for 12 hours although the possibility of such a mechanism cannot be discounted. A theoretical mechanism might include vagal stimulation of hormone release from one of these organs or possible changes in gastric motility or nutrient absorption.

5.2.3 Involvement of the Hypothalamus

Excluding Fu *et al*, all of the primary studies on ICV FGF19 focused on the hypothalamus. The evidence for hypothalamic sites of action varied. Ryan *et al.* only quantified hypothalamic FGFR expression and made no other inferences to hypothalamic function [197]. Morton *et al.* looked for co-localization of c-fos expression with POMC neurons and found that FGF19 activated non-POMC positive hypothalamic neurons [198]. Marcelin *et al.* further established that FGF19 suppressed hypothalamic AgRP/NPY neurons and that this effect relied on central ERK signaling [202]. Finally, Perry *et al.* found that ICV FGF19 decreased ACTH and corticosterone levels, implying a hypothalamic-pituitary mechanism [203]. Overall, this evidence is convincing that FGF19 does work in

the hypothalamus. However, it is possible that some of the effects in the hypothalamus still work by activating DVC neurons. As mentioned elsewhere, hypothalamic regulation of HGP seems to require the activation of DVC neurons and an intact vagus nerve [47, 92]. However, it is unknown if the same circuit is required for the changes in hepatic metabolism in glucose to lactate as was seen in Morton *et al.* [198].

It is also known that ICV FGF19 modulates the activity of a hypothalamic to DVC glucoregulatory circuit. Neuroglucopenia (CNS shortage of glucose) increases DVC neuron and vagus nerve activity, leading to increased glucagon secretion. Interestingly, ICV FGF19 dampens these effects, effectively dysregulating a physiological counterregulatory response to hypoglycemia [295]. One possible explanation for this phenomenon is that, in a physiological context, FGF19 is a gut signal that indicates a high energy balance. FGF19 is released within a few hours after eating and can be thought of in many ways as a late-acting hormone similar to insulin [358]. In this capacity, FGF19 may prevent inappropriate glucagon release by signaling to the brain to desensitize a hypothalamus-DVC-pancreas circuit that is activated by hypoglycemia. Interestingly, there are neurons within the NTS that are activated by hypoglycemia and regulate glucagon secretion through connections to the DMV [71]. In light of the widespread inhibitory effects on NTS intrinsic excitability found in Chapter 4, FGF19 might also function to inhibit this circuit as well.

5.3 The Cellular Effects of FGF19 in the DVC: Implications for Metabolism

When injected into the hindbrain, FGF19 decreased blood glucose in a peripheral muscarinic receptor-dependent manner. As outlined in Chapter 5.2.2, this is heavily suggestive that FGF19 exerts its effects via the vagus nerve. DMV neurons can regulate blood glucose concentrations and were shown to respond to FGF19 in Chapters 3 and 4. Therefore, the overarching hypothesis of this dissertation is that FGF19 modulates the excitability of neurons in the DVC that ultimately leads to altered activity of DMV neurons and thus, altered parasympathetic vagal output. Within this framework, the primary focus is DMV excitability, with all other effects being secondary contributors to DMV function. More specifically, since FGF19 in the hindbrain improved glycemia in T1DM mice only, the hypothesis proposed above holds that the FGF19-induced changes in the excitability of DMV neurons from T1DM mice must explain the observed changes in blood glucose concentrations.

Multiple models exist that may explain how FGF19 in the DVC might alter DMV activity to lower blood glucose. The first model makes the assumption that the in vitro conditions seen during electrophysiology experiments are a somewhat faithful reflection of the state of the DVC in an intact animal. In Chapters 3 and 4, it was found that FGF19 significantly increased synaptic excitability to the DMV while simultaneously causing a decrease in intrinsic excitability. This led to a decrease in I_{AP} frequency in 7/8 neurons and a decrease in 1/8. All previous data suggests that an increase in DMV activity is required for a liver-mediated decrease in blood glucose [47, 48]. This hypothesis also supported by the MSA experiment

in Chapter 3, since blockade of muscarinic activity prevented FGF19 from lowering blood glucose. It is entirely possible that the 1/8 DMV neurons that was acutely excited by FGF19 could be responsible for the metabolic changes. The hepatic branch DMV neurons consist of a small number of neurons on the left side of the DVC only and the DMV neurons in Chapter 3 were not identified by their target organ [26]. This model would imply that the organization of synaptic inputs and receptor expression of hepatic-projecting DMV neurons is such that the intrinsic inhibitory effects of FGF19 were minimized and the excitatory synaptic effects were maximized. To confirm this, future studies should include retrograde labeling so that DMV neurons that project to different organs can be compared regarding their responsiveness to FGF19.

The second model is one in which the electrophysiological recording circumstances in Chapters 3 and 4 are too far removed from intact animal physiology and are thus missing one or more key components that change how FGF19 works in the DVC. Potential confounding factors include unaccounted for effects on plasticity, the removal of synaptic inputs, and mismatch of the components in the ACSF with what is in the brain. First, there is a time mismatch between the in vitro and in vivo effects. In vitro effects were measured acutely, after five minutes of FGF19 application while in vivo effects were first measured at 6 hours after injection. It is possible that changes in synaptic plasticity occurred during this interval. This hypothesis is supported by the fact that multiple FGFs enhance long-term potentiation and paired pulse facilitation in the hippocampus after 10-20 min of application [359, 360].

Second, slice preparation like what is performed in the experiments in this work inherently remove a large proportion of the synaptic inputs to a given nucleus. Although an exact number is not known for the DVC, it was found in the hippocampus that neurons in slice preparation received approximately 4.5 fold fewer EPSCs when compared to in vivo recordings [361]. If this same relationship holds true in the DMV, then the consistent FGF19-induced increase in sEPSC frequency of T1DM would have an outsized influence and would be much more likely to overcome any intrinsic inhibitory effects. Slice preparation also removes input to the DVC from distal areas including vagal afferents and the hypothalamus. It is possible that the inclusion of input from these sources might alter how FGF19 works in the DVC. Additionally, FGF19 altered the excitability of the AP and NTS T1DM mice. Since both the AP and NTS project to the hypothalamus, it is possible that FGF19 could activate a reciprocal DVC –hypothalamus-DVC connection that modulates DMV activity in an important way [67, 89, 90].

Finally, FGF19 in the hindbrain may rely on high glucose concentrations or other hormones to produce its effect. The mice in the in vivo experiments were severely hyperglycemic (typically 500-600 mg/dL) but the ACSF used for in vitro experiments was much lower (198 mg/dL). It is not known what glucose concentration the DVC sees but it is possible that neurons in the DVC of diabetic mice experience higher glucose levels than what is found in ACSF. Since a primary effect of FGFs is the stimulation of glucose uptake, it is possible that higher ambient glucose levels may produce a greater response [286]. FGF19 may also synergize with other hormones in the DVC. The DVC responds to leptin [49, 72-

74], glucagon [79], GLP-1 [64, 80-84], and ghrelin [85-87] among others. The physiological action of one or more of these hormones may be required for FGF19 to exert its effects.

FGF19 may also require the actions of specific hormones that act on cAMP. It is known that drug modulation of inhibitory neurotransmission in the DMV often can only occur when cAMP levels are elevated. Opioids and the pancreatic polypeptides NPY and PYY fail to alter IPSCs in the DMV under resting conditions but an effect is revealed when cAMP levels are increased via forskolin, TRH, CCK-8s, or vagal deafferentiation [313, 362-366]. It was found that increasing cAMP levels alters receptor trafficking at the presynaptic terminal, allowing opioids, NPY, and PYY to act there to regulate GABA release. This system also is involved in insulin signaling in the DVC and is dysregulated by diabetes (discussed in Chapter 5.4.1). The DVC participates in endogenous TRH and CCK signaling [367, 368], and cAMP regulates FGFR trafficking in some tissues [369, 370]. It is not known whether cAMP contributes to the FGF response in the DVC but this topic could prove to be valuable for future research.

5.4 The Effects of Diabetes on the Brain

Many of the cellular effects seen in Chapters 3 and 4 were heavily modified by hyperglycemia. In Chapter 3, FGF19 caused a moderate decrease in sEPSC frequency in some neurons from control mice and a significant increase in sEPSC frequency in all neurons from T1DM mice. Also in Chapter 3, FGF19 decreased the amplitude of A-type K^+ currents in control mice only with no effects in T1DM

mice. Similarly, in Chapter 4, FGF19 increased glutamatergic neurotransmission from the NTS to the DMV in T1DM mice only. The underlying mechanism that is modified by hyperglycemia is unknown. However, there are numerous documented changes in DVC excitability and neurotransmission that occur in response to high blood glucose concentrations. Additionally, hyperglycemia modifies many of the intracellular signaling pathways that are activated by FGFRs. These changes will be outlined here with the goal of providing a background as to why FGF19 might affect neurons from diabetic mice differently.

5.4.1 The Effect of Diabetes on the DVC

First, past studies from this lab and others have shown that even a short history of hyperglycemia can lead to dramatic changes in DVC neuron excitability. Hyperglycemia causes a significant increase in EPSC frequency in the DMV [51, 282, 284]. The nature of this effect is not fully understood but it likely represents a compensatory response to hyperglycemia. Since most indications suggest that increasing DMV neuron activity suppresses blood glucose, an increase in synaptic excitability would likely be beneficial in a hyperglycemic context [44, 47, 48].

Diabetes also interferes with DVC neuron response to insulin. As discussed in Chapter 5.3, drug modulation of inhibitory transmission in the DVC is often only achievable if cAMP levels are elevated. In control mice, insulin can modulate GABA release in the DMV only when elevated cAMP levels are elevated by forskolin [77]. This effect was found to rely on Golgi protein trafficking and glucose transport. Interestingly, insulin was unable to modulate GABA release in the DMV

in diabetic mice, even in conditions of increased cAMP. Drawing parallels with previous studies, this suggests that cAMP levels regulate insulin receptor trafficking on GABA terminals presynaptic to the DMV and that hyperglycemia disrupts this response.

Diabetes also alters several other aspects of DVC excitability. Hyperglycemia increases the DMV response to GABA by increasing the proportion of GABA receptors that express the δ-subunit, likely via a posttranslational mechanism [283]. Similarly, diabetes also altered GABA responsiveness in the DMV by increasing transcription of GABA receptors containing the α1 and γ subunits [285]. It was also found that diabetes increases glutamate release to DVC GABA neurons that project to the DMV, ultimately leading to increased GABAergic activity to the DMV [281]. Finally, hyperglycemia impairs neuronal glucose sensation in the DVC. The glucose sensing response of NTS neurons involves glucokinase, an enzyme that converts glucose to glucose-6-phosphate. Diabetes decreases glucokinase expression in the DVC, leading to impaired electrophysiological responsiveness to changing extracellular glucose concentrations [280].

5.4.2 The Effect of Diabetes on FGFR Signaling Pathways

Diabetic hyperglycemia also is known to dysregulate several of the intracellular pathways that are activated by FGFRs. FGFRs signal through MAP kinases, PLCγ, and PI3K/Akt (see Chapter 1.3.5). It has been suggested that MAP kinases such as JNK, p38, and ERK mediate damaging effects of high glucose

concentrations. Diabetes causes oxidative stress in neurons through the depletion of NADPH, thereby interfering with the antioxidant defense mechanism [303]. Moreover, insulin resistance is positively correlated with oxidative damage in the brain [371]. In rat sensory neurons, high glucose activates JNK and p38 and oxidative stress activates p38 and ERK leading to damage of these cells [302]. In the dorsal root ganglia, experimentally induced diabetes causes sustained activation of all three groups of MAP kinases [302]. In this study, inhibition of p38 or ERK prevented the damage caused by oxidative stress, suggesting that these kinases serve as neuronal damage transducers in diabetes.

There is abundant evidence that diabetes interferes with the PLCγ pathway throughout the periphery but less is known about what occurs centrally [304, 372]. Both hyperglycemia and FGFR signaling activate PLC [303]. Activation of PLCγ hydrolyzes PIP_2 into IP_3, which releases Ca^{2+} from the ER, and DAG, which activates PKC. Importantly, PKC increases MAP kinase expression and promotes oxidative damage by acting on NADPH-oxidase [303]. It is well known that diabetes increases total DAG or do novo synthesis of DAG in vascular tissues, the heart, liver, and skeletal muscle [304, 372]. In nerve tissue, DAG is decreased by hyperglycemia although little is known about the effects of diabetes on DAG in the brain [373, 374]. Despite this, it is known that T1DM regulates brain expression patterns of various isoforms of PKC, the next downstream molecule from DAG [375, 376]. It is unknown what function this PKC reorganization plays but it may contribute to impairment of neurovascular coupling and modulation of multiple K^+ channels [376, 377].

Diabetes also interferes with the PI3K-Akt system. PI3K is one of the primary downstream signaling pathways of insulin and is dysregulated in many tissues following insulin resistance or loss of insulin signaling [378]. PI3K/Akt signaling is dysregulated in the vagus nerve of diabetic rats and may contribute to diabetic autonomic neuropathy [379, 380]. Moreover, diabetes decreases levels of phosphorylated PI3K and Akt in the brain, indicating a disruption in signaling [305]. It is likely that these alterations in PI3K/Akt signaling are detrimental, not compensatory, since CNS upregulation of PI3K leads to improvements in glycemia and hypothalamic-pituitary-adrenal axis activity [381].

It is unknown whether these same dysregulations occur within the DVC. However, considering the wide range of intracellular signaling defects induced by hyperglycemia throughout the body, it is unlikely that the DVC is immune to these phenomena. Glucose levels in the brain are typically tightly regulated. However, due to the local leaky blood brain barrier, it is likely that neurons in the DVC are subjected to high sustained glucose concentrations similar to what is experienced by cells in the periphery. Thus, it is possible that neurons in the DVC may have more in common with peripheral cells regarding their intracellular signaling milieu than with CNS neurons that lie inside the blood brain barrier.

5.5 Final Conclusions

Together, these data show that FGF19 decreases blood glucose when administered to the hindbrain and alters excitability in the DVC in several distinct and often opposing ways. Many of the effects seen here differed according to

disease state and were occasionally inconsistent even within the same cell types in the same animal. This is unsurprising, as none of the three nuclei contained within the DVC can be considered monolithic. It is well documented that neurons in the three DVC nuclei can be heavily subdivided based on receptor expression, response to glucose, target organ, and other criteria. However, throughout the findings in both Chapter 3 and Chapter 4, FGF19 consistently increased glutamatergic transmission in T1DM mice. This effect occurred in most neurons surveyed in both the NTS and DMV. This suggests that, despite the wide differences found between neurons in this area, FGF19 seemed to activate a mechanism that is both highly conserved and able to be modified by hyperglycemia. Moreover, prior studies support a model in which an increase in synaptic glutamate activity in the DVC leads to decreased blood glucose levels. Further research in this area should focus on identifying the particular mechanism responsible for increased glutamate release in the DVC so that it can be harnessed and understood.

The experiments outlined in this work are novel in several ways. First, there are no other published studies looking at administration of FGF19 to the hindbrain. Moreover, there is only one other study looking at FGF19 administration to T1DM mice. Next, there are no extant studies identifying the electrophysiological effects of FGF19. There are a small number of papers that performed electrophysiology with other FGFs but these mostly focused on calcium. Finally, there are vanishingly few papers that have explored the role of the AP in local DVC signaling. While there are studies that show the AP projects extensively throughout the NTS and

DMV, there are very few, if any, papers that have established that the AP can modulate activity in the DMV. This implies that the AP may participate in the vago-vagal reflex and warrants extensive future study. Due to their novelty, the papers contained in this dissertation cannot be considered the definitive work on the subject. These papers contain many novel findings but do not fully explore their underlying mechanisms or their relevance to metabolic regulation. Instead, this work should serve as the first step in a long line of research that may lead to better patient outcomes or at least a better understanding of how the brain can be harnessed to improve metabolism.

Appendices

Abbreviations

μg ..... Micrograms

4-AP 4-aminopyridine

4V ..... Fourth cerebroventricular

ACSF .....Artificial cerebrospinal fluid

AgRP ..... Agouti-related peptide

Akt ..... Protein kinase B

AMPA ..... α-amino-3-hydroxy-5-methyl-4-isoxazolepropionic acid

ANOVA ..... Analysis of variance

AP .....Area postrema

AP .....Action potential

ATP .....Adenosine triphosphate

AUC .....Area under the curve

BAT ..... Brown adipose tissue

CA ..... Citric acid

CCK ..... Cholecystokinin

CNS .....Central nervous system

CYP7A1 .....Cholesterol 7α-hydroxylase

DAG ..... Diacylglycerol

DIO ..... Diet-induced obsesity

DMV .....Dorsal motor nucleus of the vagus

DVC .....Dorsal vagal complex

EPSC ..... Excitatory post-synaptic current

FGF ..... Fibroblast growth factor

FGF19 ..... Fibroblast growth factor 19

FGFR ..... Fibroblast growth factor receptor

FXR ..... Farnesoid X receptor

GABA ..... Gamma-amino butyric acid

GFP ..... Green fluorescent protein

GI ..... Gastrointestinal

GLP-1 ..... Glucagon-like peptide-1

HEPES ..... 4-(2-hydroxyethyl)-1-piperazineethanesulfonic acid

HFD ..... High-fat diet

HGP ..... Hepatic glucose production

Hr ..... Hours

HS ..... Heparin sulfate

HSPG ..... Heparin sulfate proteoglycan

Hz ..... Hertz

I_{AP} ..... Spontaneous sodium action potential current

ICV ..... Intracerebroventricular

iFGF ..... Intracellular fibroblast growth factor

IP_3 ..... Inositol triphosphate

IPSC ..... Inhibitory post-synaptic current

K-S ..... Kolmogorov-Smirnov two sample test

KYN ..... Kynurenic acid

MAP .....Mitogen-activated protein kinase

mEPSC ..... Miniature excitatory post-synaptic current

min .....Minutes

MNI-caged glutamate 4-Methoxy-7-nitroindolinyl-caged-L-glutamate

ms .....Milliseconds

MSA ..... (-)-scopolamine methyl bromide (methylscopolamine)

mV.....Millivolts

MΩ ..... Megaohms

NADPH..... Nicotinamide adenine dinucleotide phosphate

Na_v .....Voltage-activated sodium channels

NMDA..... N-methyl-D-aspartic acid

NPY..... Neuropeptide Y

NTS ..... Nucleus tractus solitarius

pA..... Picoamps

PBS ..... Phosphate-buffered saline

PCR ..... Polymerase chain reaction

pERK..... Phosphorylated extracellular signal-related kinase

PI3K ..... Phosphoinositide 3-kinase

PIP_2 ..... Phosphatidylinositol 4,5-bisphosphate

PKC.....Protein kinase C

PLC ..... Phospholipase C

PPAR .....Peroxisome proliferator-activated receptor

PTX ..... Picrotoxin

PYY ..... Peptide YY

R_{in} ..... Input resistance

RMP ..... Resting membrane potential

S ..... seconds

sEPSC ..... spontanerous excitatory post-synaptic potential

sIPSC ..... spontaneous inhibitory post-synaptic potential

STZ ..... Streptozotocin

T1DM ..... Type I diabetes mellitus

TEA ..... Tetraethylamine

TRH ..... Thyrotropin-releasing hormone

TTX ..... Tetrodotoxin

UCP ..... Uncoupling protein

VEH ..... Vehicle

VSG ..... Vertical sleeve gastrectomy

WAT ..... White adipose tissue

Equipment Used

List of equipment used for electrophysiology and brain slice preparation

Vibrating Microtome ..... Vibratome 1000 Plus

Pipette Puller ..... Sutter P-87

Isolation Table ..... TMC

Microscope ..... Olympus BX51WI

Digitizer ..... Axon Digidata 1440A

Patch-Clamp Amplifier ..... Axon Multiclamp 700B

List of equipment used for immunohistochemistry and imaging

Microscope ..... Olympus BX41

Camera ..... Spot RT Slider

Cryostat ..... Microm HM505 E

Patch-clamp rig diagram

Front Panel Connections

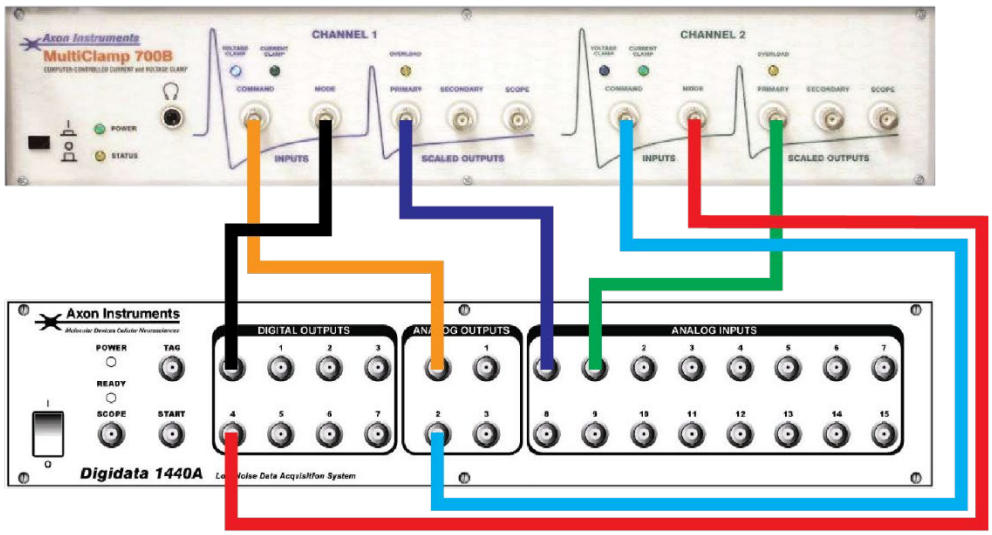

Rear Panel Connections

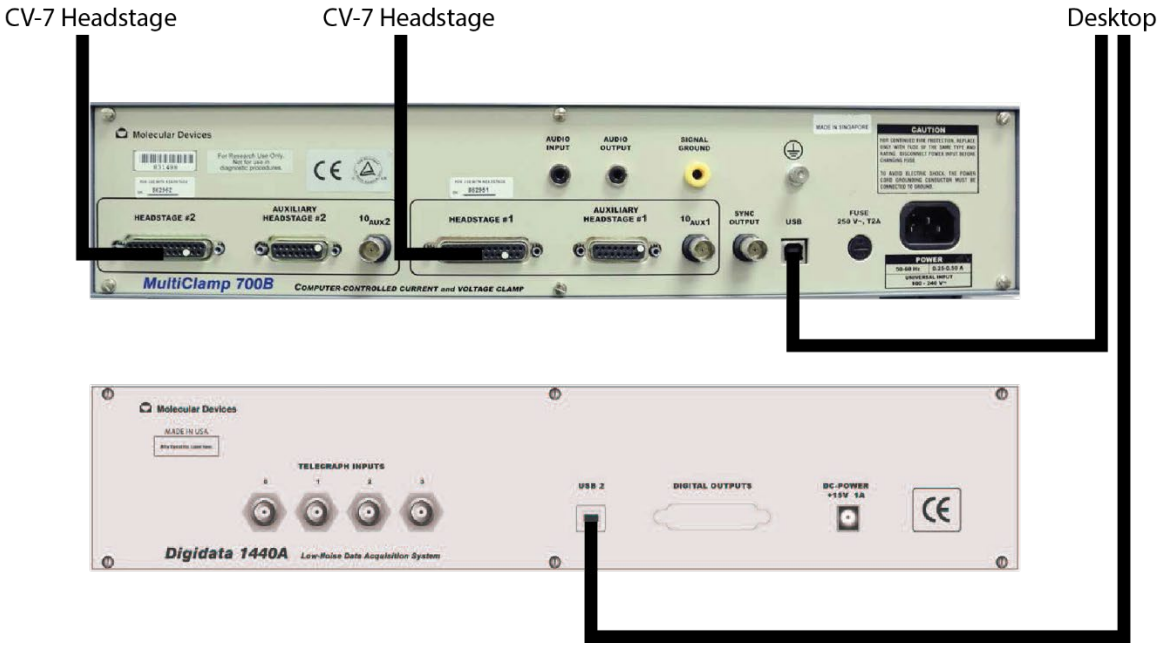

Patch Clamp Frequency Response Calculator and Circuit Diagram

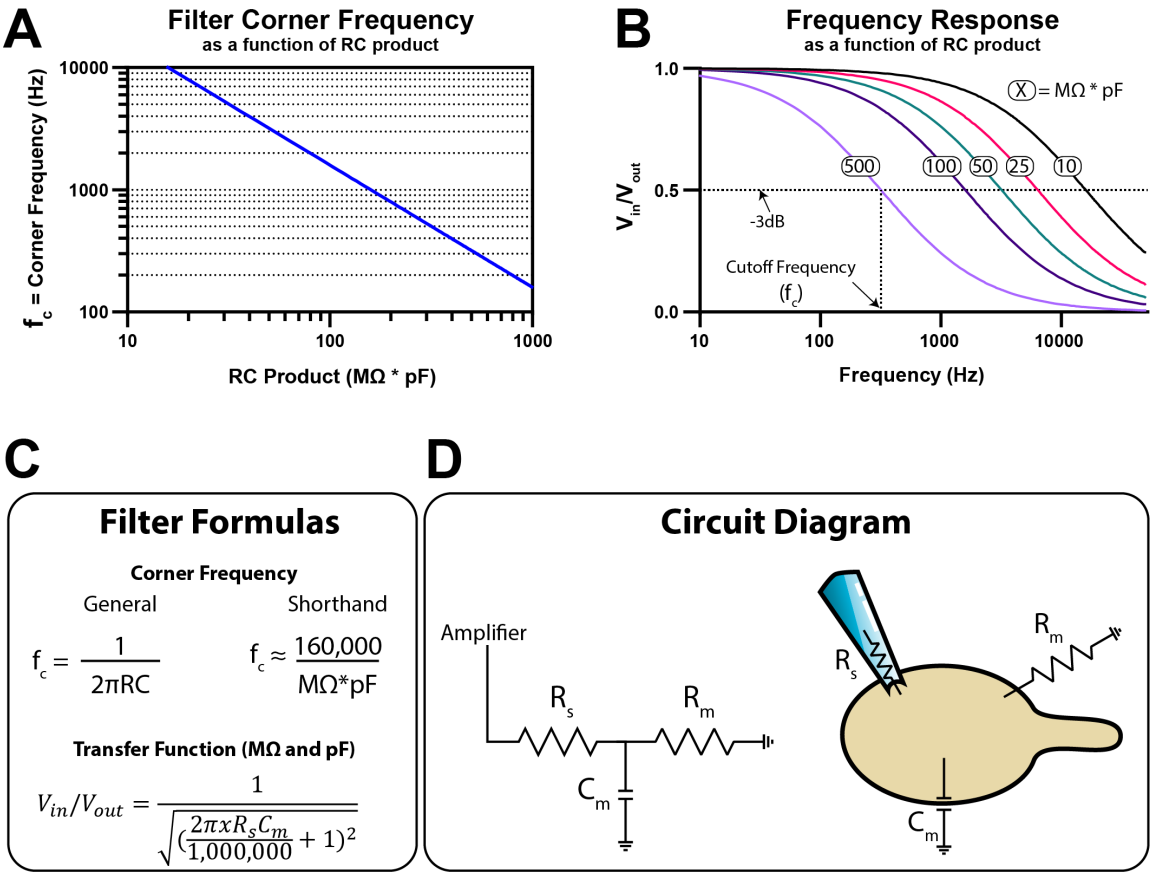

This is an infographic made to illustrate the effects of series resistance (R_s) and membrane capacitance (C_m) on the frequency response characteristics of patch clamp recordings. The resistance and capacitance of neurons are set up in such a way as to create a 1st order lowpass filter on recorded currents (also called an RC filter). Typical resistance and capacitance values are in Ohms (Ω) and Farads (F). However, R_s and C_m are usually measured in MΩ and pF so the infographic was designed with this in mind.

(**A**) Graphical representation -3dB cutoff frequency (corner frequency) as a function of the RC product (R_s*C_m = MΩ*pF). **(B)** Frequency response from 10Hz – 20,000 Hz for various RC product values. **(C)** Formula for calculation of -3dB cutoff frequency of an RC filter. General formula is given first. The shorthand formula is for "quick and dirty" calculation of cutoff frequency but is still 99.5% accurate. The final formula is the RC filter transfer function and is used to calculate the curves in B. For this formula, R_s and C_m must be in MΩ and pF respectively. **(D)** Circuit diagram for patch clamp recordings. The RC filter is created by R_s and C_m. R_m is assumed to be so much larger than R_s that it can be ignored.

References

1. Prechtl, J.C. and T.L. Powley, *The fiber composition of the abdominal vagus of the rat.* Anat Embryol (Berl), 1990. **181**(2): p. 101-15.
2. Wang, F.B. and T.L. Powley, *Topographic inventories of vagal afferents in gastrointestinal muscle.* J Comp Neurol, 2000. **421**(3): p. 302-24.
3. Zhuo, H., H. Ichikawa, and C.J. Helke, *Neurochemistry of the nodose ganglion.* Prog Neurobiol, 1997. **52**(2): p. 79-107.
4. Altschuler, S.M., et al., *Viscerotopic representation of the upper alimentary tract in the rat: sensory ganglia and nuclei of the solitary and spinal trigeminal tracts.* J Comp Neurol, 1989. **283**(2): p. 248-68.
5. Rogers, R.C., D.M. McTigue, and G.E. Hermann, *Vagovagal reflex control of digestion: afferent modulation by neural and "endoneurocrine" factors.* Am J Physiol, 1995. **268**(1 Pt 1): p. G1-10.
6. Smith, B.N., et al., *Vagally evoked synaptic currents in the immature rat nucleus tractus solitarii in an intact in vitro preparation.* J Physiol, 1998. **512 (Pt 1)**: p. 149-62.
7. Berthoud, H.R., et al., *Neuroanatomy of extrinsic afferents supplying the gastrointestinal tract.* Neurogastroenterol Motil, 2004. **16 Suppl 1**: p. 28-33.
8. Berthoud, H.R., et al., *Distribution and structure of vagal afferent intraganglionic laminar endings (IGLEs) in the rat gastrointestinal tract.* Anat Embryol (Berl), 1997. **195**(2): p. 183-91.
9. Berthoud, H.R. and T.L. Powley, *Vagal afferent innervation of the rat fundic stomach: morphological characterization of the gastric tension receptor.* J Comp Neurol, 1992. **319**(2): p. 261-76.
10. Lynn, P.A. and L.A. Blackshaw, *In vitro recordings of afferent fibres with receptive fields in the serosa, muscle and mucosa of rat colon.* J Physiol, 1999. **518**(Pt 1): p. 271-82.
11. Berthoud, H.R., P.A. Lynn, and L.A. Blackshaw, *Vagal and spinal mechanosensors in the rat stomach and colon have multiple receptive fields.* Am J Physiol Regul Integr Comp Physiol, 2001. **280**(5): p. R1371-81.
12. Johnson, L.R., *Physiology of the gastrointestinal tract*. 2012, Academic Press: London.
13. Mei, N., *Intestinal chemosensitivity.* Physiol Rev, 1985. **65**(2): p. 211-37.
14. Schwartz, G.J. and T.H. Moran, *CCK elicits and modulates vagal afferent activity arising from gastric and duodenal sites.* Ann N Y Acad Sci, 1994. **713**: p. 121-8.
15. Altschuler, S.M., et al., *The central organization of the vagus nerve innervating the colon of the rat.* Gastroenterology, 1993. **104**(2): p. 502-9.
16. Altschuler, S.M., et al., *Representation of the cecum in the lateral dorsal motor nucleus of the vagus nerve and commissural subnucleus of the nucleus tractus solitarii in rat.* J Comp Neurol, 1991. **304**(2): p. 261-74.
17. Hermann, G.E., et al., *Proteinase-activated receptors in the nucleus of the solitary tract: evidence for glial-neural interactions in autonomic control of the stomach.* J Neurosci, 2009. **29**(29): p. 9292-300.

18. Seagard, J.L., C. Dean, and F.A. Hopp, *Role of glutamate receptors in transmission of vagal cardiac input to neurones in the nucleus tractus solitarii in dogs.* J Physiol, 1999. **520 Pt 1**: p. 243-53.
19. Fortin, G. and J. Champagnat, *Spontaneous synaptic activities in rat nucleus tractus solitarius neurons in vitro: evidence for re-excitatory processing.* Brain Res, 1993. **630**(1-2): p. 125-35.
20. McCann, M.J. and R.C. Rogers, *Impact of antral mechanoreceptor activation on the vago-vagal reflex in the rat: functional zonation of responses.* J Physiol, 1992. **453**: p. 401-11.
21. Travagli, R.A., et al., *Glutamate and GABA-mediated synaptic currents in neurons of the rat dorsal motor nucleus of the vagus.* Am J Physiol, 1991. **260**(3 Pt 1): p. G531-6.
22. Sivarao, D.V., Z.K. Krowicki, and P.J. Hornby, *Role of GABAA receptors in rat hindbrain nuclei controlling gastric motor function.* Neurogastroenterol Motil, 1998. **10**(4): p. 305-13.
23. Hornby, P.J., *Receptors and transmission in the brain-gut axis. II. Excitatory amino acid receptors in the brain-gut axis.* Am J Physiol Gastrointest Liver Physiol, 2001. **280**(6): p. G1055-60.
24. Martinez-Pena y Valenzuela, I., et al., *Norepinephrine effects on identified neurons of the rat dorsal motor nucleus of the vagus.* Am J Physiol Gastrointest Liver Physiol, 2004. **286**(2): p. G333-9.
25. Rogers, R.C., R.A. Travagli, and G.E. Hermann, *Noradrenergic neurons in the rat solitary nucleus participate in the esophageal-gastric relaxation reflex.* Am J Physiol Regul Integr Comp Physiol, 2003. **285**(2): p. R479-89.
26. Fox, E.A. and T.L. Powley, *Longitudinal columnar organization within the dorsal motor nucleus represents separate branches of the abdominal vagus.* Brain Res, 1985. **341**(2): p. 269-82.
27. Shapiro, R.E. and R.R. Miselis, *The central organization of the vagus nerve innervating the stomach of the rat.* J Comp Neurol, 1985. **238**(4): p. 473-88.
28. Norgren, R. and G.P. Smith, *Central distribution of subdiaphragmatic vagal branches in the rat.* J Comp Neurol, 1988. **273**(2): p. 207-23.
29. Berthoud, H.R., N.R. Carlson, and T.L. Powley, *Topography of efferent vagal innervation of the rat gastrointestinal tract.* Am J Physiol, 1991. **260**(1 Pt 2): p. R200-7.
30. Armstrong, D.M., et al., *Co-localization of choline acetyltransferase and tyrosine hydroxylase within neurons of the dorsal motor nucleus of the vagus.* J Chem Neuroanat, 1990. **3**(2): p. 133-40.
31. Kalia, M., et al., *Evidence for the existence of putative dopamine-, adrenaline- and noradrenaline-containing vagal motor neurons in the brainstem of the rat.* Neurosci Lett, 1984. **50**(1-3): p. 57-62.
32. Krowicki, Z.K., et al., *Distribution of nitric oxide synthase in rat dorsal vagal complex and effects of microinjection of nitric oxide compounds upon gastric motor function.* J Comp Neurol, 1997. **377**(1): p. 49-69.
33. Zheng, Z.L., R.C. Rogers, and R.A. Travagli, *Selective gastric projections of nitric oxide synthase-containing vagal brainstem neurons.* Neuroscience, 1999. **90**(2): p. 685-94.

34. Guo, J.J., et al., *Catecholaminergic neurons in rat dorsal motor nucleus of vagus project selectively to gastric corpus.* Am J Physiol Gastrointest Liver Physiol, 2001. **280**(3): p. G361-7.
35. Gao, H., et al., *Morphological and electrophysiological features of motor neurons and putative interneurons in the dorsal vagal complex of rats and mice.* Brain Res, 2009. **1291**: p. 40-52.
36. Berthoud, H.R., *Anatomical demonstration of vagal input to nicotinamide acetamide dinucleotide phosphate diaphorase-positive (nitrergic) neurons in rat fundic stomach.* J Comp Neurol, 1995. **358**(3): p. 428-39.
37. Travagli, R.A., et al., *Brainstem circuits regulating gastric function.* Annu Rev Physiol, 2006. **68**: p. 279-305.
38. Rogers, R.C. and G.E. Hermann, *Vagal afferent stimulation-evoked gastric secretion suppressed by paraventricular nucleus lesion.* J Auton Nerv Syst, 1985. **13**(3): p. 191-9.
39. Naseri, M.K., D. Hutson, and D. Grundy, *Vagal influences on gastric acid secretion in response to gastric distension in the ferret.* J Auton Nerv Syst, 1991. **36**(1): p. 25-31.
40. Raybould, H.E. and Y. Tache, *Capsaicin-sensitive vagal afferent fibers and stimulation of gastric acid secretion in anesthetized rats.* Eur J Pharmacol, 1989. **167**(2): p. 237-43.
41. Ionescu, E., et al., *Increases in plasma insulin levels in response to electrical stimulation of the dorsal motor nucleus of the vagus nerve.* Endocrinology, 1983. **112**(3): p. 904-10.
42. Mussa, B.M., et al., *Effects of nitric oxide synthase blockade on dorsal vagal stimulation-induced pancreatic insulin secretion.* Brain Res, 2011. **1394**: p. 62-70.
43. Mussa, B.M. and A.J. Verberne, *Activation of the dorsal vagal nucleus increases pancreatic exocrine secretion in the rat.* Neurosci Lett, 2008. **433**(1): p. 71-6.
44. Boychuk, C.R., et al., *A hindbrain inhibitory microcircuit mediates vagally-coordinated glucose regulation.* Sci Rep, 2019. **9**(1): p. 2722.
45. Zsombok, A., et al., *Immunohistochemical localization of transient receptor potential vanilloid type 1 and insulin receptor substrate 2 and their co-localization with liver-related neurons in the hypothalamus and brainstem.* Brain Res, 2011. **1398**: p. 30-9.
46. Berthoud, H.R., M. Kressel, and W.L. Neuhuber, *An anterograde tracing study of the vagal innervation of rat liver, portal vein and biliary system.* Anat Embryol (Berl), 1992. **186**(5): p. 431-42.
47. Pocai, A., et al., *A brain-liver circuit regulates glucose homeostasis.* Cell Metab, 2005. **1**(1): p. 53-61.
48. Lam, C.K., et al., *Activation of N-methyl-D-aspartate (NMDA) receptors in the dorsal vagal complex lowers glucose production.* J Biol Chem, 2010. **285**(29): p. 21913-21.
49. Williams, K.W., A. Zsombok, and B.N. Smith, *Rapid inhibition of neurons in the dorsal motor nucleus of the vagus by leptin.* Endocrinology, 2007. **148**(4): p. 1868-81.

50. Blake, C.B. and B.N. Smith, *Insulin reduces excitation in gastric-related neurons of the dorsal motor nucleus of the vagus.* Am J Physiol Regul Integr Comp Physiol, 2012. **303**(8): p. R807-14.
51. Wean, J.B. and B.N. Smith, *FGF19 in the Hindbrain Lowers Blood Glucose and Alters Excitability of Vagal Motor Neurons in Hyperglycemic Mice.* Endocrinology, 2021. **162**(4).
52. Browning, K.N. and R.A. Travagli, *The peptide TRH uncovers the presence of presynaptic 5-HT1A receptors via activation of a second messenger pathway in the rat dorsal vagal complex.* J Physiol, 2001. **531**(Pt 2): p. 425-35.
53. Travagli, R.A. and R.A. Gillis, *Hyperpolarization-activated currents, IH and IKIR, in rat dorsal motor nucleus of the vagus neurons in vitro.* J Neurophysiol, 1994. **71**(4): p. 1308-17.
54. Babic, T., K.N. Browning, and R.A. Travagli, *Differential organization of excitatory and inhibitory synapses within the rat dorsal vagal complex.* Am J Physiol Gastrointest Liver Physiol, 2011. **300**(1): p. G21-32.
55. Browning, K.N., W.E. Renehan, and R.A. Travagli, *Electrophysiological and morphological heterogeneity of rat dorsal vagal neurones which project to specific areas of the gastrointestinal tract.* J Physiol, 1999. **517 (Pt 2)**: p. 521-32.
56. Merchenthaler, I., *Neurons with access to the general circulation in the central nervous system of the rat: a retrograde tracing study with fluoro-gold.* Neuroscience, 1991. **44**(3): p. 655-62.
57. Miller, A.D. and R.A. Leslie, *The area postrema and vomiting.* Front Neuroendocrinol, 1994. **15**(4): p. 301-20.
58. Borison, H.L., *Area postrema: chemoreceptor circumventricular organ of the medulla oblongata.* Prog Neurobiol, 1989. **32**(5): p. 351-90.
59. Ritter, S., J.J. McGlone, and K.W. Kelley, *Absence of lithium-induced taste aversion after area postrema lesion.* Brain Res, 1980. **201**(2): p. 501-6.
60. Barth, S.W., et al., *Peripheral amylin activates circumventricular organs expressing calcitonin receptor a/b subtypes and receptor-activity modifying proteins in the rat.* Brain Res, 2004. **997**(1): p. 97-102.
61. Hsu, J.Y., et al., *Non-homeostatic body weight regulation through a brainstem-restricted receptor for GDF15.* Nature, 2017. **550**(7675): p. 255-259.
62. Yang, L., et al., *GFRAL is the receptor for GDF15 and is required for the anti-obesity effects of the ligand.* Nat Med, 2017. **23**(10): p. 1158-1166.
63. Emmerson, P.J., et al., *The metabolic effects of GDF15 are mediated by the orphan receptor GFRAL.* Nat Med, 2017. **23**(10): p. 1215-1219.
64. Kawatani, M., Y. Yamada, and M. Kawatani, *Glucagon-like peptide-1 (GLP-1) action in the mouse area postrema neurons.* Peptides, 2018. **107**: p. 68-74.
65. Zuger, D., et al., *Amylin and GLP-1 target different populations of area postrema neurons that are both modulated by nutrient stimuli.* Physiol Behav, 2013. **112-113**: p. 61-9.
66. Vigier, D. and A. Rouviere, *Afferent and efferent connections of the area postrema demonstrated by the horseradish peroxidase method.* Arch Ital Biol, 1979. **117**(4): p. 325-39.

67. van der Kooy, D. and L.Y. Koda, *Organization of the projections of a circumventricular organ: the area postrema in the rat.* J Comp Neurol, 1983. **219**(3): p. 328-38.
68. Zhang, C., et al., *Area Postrema Cell Types that Mediate Nausea-Associated Behaviors.* Neuron, 2021. **109**(3): p. 461-472 e5.
69. Gross, P.M., et al., *Microvascular specializations promoting rapid interstitial solute dispersion in nucleus tractus solitarius.* Am J Physiol, 1990. **259**(6 Pt 2): p. R1131-8.
70. Boychuk, C.R., et al., *Glucose sensing by GABAergic neurons in the mouse nucleus tractus solitarii.* J Neurophysiol, 2015. **114**(2): p. 999-1007.
71. Lamy, C.M., et al., *Hypoglycemia-activated GLUT2 neurons of the nucleus tractus solitarius stimulate vagal activity and glucagon secretion.* Cell Metab, 2014. **19**(3): p. 527-38.
72. Williams, K.W. and B.N. Smith, *Rapid inhibition of neural excitability in the nucleus tractus solitarii by leptin: implications for ingestive behaviour.* J Physiol, 2006. **573**(Pt 2): p. 395-412.
73. Kanoski, S.E., et al., *Leptin signaling in the medial nucleus tractus solitarius reduces food seeking and willingness to work for food.* Neuropsychopharmacology, 2014. **39**(3): p. 605-13.
74. Grill, H.J., et al., *Evidence that the caudal brainstem is a target for the inhibitory effect of leptin on food intake.* Endocrinology, 2002. **143**(1): p. 239-46.
75. Huo, L., et al., *Leptin and the control of food intake: neurons in the nucleus of the solitary tract are activated by both gastric distension and leptin.* Endocrinology, 2007. **148**(5): p. 2189-97.
76. Hayes, M.R., et al., *Endogenous leptin signaling in the caudal nucleus tractus solitarius and area postrema is required for energy balance regulation.* Cell Metab, 2010. **11**(1): p. 77-83.
77. Blake, C.B. and B.N. Smith, *cAMP-dependent insulin modulation of synaptic inhibition in neurons of the dorsal motor nucleus of the vagus is altered in diabetic mice.* Am J Physiol Regul Integr Comp Physiol, 2014. **307**(6): p. R711-20.
78. Babic, T., et al., *Pancreatic insulin and exocrine secretion are under the modulatory control of distinct subpopulations of vagal motoneurones in the rat.* J Physiol, 2012. **590**(15): p. 3611-22.
79. LaPierre, M.P., et al., *Glucagon signalling in the dorsal vagal complex is sufficient and necessary for high-protein feeding to regulate glucose homeostasis in vivo.* EMBO Rep, 2015. **16**(10): p. 1299-307.
80. Wan, S., K.N. Browning, and R.A. Travagli, *Glucagon-like peptide-1 modulates synaptic transmission to identified pancreas-projecting vagal motoneurons.* Peptides, 2007. **28**(11): p. 2184-91.
81. Wan, S., F.H. Coleman, and R.A. Travagli, *Glucagon-like peptide-1 excites pancreas-projecting preganglionic vagal motoneurons.* Am J Physiol Gastrointest Liver Physiol, 2007. **292**(6): p. G1474-82.
82. Merchenthaler, I., M. Lane, and P. Shughrue, *Distribution of pre-pro-glucagon and glucagon-like peptide-1 receptor messenger RNAs in the rat central nervous system.* J Comp Neurol, 1999. **403**(2): p. 261-80.

83. Yamamoto, H., et al., *Glucagon-like peptide-1-responsive catecholamine neurons in the area postrema link peripheral glucagon-like peptide-1 with central autonomic control sites.* J Neurosci, 2003. **23**(7): p. 2939-46.
84. Hayes, M.R., L. Bradley, and H.J. Grill, *Endogenous hindbrain glucagon-like peptide-1 receptor activation contributes to the control of food intake by mediating gastric satiation signaling.* Endocrinology, 2009. **150**(6): p. 2654-9.
85. Swartz, E.M., et al., *Ghrelin increases vagally mediated gastric activity by central sites of action.* Neurogastroenterol Motil, 2014. **26**(2): p. 272-82.
86. Faulconbridge, L.F., et al., *Hyperphagic effects of brainstem ghrelin administration.* Diabetes, 2003. **52**(9): p. 2260-5.
87. Fry, M. and A.V. Ferguson, *Ghrelin modulates electrical activity of area postrema neurons.* Am J Physiol Regul Integr Comp Physiol, 2009. **296**(3): p. R485-92.
88. Ricardo, J.A. and E.T. Koh, *Anatomical evidence of direct projections from the nucleus of the solitary tract to the hypothalamus, amygdala, and other forebrain structures in the rat.* Brain Res, 1978. **153**(1): p. 1-26.
89. van der Kooy, D., et al., *The organization of projections from the cortex, amygdala, and hypothalamus to the nucleus of the solitary tract in rat.* J Comp Neurol, 1984. **224**(1): p. 1-24.
90. Geerling, J.C., et al., *Paraventricular hypothalamic nucleus: axonal projections to the brainstem.* J Comp Neurol, 2010. **518**(9): p. 1460-99.
91. Lam, T.K., et al., *Hypothalamic sensing of circulating fatty acids is required for glucose homeostasis.* Nat Med, 2005. **11**(3): p. 320-7.
92. Lam, C.K., et al., *Hypothalamic nutrient sensing activates a forebrain-hindbrain neuronal circuit to regulate glucose production in vivo.* Diabetes, 2011. **60**(1): p. 107-13.
93. Baek, S.J., et al., *Nonsteroidal anti-inflammatory drug-activated gene-1 over expression in transgenic mice suppresses intestinal neoplasia.* Gastroenterology, 2006. **131**(5): p. 1553-60.
94. Johnen, H., et al., *Tumor-induced anorexia and weight loss are mediated by the TGF-beta superfamily cytokine MIC-1.* Nat Med, 2007. **13**(11): p. 1333-40.
95. Mullican, S.E., et al., *GFRAL is the receptor for GDF15 and the ligand promotes weight loss in mice and nonhuman primates.* Nat Med, 2017. **23**(10): p. 1150-1157.
96. Tsai, V.W., et al., *TGF-b superfamily cytokine MIC-1/GDF15 is a physiological appetite and body weight regulator.* PLoS One, 2013. **8**(2): p. e55174.
97. Xiong, Y., et al., *Long-acting MIC-1/GDF15 molecules to treat obesity: Evidence from mice to monkeys.* Sci Transl Med, 2017. **9**(412).
98. Roep, B.O., et al., *Type 1 diabetes mellitus as a disease of the beta-cell (do not blame the immune system?).* Nat Rev Endocrinol, 2021. **17**(3): p. 150-161.
99. Rizza, R.A., *Pathogenesis of fasting and postprandial hyperglycemia in type 2 diabetes: implications for therapy.* Diabetes, 2010. **59**(11): p. 2697-707.
100. Chen, L., D.J. Magliano, and P.Z. Zimmet, *The worldwide epidemiology of type 2 diabetes mellitus--present and future perspectives.* Nat Rev Endocrinol, 2011. **8**(4): p. 228-36.
101. Cherrington, A.D., *Banting Lecture 1997. Control of glucose uptake and release by the liver in vivo.* Diabetes, 1999. **48**(5): p. 1198-214.

102. Baron, A.D., et al., *Rates and tissue sites of non-insulin- and insulin-mediated glucose uptake in humans.* Am J Physiol, 1988. **255**(6 Pt 1): p. E769-74.
103. Huang, S.C., et al., *Noninvasive determination of local cerebral metabolic rate of glucose in man.* Am J Physiol, 1980. **238**(1): p. E69-82.
104. Firth, R.G., et al., *Postprandial hyperglycemia in patients with noninsulin-dependent diabetes mellitus. Role of hepatic and extrahepatic tissues.* J Clin Invest, 1986. **77**(5): p. 1525-32.
105. Gerich, J.E., et al., *Contribution of impaired muscle glucose clearance to reduced postabsorptive systemic glucose clearance in NIDDM.* Diabetes, 1990. **39**(2): p. 211-6.
106. Campbell, P.J., L.J. Mandarino, and J.E. Gerich, *Quantification of the relative impairment in actions of insulin on hepatic glucose production and peripheral glucose uptake in non-insulin-dependent diabetes mellitus.* Metabolism, 1988. **37**(1): p. 15-21.
107. Consoli, A., et al., *Predominant role of gluconeogenesis in increased hepatic glucose production in NIDDM.* Diabetes, 1989. **38**(5): p. 550-7.
108. DeFronzo, R.A., D. Simonson, and E. Ferrannini, *Hepatic and peripheral insulin resistance: a common feature of type 2 (non-insulin-dependent) and type 1 (insulin-dependent) diabetes mellitus.* Diabetologia, 1982. **23**(4): p. 313-9.
109. Magnusson, I., et al., *Increased rate of gluconeogenesis in type II diabetes mellitus. A 13C nuclear magnetic resonance study.* J Clin Invest, 1992. **90**(4): p. 1323-7.
110. Bernard, C., *Leçons de Ohysiologie Experimentale Appliqués á lá Medecine*. 1854, Paris: J.B. Baillière.
111. Grill, H.J., *Distributed neural control of energy balance: contributions from hindbrain and hypothalamus.* Obesity (Silver Spring), 2006. **14 Suppl 5**: p. 216S-221S.
112. Scarlett, J.M. and M.W. Schwartz, *Gut-brain mechanisms controlling glucose homeostasis.* F1000Prime Rep, 2015. **7**: p. 12.
113. Schwartz, M.W., et al., *Cooperation between brain and islet in glucose homeostasis and diabetes.* Nature, 2013. **503**(7474): p. 59-66.
114. Schwartz, M.W., et al., *Central nervous system control of food intake.* Nature, 2000. **404**(6778): p. 661-71.
115. Deem, J.D., et al., *How Should We Think About the Role of the Brain in Glucose Homeostasis and Diabetes?* Diabetes, 2017. **66**(7): p. 1758-1765.
116. Trowell OA, C.B., Willmer EN, *Studies on the Growth of Tissues in vitro: VI. The Effects of some Tissue Extracts on the Growth of Periosteal Fibroblasts.* J Exp Biol, 1939. **16**: p. 60-70.
117. Armelin, H.A., *Pituitary extracts and steroid hormones in the control of 3T3 cell growth.* Proc Natl Acad Sci U S A, 1973. **70**(9): p. 2702-6.
118. Gospodarowicz, D., *Purification of a fibroblast growth factor from bovine pituitary.* J Biol Chem, 1975. **250**(7): p. 2515-20.
119. Lemmon, S.K. and R.A. Bradshaw, *Purification and partial characterization of bovine pituitary fibroblast growth factor.* J Cell Biochem, 1983. **21**(3): p. 195-208.
120. Lemmon, S.K., et al., *Bovine fibroblast growth factor: comparison of brain and pituitary preparations.* J Cell Biol, 1982. **95**(1): p. 162-9.

121. Thomas, K.A., et al., *Brain fibroblast growth factor: nonidentity with myelin basic protein fragments.* J Biol Chem, 1980. **255**(12): p. 5517-20.
122. Thomas, K.A., M. Rios-Candelore, and S. Fitzpatrick, *Purification and characterization of acidic fibroblast growth factor from bovine brain.* Proc Natl Acad Sci U S A, 1984. **81**(2): p. 357-61.
123. Ornitz, D.M. and N. Itoh, *The Fibroblast Growth Factor signaling pathway.* Wiley Interdiscip Rev Dev Biol, 2015. **4**(3): p. 215-66.
124. Matsuo, I. and C. Kimura-Yoshida, *Extracellular modulation of Fibroblast Growth Factor signaling through heparan sulfate proteoglycans in mammalian development.* Curr Opin Genet Dev, 2013. **23**(4): p. 399-407.
125. Lin, X., *Functions of heparan sulfate proteoglycans in cell signaling during development.* Development, 2004. **131**(24): p. 6009-21.
126. Belov, A.A. and M. Mohammadi, *Molecular mechanisms of fibroblast growth factor signaling in physiology and pathology.* Cold Spring Harb Perspect Biol, 2013. **5**(6).
127. Kim, M.J., et al., *The heparan sulfate proteoglycan agrin modulates neurite outgrowth mediated by FGF-2.* J Neurobiol, 2003. **55**(3): p. 261-77.
128. Cotman, S.L., W. Halfter, and G.J. Cole, *Identification of extracellular matrix ligands for the heparan sulfate proteoglycan agrin.* Exp Cell Res, 1999. **249**(1): p. 54-64.
129. Aviezer, D., et al., *Perlecan, basal lamina proteoglycan, promotes basic fibroblast growth factor-receptor binding, mitogenesis, and angiogenesis.* Cell, 1994. **79**(6): p. 1005-13.
130. Rapraeger, A.C., A. Krufka, and B.B. Olwin, *Requirement of heparan sulfate for bFGF-mediated fibroblast growth and myoblast differentiation.* Science, 1991. **252**(5013): p. 1705-8.
131. Zhang, X., et al., *Receptor specificity of the fibroblast growth factor family. The complete mammalian FGF family.* J Biol Chem, 2006. **281**(23): p. 15694-700.
132. Ornitz, D.M., et al., *Receptor specificity of the fibroblast growth factor family.* J Biol Chem, 1996. **271**(25): p. 15292-7.
133. Ornitz, D.M., et al., *Heparin is required for cell-free binding of basic fibroblast growth factor to a soluble receptor and for mitogenesis in whole cells.* Mol Cell Biol, 1992. **12**(1): p. 240-7.
134. Olwin, B.B. and A. Rapraeger, *Repression of myogenic differentiation by aFGF, bFGF, and K-FGF is dependent on cellular heparan sulfate.* J Cell Biol, 1992. **118**(3): p. 631-9.
135. Makarenkova, H.P., et al., *Differential interactions of FGFs with heparan sulfate control gradient formation and branching morphogenesis.* Sci Signal, 2009. **2**(88): p. ra55.
136. Chang, Z., et al., *Differential ability of heparan sulfate proteoglycans to assemble the fibroblast growth factor receptor complex in situ.* FASEB J, 2000. **14**(1): p. 137-44.
137. Allen, B.L. and A.C. Rapraeger, *Spatial and temporal expression of heparan sulfate in mouse development regulates FGF and FGF receptor assembly.* J Cell Biol, 2003. **163**(3): p. 637-48.

138. Shimokawa, K., et al., *Cell surface heparan sulfate chains regulate local reception of FGF signaling in the mouse embryo.* Dev Cell, 2011. **21**(2): p. 257-72.
139. Patel, V.N., et al., *Specific heparan sulfate structures modulate FGF10-mediated submandibular gland epithelial morphogenesis and differentiation.* J Biol Chem, 2008. **283**(14): p. 9308-17.
140. Escobar Galvis, M.L., et al., *Transgenic or tumor-induced expression of heparanase upregulates sulfation of heparan sulfate.* Nat Chem Biol, 2007. **3**(12): p. 773-8.
141. Prudovsky, I., et al., *Protein-phospholipid interactions in nonclassical protein secretion: problem and methods of study.* Int J Mol Sci, 2013. **14**(2): p. 3734-72.
142. Prudovsky, I., et al., *The non-classical export routes: FGF1 and IL-1alpha point the way.* J Cell Sci, 2003. **116**(Pt 24): p. 4871-81.
143. Miyakawa, K., et al., *A hydrophobic region locating at the center of fibroblast growth factor-9 is crucial for its secretion.* J Biol Chem, 1999. **274**(41): p. 29352-7.
144. Revest, J.M., L. DeMoerlooze, and C. Dickson, *Fibroblast growth factor 9 secretion is mediated by a non-cleaved amino-terminal signal sequence.* J Biol Chem, 2000. **275**(11): p. 8083-90.
145. Miyakawa, K. and T. Imamura, *Secretion of FGF-16 requires an uncleaved bipartite signal sequence.* J Biol Chem, 2003. **278**(37): p. 35718-24.
146. Yuan, H., et al., *Developmental-specific activity of the FGF-4 enhancer requires the synergistic action of Sox2 and Oct-3.* Genes Dev, 1995. **9**(21): p. 2635-45.
147. Krawchuk, D., et al., *FGF4 is a limiting factor controlling the proportions of primitive endoderm and epiblast in the ICM of the mouse blastocyst.* Dev Biol, 2013. **384**(1): p. 65-71.
148. Wang, J., et al., *FGF signaling is required for anterior but not posterior specification of the murine liver bud.* Dev Dyn, 2015. **244**(3): p. 431-43.
149. Yu, K. and D.M. Ornitz, *FGF signaling regulates mesenchymal differentiation and skeletal patterning along the limb bud proximodistal axis.* Development, 2008. **135**(3): p. 483-91.
150. Lu, P., et al., *The apical ectodermal ridge is a timer for generating distal limb progenitors.* Development, 2008. **135**(8): p. 1395-405.
151. Fukuchi-Shimogori, T. and E.A. Grove, *Neocortex patterning by the secreted signaling molecule FGF8.* Science, 2001. **294**(5544): p. 1071-4.
152. Terauchi, A., et al., *Distinct FGFs promote differentiation of excitatory and inhibitory synapses.* Nature, 2010. **465**(7299): p. 783-7.
153. Furusho, M., et al., *Fibroblast growth factor receptor signaling in oligodendrocytes regulates myelin sheath thickness.* J Neurosci, 2012. **32**(19): p. 6631-41.
154. Umemori, H., et al., *FGF22 and its close relatives are presynaptic organizing molecules in the mammalian brain.* Cell, 2004. **118**(2): p. 257-70.
155. Olsen, S.K., et al., *Fibroblast growth factor (FGF) homologous factors share structural but not functional homology with FGFs.* J Biol Chem, 2003. **278**(36): p. 34226-36.
156. Goldfarb, M., et al., *Fibroblast growth factor homologous factors control neuronal excitability through modulation of voltage-gated sodium channels.* Neuron, 2007. **55**(3): p. 449-63.

157. Hsu, W.C., C.L. Nilsson, and F. Laezza, *Role of the axonal initial segment in psychiatric disorders: function, dysfunction, and intervention.* Front Psychiatry, 2014. **5**: p. 109.
158. Xiao, M., et al., *FGF14 localization and organization of the axon initial segment.* Mol Cell Neurosci, 2013. **56**: p. 393-403.
159. Lou, J.Y., et al., *Fibroblast growth factor 14 is an intracellular modulator of voltage-gated sodium channels.* J Physiol, 2005. **569**(Pt 1): p. 179-93.
160. Wang, C., et al., *Fibroblast growth factor homologous factor 13 regulates Na+ channels and conduction velocity in murine hearts.* Circ Res, 2011. **109**(7): p. 775-82.
161. Goetz, R., et al., *Molecular insights into the klotho-dependent, endocrine mode of action of fibroblast growth factor 19 subfamily members.* Mol Cell Biol, 2007. **27**(9): p. 3417-28.
162. Kurosu, H. and O.M. Kuro, *Endocrine fibroblast growth factors as regulators of metabolic homeostasis.* Biofactors, 2009. **35**(1): p. 52-60.
163. Kurosu, H., et al., *Regulation of fibroblast growth factor-23 signaling by klotho.* J Biol Chem, 2006. **281**(10): p. 6120-3.
164. Kurosu, H., et al., *Tissue-specific expression of betaKlotho and fibroblast growth factor (FGF) receptor isoforms determines metabolic activity of FGF19 and FGF21.* J Biol Chem, 2007. **282**(37): p. 26687-26695.
165. Urakawa, I., et al., *Klotho converts canonical FGF receptor into a specific receptor for FGF23.* Nature, 2006. **444**(7120): p. 770-4.
166. Ogawa, Y., et al., *BetaKlotho is required for metabolic activity of fibroblast growth factor 21.* Proc Natl Acad Sci U S A, 2007. **104**(18): p. 7432-7.
167. Wu, X., et al., *Co-receptor requirements for fibroblast growth factor-19 signaling.* J Biol Chem, 2007. **282**(40): p. 29069-72.
168. Fon Tacer, K., et al., *Research resource: Comprehensive expression atlas of the fibroblast growth factor system in adult mouse.* Mol Endocrinol, 2010. **24**(10): p. 2050-64.
169. Jonker, J.W., et al., *A PPARgamma-FGF1 axis is required for adaptive adipose remodelling and metabolic homeostasis.* Nature, 2012. **485**(7398): p. 391-4.
170. Inagaki, T., et al., *Fibroblast growth factor 15 functions as an enterohepatic signal to regulate bile acid homeostasis.* Cell Metab, 2005. **2**(4): p. 217-25.
171. Inagaki, T., et al., *Endocrine regulation of the fasting response by PPARalpha-mediated induction of fibroblast growth factor 21.* Cell Metab, 2007. **5**(6): p. 415-25.
172. Nishimura, T., et al., *Structure and expression of a novel human FGF, FGF-19, expressed in the fetal brain.* Biochim Biophys Acta, 1999. **1444**(1): p. 148-51.
173. Potthoff, M.J., et al., *FGF15/19 regulates hepatic glucose metabolism by inhibiting the CREB-PGC-1alpha pathway.* Cell Metab, 2011. **13**(6): p. 729-38.
174. Borello, U., et al., *FGF15 promotes neurogenesis and opposes FGF8 function during neocortical development.* Neural Dev, 2008. **3**: p. 17.
175. Fisher, F.M., et al., *Integrated regulation of hepatic metabolism by fibroblast growth factor 21 (FGF21) in vivo.* Endocrinology, 2011. **152**(8): p. 2996-3004.
176. Russell, D.W., *The enzymes, regulation, and genetics of bile acid synthesis.* Annu Rev Biochem, 2003. **72**: p. 137-74.

177. Pandak, W.M., et al., *Regulation of cholesterol 7 alpha-hydroxylase mRNA and transcriptional activity by taurocholate and cholesterol in the chronic biliary diverted rat.* J Biol Chem, 1991. **266**(6): p. 3416-21.
178. Kalaany, N.Y. and D.J. Mangelsdorf, *LXRS and FXR: the yin and yang of cholesterol and fat metabolism.* Annu Rev Physiol, 2006. **68**: p. 159-91.
179. Holt, J.A., et al., *Definition of a novel growth factor-dependent signal cascade for the suppression of bile acid biosynthesis.* Genes Dev, 2003. **17**(13): p. 1581-91.
180. Yu, C., et al., *Elevated cholesterol metabolism and bile acid synthesis in mice lacking membrane tyrosine kinase receptor FGFR4.* J Biol Chem, 2000. **275**(20): p. 15482-9.
181. Ito, S., et al., *Impaired negative feedback suppression of bile acid synthesis in mice lacking betaKlotho.* J Clin Invest, 2005. **115**(8): p. 2202-8.
182. Tomiyama, K., et al., *Relevant use of Klotho in FGF19 subfamily signaling system in vivo.* Proc Natl Acad Sci U S A, 2010. **107**(4): p. 1666-71.
183. Tomlinson, E., et al., *Transgenic mice expressing human fibroblast growth factor-19 display increased metabolic rate and decreased adiposity.* Endocrinology, 2002. **143**(5): p. 1741-7.
184. Lowell, B.B., et al., *Development of obesity in transgenic mice after genetic ablation of brown adipose tissue.* Nature, 1993. **366**(6457): p. 740-2.
185. Pinkney, J.H., et al., *Physiological relationships of uncoupling protein-2 gene expression in human adipose tissue in vivo.* J Clin Endocrinol Metab, 2000. **85**(6): p. 2312-7.
186. Fu, L., et al., *Fibroblast growth factor 19 increases metabolic rate and reverses dietary and leptin-deficient diabetes.* Endocrinology, 2004. **145**(6): p. 2594-603.
187. Huang, X., et al., *FGFR4 prevents hyperlipidemia and insulin resistance but underlies high-fat diet induced fatty liver.* Diabetes, 2007. **56**(10): p. 2501-10.
188. Kir, S., et al., *FGF19 as a postprandial, insulin-independent activator of hepatic protein and glycogen synthesis.* Science, 2011. **331**(6024): p. 1621-4.
189. Mackenzie, R.W. and B.T. Elliott, *Akt/PKB activation and insulin signaling: a novel insulin signaling pathway in the treatment of type 2 diabetes.* Diabetes Metab Syndr Obes, 2014. **7**: p. 55-64.
190. Nicholes, K., et al., *A mouse model of hepatocellular carcinoma: ectopic expression of fibroblast growth factor 19 in skeletal muscle of transgenic mice.* Am J Pathol, 2002. **160**(6): p. 2295-307.
191. Suh, J.M., et al., *Endocrinization of FGF1 produces a neomorphic and potent insulin sensitizer.* Nature, 2014. **513**(7518): p. 436-9.
192. Wu, X., et al., *FGF19-induced hepatocyte proliferation is mediated through FGFR4 activation.* J Biol Chem, 2010. **285**(8): p. 5165-70.
193. Yang, C., et al., *Differential specificity of endocrine FGF19 and FGF21 to FGFR1 and FGFR4 in complex with KLB.* PLoS One, 2012. **7**(3): p. e33870.
194. Wu, A.L., et al., *FGF19 regulates cell proliferation, glucose and bile acid metabolism via FGFR4-dependent and independent pathways.* PLoS One, 2011. **6**(3): p. e17868.
195. Wu, X., et al., *Selective activation of FGFR4 by an FGF19 variant does not improve glucose metabolism in ob/ob mice.* Proc Natl Acad Sci U S A, 2009. **106**(34): p. 14379-84.

196. Lan, T., et al., *FGF19, FGF21, and an FGFR1/beta-Klotho-Activating Antibody Act on the Nervous System to Regulate Body Weight and Glycemia.* Cell Metab, 2017. **26**(5): p. 709-718 e3.
197. Ryan, K.K., et al., *Fibroblast growth factor-19 action in the brain reduces food intake and body weight and improves glucose tolerance in male rats.* Endocrinology, 2013. **154**(1): p. 9-15.
198. Morton, G.J., et al., *FGF19 action in the brain induces insulin-independent glucose lowering.* J Clin Invest, 2013. **123**(11): p. 4799-808.
199. Best, J.D., et al., *Role of glucose effectiveness in the determination of glucose tolerance.* Diabetes Care, 1996. **19**(9): p. 1018-30.
200. Alonso, L.C., et al., *Simultaneous measurement of insulin sensitivity, insulin secretion, and the disposition index in conscious unhandled mice.* Obesity (Silver Spring), 2012. **20**(7): p. 1403-12.
201. Taniguchi, A., et al., *Insulin secretion, insulin sensitivity, and glucose effectiveness in nonobese individuals with varying degrees of glucose tolerance.* Diabetes Care, 2000. **23**(1): p. 127-8.
202. Marcelin, G., et al., *Central action of FGF19 reduces hypothalamic AGRP/NPY neuron activity and improves glucose metabolism.* Mol Metab, 2014. **3**(1): p. 19-28.
203. Perry, R.J., et al., *FGF1 and FGF19 reverse diabetes by suppression of the hypothalamic-pituitary-adrenal axis.* Nat Commun, 2015. **6**: p. 6980.
204. Bozadjieva, N., K.M. Heppner, and R.J. Seeley, *Targeting FXR and FGF19 to Treat Metabolic Diseases-Lessons Learned From Bariatric Surgery.* Diabetes, 2018. **67**(9): p. 1720-1728.
205. Schauer, P.R., et al., *Bariatric surgery versus intensive medical therapy in obese patients with diabetes.* N Engl J Med, 2012. **366**(17): p. 1567-76.
206. Myronovych, A., et al., *Vertical sleeve gastrectomy reduces hepatic steatosis while increasing serum bile acids in a weight-loss-independent manner.* Obesity (Silver Spring), 2014. **22**(2): p. 390-400.
207. Kohli, R., et al., *Intestinal adaptation after ileal interposition surgery increases bile acid recycling and protects against obesity-related comorbidities.* Am J Physiol Gastrointest Liver Physiol, 2010. **299**(3): p. G652-60.
208. Patti, M.E., et al., *Serum bile acids are higher in humans with prior gastric bypass: potential contribution to improved glucose and lipid metabolism.* Obesity (Silver Spring), 2009. **17**(9): p. 1671-7.
209. Pournaras, D.J., et al., *The role of bile after Roux-en-Y gastric bypass in promoting weight loss and improving glycaemic control.* Endocrinology, 2012. **153**(8): p. 3613-9.
210. Jahansouz, C., et al., *Bile Acids Increase Independently From Hypocaloric Restriction After Bariatric Surgery.* Ann Surg, 2016. **264**(6): p. 1022-1028.
211. Bray, G.A. and T.F. Gallagher, Jr., *Suppression of appetite by bile acids.* Lancet, 1968. **1**(7551): p. 1066-7.
212. Wu, T., et al., *Effects of rectal administration of taurocholic acid on glucagon-like peptide-1 and peptide YY secretion in healthy humans.* Diabetes Obes Metab, 2013. **15**(5): p. 474-7.

213. Adrian, T.E., et al., *Rectal taurocholate increases L cell and insulin secretion, and decreases blood glucose and food intake in obese type 2 diabetic volunteers.* Diabetologia, 2012. **55**(9): p. 2343-7.
214. Broeders, E.P., et al., *The Bile Acid Chenodeoxycholic Acid Increases Human Brown Adipose Tissue Activity.* Cell Metab, 2015. **22**(3): p. 418-26.
215. Flynn, C.R., et al., *Bile diversion to the distal small intestine has comparable metabolic benefits to bariatric surgery.* Nat Commun, 2015. **6**: p. 7715.
216. Kohli, R., et al., *A surgical model in male obese rats uncovers protective effects of bile acids post-bariatric surgery.* Endocrinology, 2013. **154**(7): p. 2341-51.
217. Ryan, K.K., et al., *FXR is a molecular target for the effects of vertical sleeve gastrectomy.* Nature, 2014. **509**(7499): p. 183-8.
218. DePaoli, A.M., et al., *FGF19 Analog as a Surgical Factor Mimetic That Contributes to Metabolic Effects Beyond Glucose Homeostasis.* Diabetes, 2019. **68**(6): p. 1315-1328.
219. Chen, Y., et al., *Acute Changes of Bile Acids and FGF19 After Sleeve Gastrectomy and Roux-en-Y Gastric Bypass.* Obes Surg, 2019.
220. Nemati, R., et al., *Increased Bile Acids and FGF19 After Sleeve Gastrectomy and Roux-en-Y Gastric Bypass Correlate with Improvement in Type 2 Diabetes in a Randomized Trial.* Obes Surg, 2018. **28**(9): p. 2672-2686.
221. Myronovych, A., et al., *Assessment of the role of FGF15 in mediating the metabolic outcomes of murine Vertical Sleeve Gastrectomy (VSG).* Am J Physiol Gastrointest Liver Physiol, 2020.
222. Zhou, M., et al., *Mouse species-specific control of hepatocarcinogenesis and metabolism by FGF19/FGF15.* J Hepatol, 2017. **66**(6): p. 1182-1192.
223. Nishimura, T., et al., *Identification of a novel FGF, FGF-21, preferentially expressed in the liver.* Biochim Biophys Acta, 2000. **1492**(1): p. 203-6.
224. Kharitonenkov, A., et al., *FGF-21 as a novel metabolic regulator.* J Clin Invest, 2005. **115**(6): p. 1627-35.
225. Kharitonenkov, A., et al., *The metabolic state of diabetic monkeys is regulated by fibroblast growth factor-21.* Endocrinology, 2007. **148**(2): p. 774-81.
226. Coskun, T., et al., *Fibroblast growth factor 21 corrects obesity in mice.* Endocrinology, 2008. **149**(12): p. 6018-27.
227. Xu, J., et al., *Fibroblast growth factor 21 reverses hepatic steatosis, increases energy expenditure, and improves insulin sensitivity in diet-induced obese mice.* Diabetes, 2009. **58**(1): p. 250-9.
228. Xu, J., et al., *Acute glucose-lowering and insulin-sensitizing action of FGF21 in insulin-resistant mouse models--association with liver and adipose tissue effects.* Am J Physiol Endocrinol Metab, 2009. **297**(5): p. E1105-14.
229. Potthoff, M.J., et al., *FGF21 induces PGC-1alpha and regulates carbohydrate and fatty acid metabolism during the adaptive starvation response.* Proc Natl Acad Sci U S A, 2009. **106**(26): p. 10853-8.
230. Fisher, F.M., et al., *Obesity is a fibroblast growth factor 21 (FGF21)-resistant state.* Diabetes, 2010. **59**(11): p. 2781-9.
231. Sarruf, D.A., et al., *Fibroblast growth factor 21 action in the brain increases energy expenditure and insulin sensitivity in obese rats.* Diabetes, 2010. **59**(7): p. 1817-24.

232. Badman, M.K., et al., *Hepatic fibroblast growth factor 21 is regulated by PPARalpha and is a key mediator of hepatic lipid metabolism in ketotic states.* Cell Metab, 2007. **5**(6): p. 426-37.
233. Geiser, F., *Metabolic rate and body temperature reduction during hibernation and daily torpor.* Annu Rev Physiol, 2004. **66**: p. 239-74.
234. Zhang, J., et al., *Constant darkness is a circadian metabolic signal in mammals.* Nature, 2006. **439**(7074): p. 340-3.
235. Chartoumpekis, D.V., et al., *Brown adipose tissue responds to cold and adrenergic stimulation by induction of FGF21.* Mol Med, 2011. **17**(7-8): p. 736-40.
236. Hondares, E., et al., *Thermogenic activation induces FGF21 expression and release in brown adipose tissue.* J Biol Chem, 2011. **286**(15): p. 12983-90.
237. Hondares, E., et al., *Hepatic FGF21 expression is induced at birth via PPARalpha in response to milk intake and contributes to thermogenic activation of neonatal brown fat.* Cell Metab, 2010. **11**(3): p. 206-12.
238. Itoh, N., Y. Nakayama, and M. Konishi, *Roles of FGFs As Paracrine or Endocrine Signals in Liver Development, Health, and Disease.* Front Cell Dev Biol, 2016. **4**: p. 30.
239. Powers, C.J., S.W. McLeskey, and A. Wellstein, *Fibroblast growth factors, their receptors and signaling.* Endocr Relat Cancer, 2000. **7**(3): p. 165-97.
240. Oomura, Y., et al., *A new brain glucosensor and its physiological significance.* Am J Clin Nutr, 1992. **55**(1 Suppl): p. 278S-282S.
241. Meek, T.H., et al., *Functional identification of a neurocircuit regulating blood glucose.* Proc Natl Acad Sci U S A, 2016. **113**(14): p. E2073-82.
242. Suzuki, S., et al., *Feeding suppression by fibroblast growth factor-1 is accompanied by selective induction of heat shock protein 27 in hypothalamic astrocytes.* Eur J Neurosci, 2001. **13**(12): p. 2299-308.
243. Suzuki, S., et al., *Intracerebroventricular infusion of fibroblast growth factor-1 increases Fos immunoreactivity in periventricular astrocytes in rat hypothalamus.* Neurosci Lett, 2001. **300**(1): p. 29-32.
244. Hanai, K., et al., *Central action of acidic fibroblast growth factor in feeding regulation.* Am J Physiol, 1989. **256**(1 Pt 2): p. R217-23.
245. Ferguson, I.A. and E.M. Johnson, Jr., *Fibroblast growth factor receptor-bearing neurons in the CNS: identification by receptor-mediated retrograde transport.* J Comp Neurol, 1991. **313**(4): p. 693-706.
246. Scarlett, J.M., et al., *Central injection of fibroblast growth factor 1 induces sustained remission of diabetic hyperglycemia in rodents.* Nat Med, 2016. **22**(7): p. 800-6.
247. Brown, J.M., et al., *The Hypothalamic Arcuate Nucleus-Median Eminence Is a Target for Sustained Diabetes Remission Induced by Fibroblast Growth Factor 1.* Diabetes, 2019. **68**(5): p. 1054-1061.
248. Scarlett, J.M., et al., *Peripheral Mechanisms Mediating the Sustained Antidiabetic Action of FGF1 in the Brain.* Diabetes, 2019. **68**(3): p. 654-664.
249. Alonge, K.M., et al., *Hypothalamic perineuronal net assembly is required for sustained diabetes remission induced by fibroblast growth factor 1 in rats.* Nat Metab, 2020. **2**(10): p. 1025-1033.

250. Bentsen, M.A., et al., *Transcriptomic analysis links diverse hypothalamic cell types to fibroblast growth factor 1-induced sustained diabetes remission.* Nat Commun, 2020. **11**(1): p. 4458.
251. Lee, P.L., et al., *Purification and complementary DNA cloning of a receptor for basic fibroblast growth factor.* Science, 1989. **245**(4913): p. 57-60.
252. Kornbluth, S., K.E. Paulson, and H. Hanafusa, *Novel tyrosine kinase identified by phosphotyrosine antibody screening of cDNA libraries.* Mol Cell Biol, 1988. **8**(12): p. 5541-4.
253. Keegan, K., et al., *Isolation of an additional member of the fibroblast growth factor receptor family, FGFR-3.* Proc Natl Acad Sci U S A, 1991. **88**(4): p. 1095-9.
254. Partanen, J., et al., *FGFR-4, a novel acidic fibroblast growth factor receptor with a distinct expression pattern.* EMBO J, 1991. **10**(6): p. 1347-54.
255. Stark, K.L., J.A. McMahon, and A.P. McMahon, *FGFR-4, a new member of the fibroblast growth factor receptor family, expressed in the definitive endoderm and skeletal muscle lineages of the mouse.* Development, 1991. **113**(2): p. 641-51.
256. Pasquale, E.B., *A distinctive family of embryonic protein-tyrosine kinase receptors.* Proc Natl Acad Sci U S A, 1990. **87**(15): p. 5812-6.
257. Wang, F., et al., *Alternately spliced NH2-terminal immunoglobulin-like Loop I in the ectodomain of the fibroblast growth factor (FGF) receptor 1 lowers affinity for both heparin and FGF-1.* J Biol Chem, 1995. **270**(17): p. 10231-5.
258. Roghani, M. and D. Moscatelli, *Prostate cells express two isoforms of fibroblast growth factor receptor 1 with different affinities for fibroblast growth factor-2.* Prostate, 2007. **67**(2): p. 115-24.
259. Miki, T., et al., *Determination of ligand-binding specificity by alternative splicing: two distinct growth factor receptors encoded by a single gene.* Proc Natl Acad Sci U S A, 1992. **89**(1): p. 246-50.
260. Chellaiah, A.T., et al., *Fibroblast growth factor receptor (FGFR) 3. Alternative splicing in immunoglobulin-like domain III creates a receptor highly specific for acidic FGF/FGF-1.* J Biol Chem, 1994. **269**(15): p. 11620-7.
261. Werner, S., et al., *Differential splicing in the extracellular region of fibroblast growth factor receptor 1 generates receptor variants with different ligand-binding specificities.* Mol Cell Biol, 1992. **12**(1): p. 82-8.
262. Min, H., et al., *Fgf-10 is required for both limb and lung development and exhibits striking functional similarity to Drosophila branchless.* Genes Dev, 1998. **12**(20): p. 3156-61.
263. Sekine, K., et al., *Fgf10 is essential for limb and lung formation.* Nat Genet, 1999. **21**(1): p. 138-41.
264. Bellusci, S., et al., *Fibroblast growth factor 10 (FGF10) and branching morphogenesis in the embryonic mouse lung.* Development, 1997. **124**(23): p. 4867-78.
265. Beyer, T.A., et al., *Fibroblast growth factor 22 and its potential role during skin development and repair.* Exp Cell Res, 2003. **287**(2): p. 228-36.
266. Goetz, R. and M. Mohammadi, *Exploring mechanisms of FGF signalling through the lens of structural biology.* Nat Rev Mol Cell Biol, 2013. **14**(3): p. 166-80.

267. House, S.L., et al., *Cardioprotection induced by cardiac-specific overexpression of fibroblast growth factor-2 is mediated by the MAPK cascade.* Am J Physiol Heart Circ Physiol, 2005. **289**(5): p. H2167-75.
268. Liao, S., et al., *The cardioprotective effect of the low molecular weight isoform of fibroblast growth factor-2: the role of JNK signaling.* J Mol Cell Cardiol, 2007. **42**(1): p. 106-20.
269. Kanazawa, S., et al., *bFGF regulates PI3-kinase-Rac1-JNK pathway and promotes fibroblast migration in wound healing.* PLoS One, 2010. **5**(8): p. e12228.
270. Tsang, M. and I.B. Dawid, *Promotion and attenuation of FGF signaling through the Ras-MAPK pathway.* Sci STKE, 2004. **2004**(228): p. pe17.
271. Tan, Y., et al., *FGF and stress regulate CREB and ATF-1 via a pathway involving p38 MAP kinase and MAPKAP kinase-2.* EMBO J, 1996. **15**(17): p. 4629-42.
272. Manning, B.D. and L.C. Cantley, *AKT/PKB signaling: navigating downstream.* Cell, 2007. **129**(7): p. 1261-74.
273. Loh, C.Y., et al., *Signal Transducer and Activator of Transcription (STATs) Proteins in Cancer and Inflammation: Functions and Therapeutic Implication.* Front Oncol, 2019. **9**: p. 48.
274. Okumura, T., I.L. Taylor, and T.N. Pappas, *Microinjection of TRH analogue into the dorsal vagal complex stimulates pancreatic secretion in rats.* Am J Physiol, 1995. **269**(3 Pt 1): p. G328-34.
275. Travagli, R.A. and L. Anselmi, *Vagal neurocircuitry and its influence on gastric motility.* Nat Rev Gastroenterol Hepatol, 2016. **13**(7): p. 389-401.
276. Ferreira, M., Jr., et al., *Glucose effects on gastric motility and tone evoked from the rat dorsal vagal complex.* J Physiol, 2001. **536**(Pt 1): p. 141-52.
277. Belluardo, N., et al., *Comparative localization of fibroblast growth factor receptor-1, -2, and -3 mRNAs in the rat brain: in situ hybridization analysis.* J Comp Neurol, 1997. **379**(2): p. 226-46.
278. Bookout, A.L., et al., *FGF21 regulates metabolism and circadian behavior by acting on the nervous system.* Nat Med, 2013. **19**(9): p. 1147-52.
279. Hultman, K., et al., *The central fibroblast growth factor receptor/beta klotho system: Comprehensive mapping in Mus musculus and comparisons to nonhuman primate and human samples using an automated in situ hybridization platform.* J Comp Neurol, 2019.
280. Halmos, K.C., et al., *Molecular and functional changes in glucokinase expression in the brainstem dorsal vagal complex in a murine model of type 1 diabetes.* Neuroscience, 2015. **306**: p. 115-22.
281. Boychuk, C.R. and B.N. Smith, *Glutamatergic drive facilitates synaptic inhibition of dorsal vagal motor neurons after experimentally induced diabetes in mice.* J Neurophysiol, 2016. **116**(3): p. 1498-506.
282. Bach, E.C., K.C. Halmos, and B.N. Smith, *Enhanced NMDA receptor-mediated modulation of excitatory neurotransmission in the dorsal vagal complex of streptozotocin-treated, chronically hyperglycemic mice.* PLoS One, 2015. **10**(3): p. e0121022.
283. Boychuk, C.R., K.C. Halmos, and B.N. Smith, *Diabetes induces GABA receptor plasticity in murine vagal motor neurons.* J Neurophysiol, 2015. **114**(1): p. 698-706.

284. Zsombok, A., et al., *Functional plasticity of central TRPV1 receptors in brainstem dorsal vagal complex circuits of streptozotocin-treated hyperglycemic mice.* J Neurosci, 2011. **31**(39): p. 14024-31.
285. Boychuk, C.R., K.C. Smith, and B.N. Smith, *Functional and molecular plasticity of gamma and alpha1 GABAA receptor subunits in the dorsal motor nucleus of the vagus after experimentally induced diabetes.* J Neurophysiol, 2017. **118**(5): p. 2833-2841.
286. Adams, A.C., et al., *Fundamentals of FGF19 & FGF21 action in vitro and in vivo.* PLoS One, 2012. **7**(5): p. e38438.
287. RRID:AB_11178519, *https://scicrunch.org/resolver/AB_11178519*.
288. RRID:AB_143157, *https://scicrunch.org/resolver/AB_143157*.
289. Ayer, A., et al., *Hemodynamic consequences of chronic parasympathetic blockade with a peripheral muscarinic antagonist.* Am J Physiol Heart Circ Physiol, 2007. **293**(2): p. H1265-72.
290. Lechner, S.G., M. Mayer, and S. Boehm, *Activation of M1 muscarinic receptors triggers transmitter release from rat sympathetic neurons through an inhibition of M-type K+ channels.* J Physiol, 2003. **553**(Pt 3): p. 789-802.
291. Carnagarin, R., et al., *Effects of sympathetic modulation in metabolic disease.* Ann N Y Acad Sci, 2019. **1454**(1): p. 80-89.
292. Filippi, B.M., et al., *Insulin signals through the dorsal vagal complex to regulate energy balance.* Diabetes, 2014. **63**(3): p. 892-9.
293. Filippi, B.M., et al., *Insulin activates Erk1/2 signaling in the dorsal vagal complex to inhibit glucose production.* Cell Metab, 2012. **16**(4): p. 500-10.
294. Browning, K.N., S. Verheijden, and G.E. Boeckxstaens, *The Vagus Nerve in Appetite Regulation, Mood, and Intestinal Inflammation.* Gastroenterology, 2017. **152**(4): p. 730-744.
295. Picard, A., et al., *A Genetic Screen Identifies Hypothalamic Fgf15 as a Regulator of Glucagon Secretion.* Cell Rep, 2016. **17**(7): p. 1795-1806.
296. Scarlett, J.M., et al., *Peripheral Mechanisms Mediating the Sustained Anti-Diabetic Action of FGF1 in the Brain.* Diabetes, 2018.
297. Lun, M.P., E.S. Monuki, and M.K. Lehtinen, *Development and functions of the choroid plexus-cerebrospinal fluid system.* Nat Rev Neurosci, 2015. **16**(8): p. 445-57.
298. Browning, K.N., et al., *Plasticity in the brainstem vagal circuits controlling gastric motor function triggered by corticotropin releasing factor.* J Physiol, 2014. **592**(20): p. 4591-605.
299. Davis, S.F., et al., *Excitatory and inhibitory local circuit input to the rat dorsal motor nucleus of the vagus originating from the nucleus tractus solitarius.* Brain Res, 2004. **1017**(1-2): p. 208-17.
300. Rasmussen, B.A., et al., *Duodenal activation of cAMP-dependent protein kinase induces vagal afferent firing and lowers glucose production in rats.* Gastroenterology, 2012. **142**(4): p. 834-843 e3.
301. Sutton, G.M., L.M. Patterson, and H.R. Berthoud, *Extracellular signal-regulated kinase 1/2 signaling pathway in solitary nucleus mediates cholecystokinin-induced suppression of food intake in rats.* J Neurosci, 2004. **24**(45): p. 10240-7.

302. Purves, T., et al., *A role for mitogen-activated protein kinases in the etiology of diabetic neuropathy.* FASEB J, 2001. **15**(13): p. 2508-14.
303. Volpe, C.M.O., et al., *Cellular death, reactive oxygen species (ROS) and diabetic complications.* Cell Death Dis, 2018. **9**(2): p. 119.
304. Das Evcimen, N. and G.L. King, *The role of protein kinase C activation and the vascular complications of diabetes.* Pharmacol Res, 2007. **55**(6): p. 498-510.
305. Bathina, S. and U.N. Das, *Dysregulation of PI3K-Akt-mTOR pathway in brain of streptozotocin-induced type 2 diabetes mellitus in Wistar rats.* Lipids Health Dis, 2018. **17**(1): p. 168.
306. Haeusler, R.A., T.E. McGraw, and D. Accili, *Biochemical and cellular properties of insulin receptor signalling.* Nat Rev Mol Cell Biol, 2018. **19**(1): p. 31-44.
307. Taniguchi, C.M., B. Emanuelli, and C.R. Kahn, *Critical nodes in signalling pathways: insights into insulin action.* Nat Rev Mol Cell Biol, 2006. **7**(2): p. 85-96.
308. Bailey, T.W., et al., *A-type potassium channels differentially tune afferent pathways from rat solitary tract nucleus to caudal ventrolateral medulla or paraventricular hypothalamus.* J Physiol, 2007. **582**(Pt 2): p. 613-28.
309. Browning, K.N. and R.A. Travagli, *Central nervous system control of gastrointestinal motility and secretion and modulation of gastrointestinal functions.* Compr Physiol, 2014. **4**(4): p. 1339-68.
310. Cunningham, E.T., Jr., R.R. Miselis, and P.E. Sawchenko, *The relationship of efferent projections from the area postrema to vagal motor and brain stem catecholamine-containing cell groups: an axonal transport and immunohistochemical study in the rat.* Neuroscience, 1994. **58**(3): p. 635-48.
311. Mussa, B.M. and A.J. Verberne, *The dorsal motor nucleus of the vagus and regulation of pancreatic secretory function.* Exp Physiol, 2013. **98**(1): p. 25-37.
312. Willis, A., et al., *Three types of postsynaptic glutamatergic receptors are activated in DMNX neurons upon stimulation of NTS.* Am J Physiol, 1996. **271**(6 Pt 2): p. R1614-9.
313. Browning, K.N. and R.A. Travagli, *Short-term receptor trafficking in the dorsal vagal complex: an overview.* Auton Neurosci, 2006. **126-127**: p. 2-8.
314. Davis, S.F., et al., *Selective enhancement of synaptic inhibition by hypocretin (orexin) in rat vagal motor neurons: implications for autonomic regulation.* J Neurosci, 2003. **23**(9): p. 3844-54.
315. Derbenev, A.V., T.C. Stuart, and B.N. Smith, *Cannabinoids suppress synaptic input to neurones of the rat dorsal motor nucleus of the vagus nerve.* J Physiol, 2004. **559**(Pt 3): p. 923-38.
316. Glatzer, N.R., et al., *Endomorphin-1 modulates intrinsic inhibition in the dorsal vagal complex.* J Neurophysiol, 2007. **98**(3): p. 1591-9.
317. D'Agostino, G., et al., *Appetite controlled by a cholecystokinin nucleus of the solitary tract to hypothalamus neurocircuit.* Elife, 2016. **5**.
318. Kawai, Y. and E. Senba, *Electrophysiological and morphological characteristics of nucleus tractus solitarii neurons projecting to the ventrolateral medulla.* Brain Res, 2000. **877**(2): p. 374-8.
319. Norgren, R., *Projections from the nucleus of the solitary tract in the rat.* Neuroscience, 1978. **3**(2): p. 207-18.

320. Browning, K.N. and R.A. Travagli, *Plasticity of vagal brainstem circuits in the control of gastric function.* Neurogastroenterol Motil, 2010. **22**(11): p. 1154-63.
321. Zsombok, A. and B.N. Smith, *Plasticity of central autonomic neural circuits in diabetes.* Biochim Biophys Acta, 2009. **1792**(5): p. 423-31.
322. Kalia, M. and J.M. Sullivan, *Brainstem projections of sensory and motor components of the vagus nerve in the rat.* J Comp Neurol, 1982. **211**(3): p. 248-65.
323. Contreras, R.J., R.M. Beckstead, and R. Norgren, *The central projections of the trigeminal, facial, glossopharyngeal and vagus nerves: an autoradiographic study in the rat.* J Auton Nerv Syst, 1982. **6**(3): p. 303-22.
324. Leslie, R.A., D.G. Gwyn, and D.A. Hopkins, *The central distribution of the cervical vagus nerve and gastric afferent and efferent projections in the rat.* Brain Res Bull, 1982. **8**(1): p. 37-43.
325. Shapiro, R.E. and R.R. Miselis, *The central neural connections of the area postrema of the rat.* J Comp Neurol, 1985. **234**(3): p. 344-64.
326. Rinaman, L. and G. Schwartz, *Anterograde transneuronal viral tracing of central viscerosensory pathways in rats.* J Neurosci, 2004. **24**(11): p. 2782-6.
327. Baptista, V., et al., *Cholecystokinin octapeptide increases spontaneous glutamatergic synaptic transmission to neurons of the nucleus tractus solitarius centralis.* J Neurophysiol, 2005. **94**(4): p. 2763-71.
328. Shitaka, Y., et al., *Basic fibroblast growth factor increases functional L-type Ca2+ channels in fetal rat hippocampal neurons: implications for neurite morphogenesis in vitro.* J Neurosci, 1996. **16**(20): p. 6476-89.
329. Mergler, S., et al., *Calcium influx induced by activation of receptor tyrosine kinases in SV40-transfected human corneal endothelial cells.* Exp Eye Res, 2003. **77**(4): p. 485-95.
330. Glatzer, N.R., et al., *Synaptic and morphologic properties in vitro of premotor rat nucleus tractus solitarius neurons labeled transneuronally from the stomach.* J Comp Neurol, 2003. **464**(4): p. 525-39.
331. Pitra, M.S. and B.N. Smith, *"Musings on the wanderer: What's new in our understanding of vago-vagal reflexes? VI. Central vagal circuits that control glucose metabolism.".* Am J Physiol Gastrointest Liver Physiol, 2020.
332. Roman, C.W., V.A. Derkach, and R.D. Palmiter, *Genetically and functionally defined NTS to PBN brain circuits mediating anorexia.* Nat Commun, 2016. **7**: p. 11905.
333. Blevins, J.E. and D.G. Baskin, *Hypothalamic-brainstem circuits controlling eating.* Forum Nutr, 2010. **63**: p. 133-140.
334. Garza, A., et al., *Expression of nicotinic acetylcholine receptors and subunit messenger RNAs in the enteric nervous system of the neonatal rat.* Neuroscience, 2009. **158**(4): p. 1521-9.
335. Schemann, M. and D. Grundy, *Electrophysiological identification of vagally innervated enteric neurons in guinea pig stomach.* Am J Physiol, 1992. **263**(5 Pt 1): p. G709-18.
336. Pandol, S., *The Exocrine Pancreas*. 2010, San Rafael, CA: Morgan and Claypool Life Sciences.
337. Laughton, W.B. and T.L. Powley, *Localization of efferent function in the dorsal motor nucleus of the vagus.* Am J Physiol, 1987. **252**(1 Pt 2): p. R13-25.

338. Ahren, B., *Autonomic regulation of islet hormone secretion--implications for health and disease.* Diabetologia, 2000. **43**(4): p. 393-410.
339. Gilon, P. and J.C. Henquin, *Mechanisms and physiological significance of the cholinergic control of pancreatic beta-cell function.* Endocr Rev, 2001. **22**(5): p. 565-604.
340. Brunicardi, F.C., D.M. Shavelle, and D.K. Andersen, *Neural regulation of the endocrine pancreas.* Int J Pancreatol, 1995. **18**(3): p. 177-95.
341. Duttaroy, A., et al., *Muscarinic stimulation of pancreatic insulin and glucagon release is abolished in m3 muscarinic acetylcholine receptor-deficient mice.* Diabetes, 2004. **53**(7): p. 1714-20.
342. Rix I, N.-L.C., Bergmann NC, et al., *Glucagon Physiology*, in *Endotext*, A.B. Feingold KR, Boyce A, et al., Editor. 2019.
343. Reaven, G.M., et al., *Documentation of hyperglucagonemia throughout the day in nonobese and obese patients with noninsulin-dependent diabetes mellitus.* J Clin Endocrinol Metab, 1987. **64**(1): p. 106-10.
344. Cryer, P.E., *Minireview: Glucagon in the pathogenesis of hypoglycemia and hyperglycemia in diabetes.* Endocrinology, 2012. **153**(3): p. 1039-48.
345. Svoboda, M., et al., *Relative quantitative analysis of glucagon receptor mRNA in rat tissues.* Mol Cell Endocrinol, 1994. **105**(2): p. 131-7.
346. Unger, R.H., *Glucagon physiology and pathophysiology in the light of new advances.* Diabetologia, 1985. **28**(8): p. 574-8.
347. Vatamaniuk, M.Z., et al., *Acetylcholine affects rat liver metabolism via type 3 muscarinic receptors in hepatocytes.* Life Sci, 2003. **72**(16): p. 1871-82.
348. Berthoud, H.R., *Anatomy and function of sensory hepatic nerves.* Anat Rec A Discov Mol Cell Evol Biol, 2004. **280**(1): p. 827-35.
349. Akiyoshi, H., T. Gonda, and T. Terada, *A comparative histochemical and immunohistochemical study of aminergic, cholinergic and peptidergic innervation in rat, hamster, guinea pig, dog and human livers.* Liver, 1998. **18**(5): p. 352-9.
350. el-Salhy, M., R. Stenling, and L. Grimelius, *Peptidergic innervation and endocrine cells in the human liver.* Scand J Gastroenterol, 1993. **28**(9): p. 809-15.
351. Burt, A.D., et al., *Localization of adrenergic and neuropeptide tyrosine-containing nerves in the mammalian liver.* Hepatology, 1989. **9**(6): p. 839-45.
352. Goehler, L.E. and C. Sternini, *Neuropeptide Y immunoreactivity in the mammalian liver: pattern of innervation and coexistence with tyrosine hydroxylase immunoreactivity.* Cell Tissue Res, 1991. **265**(2): p. 287-95.
353. Stoyanova, II and M.V. Gulubova, *Peptidergic nerve fibres in the human liver.* Acta Histochem, 1998. **100**(3): p. 245-56.
354. Ding, W.G., H. Kitasato, and H. Kimura, *Development of neuropeptide Y innervation in the liver.* Microsc Res Tech, 1997. **39**(4): p. 365-71.
355. Ding, W.G., et al., *Phylogenetic and ontogenetic study of neuropeptide Y-containing nerves in the liver.* Histochem J, 1994. **26**(5): p. 453-9.
356. Cheng, Z., et al., *Projections of the dorsal motor nucleus of the vagus to cardiac ganglia of rat atria: an anterograde tracing study.* J Comp Neurol, 1999. **410**(2): p. 320-41.

357. Fontan, J.J., C.T. Diec, and C.R. Velloff, *Bilateral distribution of vagal motor and sensory nerve fibers in the rat's lungs and airways.* Am J Physiol Regul Integr Comp Physiol, 2000. **279**(2): p. R713-28.
358. Potthoff, M.J., S.A. Kliewer, and D.J. Mangelsdorf, *Endocrine fibroblast growth factors 15/19 and 21: from feast to famine.* Genes Dev, 2012. **26**(4): p. 312-24.
359. Sasaki, K., et al., *Acidic fibroblast growth factor facilitates generation of long-term potentiation in rat hippocampal slices.* Brain Res Bull, 1994. **33**(5): p. 505-11.
360. Terlau, H. and W. Seifert, *Fibroblast Growth Factor Enhances Long-term Potentiation in the Hippocampal Slice.* Eur J Neurosci, 1990. **2**(11): p. 973-977.
361. Pernia-Andrade, A.J., et al., *A deconvolution-based method with high sensitivity and temporal resolution for detection of spontaneous synaptic currents in vitro and in vivo.* Biophys J, 2012. **103**(7): p. 1429-39.
362. Browning, K.N., A.E. Kalyuzhny, and R.A. Travagli, *Mu-opioid receptor trafficking on inhibitory synapses in the rat brainstem.* J Neurosci, 2004. **24**(33): p. 7344-52.
363. Browning, K.N., A.E. Kalyuzhny, and R.A. Travagli, *Opioid peptides inhibit excitatory but not inhibitory synaptic transmission in the rat dorsal motor nucleus of the vagus.* J Neurosci, 2002. **22**(8): p. 2998-3004.
364. Browning, K.N. and R.A. Travagli, *Functional organization of presynaptic metabotropic glutamate receptors in vagal brainstem circuits.* J Neurosci, 2007. **27**(34): p. 8979-88.
365. Browning, K.N. and R.A. Travagli, *Modulation of inhibitory neurotransmission in brainstem vagal circuits by NPY and PYY is controlled by cAMP levels.* Neurogastroenterol Motil, 2009. **21**(12): p. 1309-e126.
366. Browning, K.N., et al., *Vagal afferent control of opioidergic effects in rat brainstem circuits.* J Physiol, 2006. **575**(Pt 3): p. 761-76.
367. Sullivan, C.N., et al., *Endogenous cholecystokinin reduces food intake and increases Fos-like immunoreactivity in the dorsal vagal complex but not in the myenteric plexus by CCK1 receptor in the adult rat.* Am J Physiol Regul Integr Comp Physiol, 2007. **292**(3): p. R1071-80.
368. Yang, H., G. Ohning, and Y. Tache, *TRH in dorsal vagal complex mediates acid response to excitation of raphe pallidus neurons in rats.* Am J Physiol, 1993. **265**(5 Pt 1): p. G880-6.
369. Stachowiak, E.K., et al., *cAMP-induced differentiation of human neuronal progenitor cells is mediated by nuclear fibroblast growth factor receptor-1 (FGFR1).* J Neurochem, 2003. **84**(6): p. 1296-312.
370. Stachowiak, M.K., et al., *Nuclear accumulation of fibroblast growth factor receptors is regulated by multiple signals in adrenal medullary cells.* Mol Biol Cell, 1996. **7**(8): p. 1299-317.
371. Maciejczyk, M., et al., *Redox Balance, Antioxidant Defense, and Oxidative Damage in the Hypothalamus and Cerebral Cortex of Rats with High Fat Diet-Induced Insulin Resistance.* Oxid Med Cell Longev, 2018. **2018**: p. 6940515.
372. Geraldes, P. and G.L. King, *Activation of protein kinase C isoforms and its impact on diabetic complications.* Circ Res, 2010. **106**(8): p. 1319-31.
373. Ido, Y., et al., *Neural dysfunction and metabolic imbalances in diabetic rats. Prevention by acetyl-L-carnitine.* Diabetes, 1994. **43**(12): p. 1469-77.

374. Zhu, X. and J. Eichberg, *1,2-diacylglycerol content and its arachidonyl-containing molecular species are reduced in sciatic nerve from streptozotocin-induced diabetic rats.* J Neurochem, 1990. **55**(3): p. 1087-90.
375. Ramakrishnan, R., R. Sheeladevi, and N. Suthanthirarajan, *PKC-alpha mediated alterations of indoleamine contents in diabetic rat brain.* Brain Res Bull, 2004. **64**(2): p. 189-94.
376. Vetri, F., et al., *Complex modulation of the expression of PKC isoforms in the rat brain during chronic type 1 diabetes mellitus.* Brain Res, 2013. **1490**: p. 202-9.
377. Vetri, F., et al., *Impairment of neurovascular coupling in type 1 diabetes mellitus in rats is linked to PKC modulation of BK(Ca) and Kir channels.* Am J Physiol Heart Circ Physiol, 2012. **302**(6): p. H1274-84.
378. Maffei, A., G. Lembo, and D. Carnevale, *PI3Kinases in Diabetes Mellitus and Its Related Complications.* Int J Mol Sci, 2018. **19**(12).
379. Verrotti, A., et al., *Autonomic neuropathy in diabetes mellitus.* Front Endocrinol (Lausanne), 2014. **5**: p. 205.
380. Cai, F. and C.J. Helke, *Abnormal PI3 kinase/Akt signal pathway in vagal afferent neurons and vagus nerve of streptozotocin-diabetic rats.* Brain Res Mol Brain Res, 2003. **110**(2): p. 234-44.
381. Torres, R.C., et al., *Activation of PPAR-gamma reduces HPA axis activity in diabetic rats by up-regulating PI3K expression.* Exp Mol Pathol, 2016. **101**(2): p. 290-301.

VITA

Education

B.S. in Biology ..... West Virginia University – 2008-2013

B.A. in Chemistry..... West Virginia University – 2008-2013

Minor in Philosophy ..... West Virginia University – 2008-2013

Scientific Work Experience

Analytical Chemist

WVU National Research Center for Coal and Energy 2012-2014

Analytical Chemist

MSES Corrosion Products..... 2014-2016

Teaching Assistant – Human Anatomy and Physiology

Bluegrass Community and Technical College 2020

Awards and Honors

UKY Graduate Training in Integrative Physiology T32 Training Grant... 2017-2018

Graduate Student Congress Travel Award 2019

Publications

Wean, J.B. and Smith, B.N. (2021) FGF19 in the hindbrain lowers blood glucose and alters excitability of vagal motor neurons in hyperglycemic mice. *Endocrinology,* Volume 162. *PubMed*

Abstracts

2018 Bluegrass Society for Neuroscience Conference, Lexington, KY.
Poster
"Fibroblast Growth Factor 19 Alters Parasympathetic Output of the Dorsal Motor Nucleus of the Vagus".

2018 University of Kentucky Physiology Retreat, Lexington, KY.
Poster and One-Minute Data Blitz
"Fibroblast Growth Factor 19 Alters Parasympathetic Output of the Dorsal Motor Nucleus of the Vagus" poster and one minute data blitz presentation.

2018 Kentucky Neuroscience Institute Translational Research Symposium, Lexington, KY.
"Fibroblast Growth Factor 19 Alters Excitability in the
Dorsal Motor Nucleus of the Vagus".

2018 Society for Neuroscience Conference, San Diego, CA.
"Fibroblast Growth Factor 19 Alters Excitability in the Dorsal Motor Nucleus of the Vagus".

2019 Bluegrass Society for Neuroscience Conference, Lexington, KY.
"Fibroblast Growth Factor 19 Alters Excitability in the Dorsal Motor Nucleus of the Vagus".

2019 University of Kentucky Physiology Retreat, Lexington, KY.
Poster and One-minute Data Blitz
"Fibroblast Growth Factor 19 Alters Parasympathetic Output of the Dorsal Motor Nucleus of the Vagus"

2019 Barnstable Brown Diabetes Center Research Day, Lexington, KY.
Poster
"Fibroblast Growth Factor 19 Alters Excitability in the Dorsal Motor Nucleus of the Vagus".

2019 Society for Neuroscience Conference, Chicago, IL.
Nanosymposium Presentation
"Fibroblast Growth Factor 19 Alters Excitability in the Dorsal Motor Nucleus of the Vagus and Lowers Blood Glucose Concentration".

2020 University of Kentucky Physiology Retreat, Lexington, KY.
Virtual Poster Presentation
"FGF19 in the Dorsal Vagal Complex".

2020 Barnstable Brown Diabetes Center Research Day, Lexington, KY.
Virtual Poster Presentation
"FGF19 in the Dorsal Vagal Complex".